# Control of B cell participation in the T-dependent humoral immune response by follicular regulatory T cells and other factors

By
Zachary Benet

A dissertation submitted in partial fulfillment
of the requirements for the degree of
Doctor of Philosophy
(Immunology)
In the University of Michigan
2017

Doctoral committee:

Assistant Professor Irina Grigorova, Chair
Professor Cheong-Hee Chang
Professor Gabriel Nuñez
Professor Bruce Richardson
Professor Weiping Zou

Zachary Benet

benetzl@umich.edu

ORCID ID: 0000-0002-8679-7545

## Dedication

To my parents for their unending support. To Carrie for her love and patience.

## Acknowledgements

First and foremost, I would like to thank my advisor, Dr. Irina Grigorova, for her unwavering support and willingness to provide the best mentorship a student could hope for throughout this whole process. I would also like to acknowledge my committee members for their advice and input on forwarding my project.

I also want to acknowledge the many members of Grigorova Lab who have helped with my project. I would like to thank Jackson Turner for putting up with me for the past 6 years every day. I'm not the most organized individual so I would like to thank the mouse technicians we have had over the years including Eunjung Lyu, Trisha Denike, and Jenny Jiang. I would also like to acknowledge the many undergraduates who worked on this project. Their hard work has saved me from developing carpal tunnel syndrome.

And finally, I would like to acknowledge the students and faculty in the Immunology Program. From discussions on science to just having some beers at ABC, it has been amazing watching everyone grow into the scientists they are now. I wish you all the best of luck. I would also like to thank Dr. Bethany Moore for being the amazing support that she is by always having her door open to students. Finally, I would like to thank Zarinah Aquil. I am the worst to respond to emails which likely drives her crazy but she always responds quickly when I need something from her. Sorry, but thank you!

## Table of Contents

# List of Figures

## Abstract

High affinity, long lasting antibodies and memory B cells provide protection from foreign pathogens and their generation has been the target of nearly all succesful vaccines to date. Their development requires that B cells participate in the T-dependent humoral response and form Germinal Centers (GCs) where B cell affinity maturation and differentiation of long-lived antibody-secreting cells and high-affinity memory B cells takes place. The T-dependent humoral response must be tightly regulated because of its potential to recruit or generate B cells with self-reactivity that can lead to the development of autoimmune diseases. While it is well known that follicular helper and follicular regulatory T cells (Tfh and Tfr) are required for the control of GC responses and Tfh cells are widely studied, the mechanisms of Tfr cell action on newly recruited activated B cells and GC B cells are not fully understood.

In my thesis work I found that follicular regulatory T cells can respond to the proinflammatory cytokines CCL3 and CCL4 (which can be secreted by GC B cells) *ex vivo* and make more frequent interactions with wild-type (WT) than CCL3-deficient GC B cells *in vivo*. Moreover, I showed that B cell intrinsic production of CCL3 is required for control of GC B cell expansion and is important for limiting the development of antinuclear antibodies. Together, our data suggests that CCL3 secreted by GC B cells promotes their direct interactions and control by Tfr cells *in vivo*.

In addition to analysis of the cellular and molecular mechanisms of Tfr action on GC B cells, we also examined how kinetics of Tfh and Tfr cell response affects the recruitment of newly arriving antigen-specific B cells into the GC response. We found that B cells have a short, limited time frame in which they can participate in ongoing immune responses. Preloading B cells with activating antigen alone is sufficient to promote their participation at all stages of the GCs despite differences in the number and quality of

follicular T cells. Our data suggests that antigen-triggered activation may be the limiting factor for continuous recruitment of antigen-specific B cells into immunization-induced response. Overall, the findings of this work may be important for future improvements of vaccination approaches against pathogenic diseases and better treatments or prevention of autoimmune diseases.

# Chapter 1 – Introduction

## The role of antibody responses in immunity

Emil von Behring and Shibasabura Kitasato in 1890 showed that serum transfer from immunized to unimmunized hosts could render both diphtheria and tetanus toxin harmless [1]. It was later discovered that the molecules responsible for the protection to a wide variety of inoculum comprised of the gamma globulin fraction in human serum. The source of gamma globulins, termed antibodies or immunoglobulins, was traced back to plasma cells found residing in bone marrow [2]. Since then antibodies have been shown to recognize a wide variety of foreign antigens and be the key feature of the adaptive humoral immune response. The importance of antibodies in providing protection in humans was made clear by Charles Janeway who, along with Fred Rosen, pioneered intravenous antibody therapy for patients who lack the ability to mount their own humoral response and are subject to recurrent infections [3, 4]. Subsequently, the generation of antibodies has been the goal of nearly all vaccination strategies up-to-date.

## T-independent and T-dependent B cell responses

Antibody responses are mounted by B lymphocytes (B cells). Mature B cells express immunoglobulins in a membrane-attached form called B cell receptors (BCRs). During development, B cells undergo the process of random VDJ recombination of germline DNA encoding their BCRs. This process renders mature B cells expressing BCRs with unique antigen recognition sites and specificity. Because of the outstanding variability of the BCR repertoire between various B cells, a wide variety of antigens including proteins, lipids, DNA, RNA and polysaccharides can trigger B cell responses [5]. Antigen-dependent cross-linking of BCRs promotes B cell activation and may lead to proliferation and the generation of antibody secreting plasma cells [6]. Antibody

generated from these cells helps facilitate opsonization of foreign antigen, generate immune complexes, and promotes antigen capture to the follicles to further enhance the humoral immune response [7]. Memory cells may also be generated early in the response. These cells can be reactivated upon secondary challenge for rapid, secondary responses [7].

While initial activation of B cells is triggered by antigen-dependent cross-linking of BCRs, complete B cell activation depends on the nature of antigens and the signals from helper T cells (Th cells). Multivalent antigens that induce very strong cross-linking of BCRs or antigens that work in conjunction with innate immune Toll-like receptors can induce thymus-independent (T-independent) B cell response that require little to no involvement of Th cells. These antigens can directly trigger B cells to form short-lived plasma cells reside in local secondary lymphoid organs (SLOs) and produce antibodies. In some cases, they can also promote formation of memory B cells [8, 9]. Common to the T-independent response is that antigen affinity of the antibodies and memory B cells produced is relatively low.

Protein or peptide-containing antigens can trigger thymus-dependent (T-dependent) B cell responses by enabling B cells interactions and acquisition of costimulatory signals from cognate Th cells [10]. Activated B cells internalize antigen-bound BCRs and direct them to endosomes, where antigenic proteins are processed into peptides and loaded onto major histocompatibility complex II (MHCII) molecules. Th cells that recognize pMHCII/peptide complexes presented on antigen-primed B cells through their T cell receptor (TCR) can engage into cognate interactions and provide survival, proliferation, and differentiation signals to their cognate B cells [10]. Like the T-independent response, in T-dependent response B cells form short-lived plasma cells and memory cells that express immunoglobulins of low affinity towards antigen. However, T-dependent antigens also lead to the formation of transient, microanatomical structures in the B cell follicles of secondary lymphoid organs (SLOs) called germinal centers (GCs) [10]. Within the GCs, B cells undergo a process called affinity maturation where

their BCRs increase in affinity overtime. They also undergo extensive class-switching – the process that leads to the expression of immunoglobulins of IgG, IgA, or IgE isotype by activated B cells. GCs give rise to high affinity, class-switched memory B cells and long lived plasma cells (LLPCs) that migrate to the bone marrow, the gut or mammary glands and that can persist for months/years secreting higher affinity antibodies [11] . Generation of long-term high-affinity, class-switched antibody responses is a hall-mark of the T-dependent humoral response. Thus, understanding how the T-dependent process is controlled can provide new insights into vaccine design.

**Complex Regulation of B cells by T cells**

T cells play a multifunctional role in orchestrating B cell responses to foreign antigen. Early in the response, T cells provide signals that promote B cell survival and prompt differentiation into plasmablasts, early memory B cells, and GC B cells [6]. Within GCs, T cells are required for GC B cell survival, proliferation, class-switching, affinity maturation and generation of effector cells. Observations made in mice and humans in which T cells are incapable of helping B cells have shown that the resulting immune response and protection from disease are significantly impaired [12-14]. At the same time, excessive T cell help was also found to be disadvantageous and result in decreased overall affinity of the foreign antibody response and the recruitment of B cells that harbor BCRs specific to self-antigens [15-17].

Two types of $CD4^+$ T cells are thought to be playing the major role in promoting and regulating T-dependent B cell responses: follicular helper T cells (Tfh) and follicular regulatory T cells (Tfr).

While it has been known for several decades that $CD4^+$ T cells are required for the formation of productive GCs, as well as for generating antigen-specific memory and LLPCs, the exact Th cell subset had initially remained elusive. Interleukin (IL)-4 producing $CD4^+$ T cells, or Th2 cells, were a candidate subset since IL-4 can stimulate immunoglobulin secretion and induce isotype switching. However, mice in which $CD4^+$ T

cells cannot differentiate into Th2 develop GCs and can produce T-dependent antibody responses [18]. In the past decade, a subset of T cells termed Tfh cells, have been identified as the T cell required for the T-dependent humoral response [10, 19]. Tfh cells differentiate from foreign antigen-specific Th cells during infection or following an immunization and move into the follicles of SLO to support GC responses. Functionally, Tfh help regulate the magnitude of the GC response, restrict the entry of low affinity clones into the GC, and are critical to the process of affinity maturation [10, 19-22].

While Tfh have been extensively studied, until recently much less attention has been paid to Tfr cells. Tfr cells arise predominantly, but not exclusively, from natural Tregs and appear to regulate the magnitude of the GC and the humoral response, class-switching, and antigen specificity. Together Tfh and Tfr cells play a complex and multifaceted role in the T-dependent humoral response. These cells will be described more in detail below once the process which they influence has been outlined.

**Initiation of T-dependent B cell response**

*Early anatomy of B cell activation*

The first steps in the initiation of T-dependent B cell response is activation of naïve B cells by foreign antigens. This must be followed by acquisition of help from cognate Th cells. The spatial-temporal dynamics of these events depends greatly on the anatomy of secondary lymphoid organs (SLO), the types of antigens that drain or are actively delivered into SLO [23], and multiple molecular cues that orchestrate movements of lymphocytes within secondary lymphoid organs at different stages of their activation [10, 24].

The lymph nodes and the white pulp of the spleen can be broadly characterized by as a central T zone bordered by B cell follicles with interfollicular regions (IF) between adjacent follicles. Within the spleen, follicles are bordered by the marginal zone (MZ) while within the lymph node the follicles are adjacent to the subcapsular sinus (SCS) which both contain specialized cells to facilitate antigen capture and presentation [24] (Fig 1.1). B cells have been shown to acquire antigen at these sites or in other regions

of the SLO, depending on the type of antigen and its' access into SLO [25].

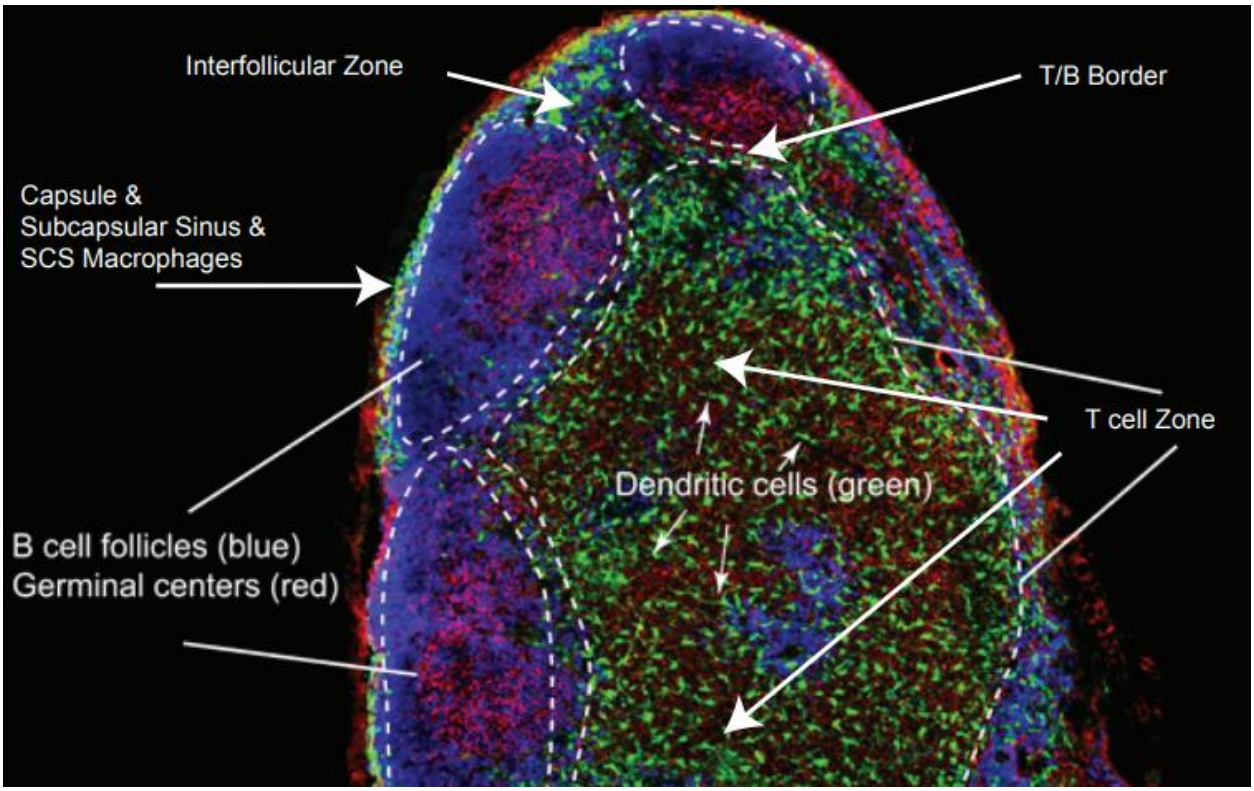


**Figure 1.1. Anatomy of the Lymph Node**
Adapted from http://www.cell.com/immunity/image-resource-lymphnode. Credit: Ashley Moseman and Ulrich von Andrian, Harvard Medical School

The coordinated migration of B cells following antigen-driven activation depends on the secretion of chemokines and other factors by stromal and other cells types of the SLO and several different G-protein coupled receptors (GPCRs) expressed by B cells. Follicular stromal cells express CXCL13, which promotes B cell localization and migration within the B cell follicle via CXCR5 receptor [26]. Critical to the positioning of B cells following their initial activation is the increased expression of the EBV-induced molecule 2 (EBI2) receptor [27-29]. EBI2 is responsible for the initial movement of activated B cells towards the back of the follicle where its ligand, 7α,25-dihydroxycholesterol (7α,25-OHC), is thought to be in high concentrations [29] and where B cells are likely to acquire additional antigen associated with the MZ or SCS [25, 30]. CCR7 expression then guides B cells to the border between B cell follicles and the T zone and interfollicular areas [24, 31], where CCR7 ligands CCL21/19 are secreted by

interfollicular and T zone stromal cells [26, 32]. Uniform distribution of activated B cells along B-T border depends on both EBI2 and CCR7 [30, 31]. Migration to these regions helps position B cells to receive cognate CD4+ T cell help and promote their participation in the T-dependent humoral immune response. Following acquisition of T cell help, proliferating B cells can be visualized in the back of the follicle and interfollicular areas where they move in an EBI2-dependent fashion and where their initial differentiation into plasma, memory and GC B cells is thought to take place [30, 33]. The following movement of GC B cells to the middle of the follicle is facilitated by the downregulation of CCR7, loss of EBI2, and by increasingly dominant CXCR5 signals [30, 34].

*Early T/B cell interactions*

At the T/B border, cognate Th cells and activated B cells undergo long-lived interactions that typically are longer than 10 min with some lasting for over an hour [31]. These interactions are dependent on factors such as the expression of integrins [35], the amount of antigen presented by B cells [21], and adhesion molecules [35, 36]. Interestingly, intravital microscopy has also revealed that B and T cells can perform a series of short, sequential interactions [31, 36]. These short interactions may be important in increasing the activation state of the B cell by enhancing the expression of pro-adhesion molecules and may eventually lead to longer duration contacts. Stabilization of contacts between B and T cells is critical for subsequent development into either early effector B cells or GC B cells [36, 37]. During contacts, T cells may provide a number of signals to cognate B cells including, but not limited to, IL-4, IL-21, and CD40L which influence the expression and activation of transcription factors such as Bcl6, Blimp1, and IRF4 [10].

*Early differentiation of activated B cells*

During early cognate interactions, B cells integrate BCR signals and the many T cell derived signals being provided and differentiate into early effector cells or GC B cells. The presence and amount of these signals seemingly enable differentiation into

memory cells and plasmablasts as early as 2-3 days after activation and GC B cells as early as 4-5 days [33, 38]. The differentiation of B cells into one of these subsets is dependent on inducing the expression of the mutually antagonistic master transcription factors Bimp1 and Bcl6 [39].

Plasmablasts are early plasma cells that still retain the ability to capture and present antigen to T cells despite their production of high amounts of soluble antibody [40]. Differentiation into plasmablasts critically depends on Blimp1 (encoded by *Prdm1)* which suppresses Bcl6. CD40 signaling, which can enhance Blimp1 expression, increases plasmablast numbers and is dependent on the amount of antigen which a B cell can present to T cells [11, 40]. High affinity B cells early in the response present more antigen and receive more T cell help for differentiation into and proliferate as plasmablasts [40, 41]. Long, durable cognate interactions between B and T cells will expose B cells to greater amounts of cytokines like IL-21 which can enhance IRF4 expression and activity [42]. High expression of IRF4 helps repress Bcl6, and thus potentiates Blimp1 expression [43].

Memory B cell generation early on may require the least amount of T cell help or is a default differentiation pathway after BCR engagement. At the same time, CD40 signaling has been suggested in promoting the generation of memory cells prior to GC formation [44].

Finally, activated B cells may also differentiate into GC B cells. GC B cells express Bcl6 and may also express low levels of IRF4 for class switching and somatic hypermutation [45, 46]. T cell help is indeed required for the differentiation of GC B cells and long, durable contacts facilitate this process [31, 36].

**Germinal Centers**

GCs arise and are visible at the center of B cell follicles 4-6 days after antigen challenge. Within GCs, B cells undergo rapid proliferation, somatic hypermutation of their BCRs, and are selected based on increased affinity towards antigen [10]. GC B

cells that are not selected undergo rapid apoptosis. This process leads to affinity maturation of antibody responses critically important for generation of neutralizing antibodies against many pathogens and toxins.

*Polarization of germinal centers into light and dark zones*

Early structural observations indicated that GCs are made of two zones: the light and dark zones (LZ and DZ, respectively). These names derive from microscopic observations because the dark zone, dense in dividing GC cells with high amounts of chromatin, appeared dark due to their ability to block light. Comparatively, the light zone does not have many dividing cells and B cells are interspaced by follicular dendritic cells (FDCs) [47].

Light zone FDCs are stromal cells that produce the chemokine CXCL13 and are positioned at the center of B cell follicles [48]. In contrast, the dark zone is found closer to the T/B border. Here, specialized stromal cells called *Cxl12*-expressing reticular cells (CRCs) produce CXCL12 [49, 50]. The polarization of the GC into two distinct regions appears necessary for the proper development of the humoral immune response since special biological processes occur within each zone [51, 52].

Within the LZ, GC B cells are thought to acquire antigen and T cell help. FDCs are decorated with immune complexed antigen via Fc and complement receptors and can internalize and store antigen for an extended period [53-55]. GC B cell clones compete for limited amounts of antigen and pro-survival signals displayed on FDCs [56-58]. LZ GC B cells present antigen to resident Tfh cells who subsequently provide survival and activation signals. Taken together, the B cells within the LZ are activated, both from the reacquisition of antigen and from Tfh cells [22, 59, 60] and are poised for proliferation suggesting that LZ B cells are undergoing positive selection within this region. Paradoxically, evidence of actively proliferating cells in the LZ is rare with only B cells currently in the S-phase appearing in the LZ [22, 61].

In contrast to LZ B cells, B cells within the DZ are characterized as highly proliferative. Observations made with the proliferation antigen Ki67 revealed nearly ubiquitous expression of this marker within the DZ and nearly universal uptake of thymidine analogs such as BrdU [61, 62]. In contrast to the LZ, B cells that are currently in the G2/M phase of cell division are significantly enriched in the DZ [22, 61]. During division, activation-induced cytidine deaminase (AID), which deaminates cytidine residues in the BCR genes randomly and enables class switching to different immunoglobulin genes (IgG, IgA, etc.), is active [10, 63]. B cells in the DZ do not share a similar gene profile to that seen in the LZ, most notably BCR and CD40 signaling profiles are absent [22, 60]. Consistent with this observation is the relative lack of T follicular helper cells and FDC-laden antigen in the region. Together, this data implicates that the DZ is largely a region within the GC that supports proliferation, somatic hypermutation (SHM), and class switch recombination.

*Interzonal migration*

The division of labor suggests that B cells must travel between each zone before undergoing either proliferation or selection. Original observations suggested GC B cells first start in the DZ, move to the LZ, and then are either selected to become effector B cells or undergo apoptosis [7, 64]. However, this model does not account for the increase in affinity of antigen-specific antibodies observed in the serum nor the evolution of the DNA sequences obtained from B cell clones within the GC [65-67]. In contrast, three independent groups were able to observe that B cells shuttle and recycle between each zone [61, 62, 68]. Building on these studies one group observed that while nearly 50% of the B cells in the DZ moved to the LZ, only 10% moved from the LZ to DZ indicating only a relatively small number of cells are selected to continue participating in the GC [22]. Movement between the two zones appeared to be dependent on the surface expression of the chemokine receptor CXCR4. GC B cells that upregulate CXCR4 are thought to move to its ligand CXCL12, secreted by a resident reticular cell within the DZ [49, 50, 61, 69]. These observations provide strong evidence that antigen specific B cells within the GC are not restricted to one zone nor

do they progress in a linear fashion but instead undergo recycling following certain selective cues.

The division of labor within the GC and interzonal migration appears to play an important role in proper humoral responses. While migration to the DZ is not required for the biological events that occur within that region, fewer mutations accumulate and thus proper SHM is not maintained in CXCR4-deficient GC B cells [69]. FOXO1 appears to be a critical transcription factor that promotes the 'DZ B cell transcriptional program'. B cells that FOXO1 can still form GCs but there is no apparent polarization of the GC. SHM still occurs, but the proper selection of high affinity clones is not maintained [51, 52]. These data suggest that selection and proliferation might be segregated to maintain development of high affinity B cell clones.

*Model of selection and cell fate decisions*

Within an individual GC, B cell clones compete both inter- and intra-clonally for limited resources. A critical factor for selection is the relative affinity of each clone for antigen within the same GC [21, 67, 70, 71]. Within the GC, competition for limited amounts of resources could be derived from two sources: antigen or Tfh help. In the antigen driven scenario, B cells would compete solely for antigen found on the FDCs. Higher affinity B cells would acquire more antigen through their BCR than lower affinity cells, have stronger BCR-mediated signaling, and go on to proliferate following the acquisition of T cell help. However, BCR signaling may be partially repressed in GC compared to naive B cells [72]. Additionally, this model would also suggest that the amount of T cell help is not limiting. Alternatively, Tfh help could represent the limiting resource in the GC. GC B cells would still compete for antigen from FDCs but the BCR would primarily mediate internalization of antigen. Higher affinity B cells would acquire, process, and finally load more antigen onto surface MHC than lower affinity cells. T cells would then provide stronger survival and differential cues to B cells that express the highest amount of peptide-MHC. Consistent with that the second model, increased T cell numbers can increase the size of the GC [16, 73] and T cells are the limiting factor for a variety of vaccine development efforts [74, 75]. Additionally, evidence for T cell mediated

selection has been provided using antigen targeted to GC B cells in a BCR-independent manner [21, 22, 76, 77]. In these experiments, GC B cells that presented more antigen for T cells outcompeted those that presented less antigen to Th cells [76, 77]. Together these findings strongly suggest that T cell help may be the limiting in GC B cell selection. However, whether BCR engagement may also contribute to GC selection in a BCR signaling-dependent fashion is unclear.

*Selection into the plasma cell fate*

In addition to being selected to continue developing within the GC, B cells may also be selected to differentiate into plasma cells that then persist for long periods of time in the bone marrow or the gut and secrete high affinity antibodies. The differentiation into LLPCs seems to depend strongly on the affinity of the B cell as plasma cells harvested from the bone marrow are all high affinity [78]. Like the models proposed above for selection, it is not entirely understood whether high amounts of BCR cross-linking in addition to T cell help contributes to the recruitment of high affinity GC B cells into the plasma cell compartment. However, strong evidence suggests that Tfh cells play a fundamental role in driving PC generation from GC B cells.

*Selection into memory B cells*

In contrast to plasma cells, GC B cells that differentiate into memory B cells do not seem to have an obvious distinguishing characteristic. The default pathway of GC B cells is to undergo apoptosis which they can be rescued from by successfully competing for limited amounts of survival signals [10]. While high affinity cells are either selected to become plasma cells or re-enter into the DZ following selection, moderate to low affinity clones are thought to either die or receive adequate signals to overcome apoptosis. Memory B cells may derive from populations of cells that receive ‘just enough’ signals to overcome apoptosis. Indeed, blocking apoptosis enhances memory B cell formation [79]. Disruption of the ability to receive T cell help through CD40 does not have an effect on memory cell formation after GCs are formed [80]. Indeed, GC-derived memory B cells’ development inversely correlates with the ability to receive T cell help [59]. Additionally, in experimental conditions where proper affinity maturation of a select GC

B cell population is disrupted, the generation of memory B cells is increased [69]. Confounding the study of memory B cells derived from the GC is that no reliable markers can differentiate them from memory B cells that arise prior to the GC [80]. Together, the decision to choose memory cell fate over apoptosis or reentry into the GC remains poorly understood but may be the default pathway for GC B cells that do not receive enough positive signals to either renter the DZ or differentiate into plasma cells.

## Follicular helper T cells

*Differentiation of Tfh cells*

The current paradigm of T cell differentiation suggests that specific transcription factors, or so called 'master transcription factors,' orchestrate the unique transcriptional profiles observed in each effector T cell lineage. Through observations of $CXCR5^+$ T cells, multiple groups in 2009 identified that Bcl6, a powerful transcriptional repressor, was required for the development of T follicular helper cells [39, 81, 82]. Bcl6 directly represses the transcription factor Blimp1, which is high in other T cell lineages but is detrimental to the development of Tfh cells. By binding to the enhancer and promoter regions of various genes, Bcl6 drives expression of CXCR5 and multiple other factors that determine unique characteristics of Tfh cells. Forced expression of Bcl6 is sufficient to promote development of Tfh-like phenotype in $CD4^+$ T cells [39].

The stable expression of Bcl6 in T cells appears to depend on three signals. First, T cells undergoing priming by dendritic cells must receive strong T cell receptor signaling and CD28 stimulation that promotes the initial expression of Bcl6 [83, 84]. Secondly, T cells must receive IL-6 and IL-21 STAT1- and, to a lesser extent, STAT3- dependent signaling for continued expression of Bcl6 [85]. And finally, presentation of ICOSL on antigen-presenting cells and its recognition by ICOS on T cells is responsible for stabilization of Bcl6 expression, expression of CXCR5, and inhibition of Blimp1 [39, 86, 87]. Intimate contact between differentiating T cells and APCs mediated by the SLAM-associated protein, SAP, is also required [36].

*Suggested three stages of Tfh cell development*

Development of primed T cells into Tfh cells is a multistep process that can be arbitrarily divided into Pre-Tfh, Follicular Tfh and GC Tfh stages based on their anatomical location and expression levels of Bcl6, PD1 and CXCR5. Pre-Tfh cells express moderate levels of Bcl6, CXCR5, and high levels of EBI2 and can be visualized along the T-B border and interfollicular areas of SLO [33, 88-90]. While $Bcl6^{pos}$ antigen-specific Th cells may be detected by FACS as early as 24 hours after immunization [33, 85, 88], arrival of pre-Tfh cells at the T-B border often isn't observed until 2-3 days following immunization [31, 33]. Follicular Tfh cells typically have higher expression levels CXCR5, PD-1 and ICOS compared to pre-Tfh cells, have decreased expression of CCR7 and EBI2, and can be found in the follicles at 2-4 days following immunization [33]. Of note, in addition to the developing Tfh cells that are migrating towards GCs in primary responses, memory Tfh cells also have a $CXCR5^{int}$ $PD\text{-}1^{int}$ surface staining phenotype [91]. Tfh cells that enter GCs express the highest amounts of Bcl6, CXCR5 and PD-1 [89]. They begin seeding the GCs along with GC B cells around 3-5 days following immunization [33]. GC Tfh cells express S1PR2 receptor, which helps retain them within sphingosine -1-phosphate-low GCs in the primary immune responses [91, 92]. Interestingly, in secondary responses, GC Tfh cells confinement within a single GCs is reduced and they can migrate between different GC-containing follicles [91, 93].

Within GCs Tfh cells appear to undergo further development. Early on, GC Tfh cells predominately express IL-21 and can be found proximal to GC B cells that are mutating. As the response progresses, GC Tfh upregulate CD40L and production of IL-4 (and IFN-γ), decrease production of IL-21, and can be found more associated with GC B cells within the light zone [94-96]. These GC Tfh cells have functional differences in that $IL\text{-}21^{+}$ GC Tfh cells support affinity maturation while $IL\text{-}4^{+}$ GC Tfh are more tuned to induce class switching and plasma cell generation [95].

*Tfh cell derived signals important for selection of high-affinity GC B cells and generation of memory and plasma cells*

The signals which are provided by Tfh to GC B cells predominantly include the cytokines IL-21, IL-4, IFNγ and surface receptors such as CD40L. These signals are important for survival, class-switching, continued affinity maturation and differentiation of GC B cells. Within the GCs, IL-21 reinforces expression of Bcl6 and is required for optimal affinity maturation [95, 97]. IL-4 promotes GC B cell proliferation, survival [98, 99], and the generation of plasma cells [95]. IL-4 and IFNγ also promote GC B cell class-switching to IgG1 and IgG2a and IgG3 isotypes, respectively [100, 101]. CD40L-induced signaling has a critical role in maintaining GC responses and is required to support GC B cell survival [102], affinity maturation [100], and formation of memory and plasma cells [103, 104]. Strong CD40 signaling in B cells blocks Bcl6 expression and induces Blimp1 [19, 105-107]. Interestingly, rapid delivery of preformed CD40L molecules to the Tfh cell surface is dependent on the extensive GC B cell-Tfh cell contacts and ICOS signaling [108]. It is during these interactions when GC B cells are thought to integrate all Tfh cell-derived signals that ultimately dictate GC B cell fate.

*Tfh cell contacts with B cells within GCs*

GC B cell selection and differentiation depends on their direct interactions with cognate Tfh cells. Productive interactions between B and T cells require over 5 minutes of contact time to ‘scan’ presented pMHCII/peptides, generate an immunological synapse and directionally release cytokines to the target cell [109-112]. Therefore, prolonged cognate interactions between GC B cells and Tfh cells are thought to be important for selection and differentiation of GC B cells, as well as maintenance of GC Tfh cells [35, 36, 113].

While prolonged interactions between cognate B and T cells at the B/T border are common, the dynamics of GC B cells and Tfh cell interactions is very different. GC Tfh make many short contacts with few lasting longer than 5 minutes [61]. It is believed that GC Tfh cells are constantly scanning GC B cells looking for where activating signals are the highest relative to other B cells within their immediate vicinity [61, 108, 114]. While

serial, short interactions with cognate GC B cells may be important for the *de novo* synthesis of GC Tfh-derived, pro-GC B cell molecules or for delivery of pre-formed molecules [108, 115, 116] or for the maintenance of the GC Tfh phenotype [33, 87, 115], long duration interactions are capable of inducing a feed-forward loop that strongly promotes T cell polarization towards the B cell, delivery of cytokines, and the reorganization of co-stimulatory and B cell survival and differentiation molecules [108, 110-112, 114, 117]. In this model, the amount of antigen to which B cells can display for T cell help would directly influence whether a long or short duration interaction would occur and directly affect GC B cell fate.

*Control of Tfh cells numbers and specificity of the GC response*

Tfh cells play a critical role in selecting and tuning B cells that participate in the humoral immune response. Early models proposed that the processes that occurred within GCs (affinity maturation, clonal diversification, and selection) were controlled by resident GC T cells and that they were the limiting factor within the GC [7]. These models predicted that by increasing the amount of help available to B cells, lower affinity clones or clones not specific towards the challenging antigen could receive enough T cell help to persist within the GC or differentiate into memory or plasma cells.

Consistent with this model, excessive formation of Tfh cells has been shown to lead to the generation of spontaneous GCs, production of autoantibodies and development of autoimmunity as in the case of the *sanroque* mouse model [16, 118]. The *sanroque* mutation affects the RNA-binding protein Roquin, a protein that promotes degradation of multiple mRNAs including that of *Icos* and IFNγ [119]. *Sanroque* mice express higher levels of ICOS and IFNγ ultimately leading to increased Tfh generation, dysregulated GC responses and development of autoimmunity [15, 16, 119]. Other mouse models of autoimmunity also show increased formation of Tfh such as the BXSB-Yaa and MPL/*Fas*$^{lpr}$ model [31, 120]. In humans, several reports have found that circulating CXCR5$^{+}$ CD4$^{+}$ T cells are significantly elevated in patients with autoimmune diseases such as systemic lupus erythematosus, Grave's disease, and rheumatoid arthritis [121-123]. While other factors may contribute to the development of autoimmune diseases,

increased numbers of Tfh cells and/or their activity correlate closely with disease. Thus, control over Tfh numbers and/or their specificity is believed to be important in preventing autoimmune responses.

**Follicular regulatory T cells**

It has been recognized for some time that in addition to Tfh and GC B cells, Tregs are also present within B cell follicles and GCs [124, 125]. However, whether these follicular Tregs were different from conventional Tregs and how they contributed towards protection against autoimmunity, particularly to antibody-based autoimmune diseases, was unknown. Recent work has begun to elucidate the role of Tfr cells in B cell responses.

*Differentiation of Tfr*

Tregs are known to co-opt similar transcription factor networks as non-regulatory $CD4^+$ effector cells [126]. Like Tfh cells, the differentiation of Tfr cells from Tregs depend on Bcl6 which, along with NFAT2, upregulates CXCR5 and enables them to enter the follicles [127-131]. However, unlike Tfh cells, the effector function of Tregs depends on the expression of Blimp1 and Tfr cells paradoxically express both Bcl6 and Blimp1 [127, 132]. Finally, Tfr cells express the T regulatory master transcription factor Foxp3 [127-129, 133].

The differentiation of Tfr cells occurs in response to a wide range of antigen and immunizing conditions [127, 129, 134, 135] and is dependent on DCs [134]. High levels of TCR signaling can induce the expansion or differentiation of Tfr cells since in mice that lack inhibitory PTEN, Tfr numbers are increased [136]. This would suggest that Tregs see cognate antigen being presented by APCs and/or B cells. Consistent with that, Tfr cells are more clonal a population than Tregs [137]. Tfr cells do not develop in mice that lack B cells, which could indicate that they depend on B cell interactions for full differentiation [138]. Like Tfh cells, Tfr cells depend on the molecules CD28, ICOS, and SAP for their differentiation. CD28 appears to play a critical role in proliferation and differentiation of Tfr cells [127, 134, 139]. ICOS-deficient mice are defective in their

development of Tfr cells. Finally, SAP appears critical in their differentiation since SAP-deficient Tregs do not generate Tfr cells [127].

The kinetics of Tfr differentiation is like that of Tfh helpers although with some key differences. While Tfr cells can always be detected within the follicles, and at a much higher frequency than Tfh cells, they are more prevalent following immunization. While initially thought to parallel Tfh cell differentiation, albeit at a reduced frequency, and then slowly decline as the GC wanes [127], our recent work has detailed their kinetics more closely [96]. Tfr appear to initially undergo a burst of differentiation prior to the establishment of a GC and prior to the appearance of Tfh cells. This is then followed by either a small decline or leveling of Tfr cells at the peak of the GC response and then a maintenance during the collapse of the GC.

Although Tfr cells express Foxp3 [127-129, 137], $Foxp3^+$ $CD4^+$ cells can either be derived from the thymus or induced in the periphery. Thymically-derived Tregs, or natural Tregs, have specificity to self-proteins while those induced in the periphery typically are specific to foreign antigen [140]. Most work has shown that Tfr cells express markers of thymically-derived Tregs and are not specific to foreign antigen [127, 128, 132]. However, one publication has found that under exceptional immunization conditions, Tfr cells can be induced from non-Foxp3-expressing cells that are specific towards foreign antigen. However, these foreign antigen-specific Tfr cells only represent a small fraction of the total Tfr population. Interestingly, Tfr cells' TCR usage also indicates that they do not undergo a polyclonal expansion to the same extent that Tfh cells do, suggesting that there is no dominant antigen to which Tfr cells are responding against [137]. Whether specific clones always arise or are dependent on the type of antigen, adjuvant, or site of immunization has not been addressed.

Because Tfr cells can suppress the humoral immune response, their own development must be controlled as to allow normal, antigen-specific responses to generate high affinity, high titer antibodies. Two molecules that limit the differentiation of Tfr cells are PD-1 and CTLA-4. PD-1 expression by Tregs has been shown to limit the expansion or

differentiation of Tfr cells following immunization [134]. PD-1 blocks Tfr cell differentiation by interacting with PD-L1, but not PD-L2, on antigen presenting cells (APCs). However, whether PD-1 and PD-L1 are responsible for curtailing initial Tfr cell differentiation by DCs or inhibiting their full differentiation or maintenance is not known. CTLA-4 is an inhibitory receptor that binds to CD80 and CD86 and attenuates immune responses by competing with CD28 [17]. While Tfr cells use CTLA-4 as an effector molecule (as discussed below), their differentiation is also limited by its expression. CTLA-4 deletion in Treg cells enhances the generation of Tfr cells following immunization [141, 142]. This may be because of enhanced expression of pro-Tfr cell signals and the increase in expression of ICOS on Tregs when CTLA-4 is deleted [142].

*Functions of Tfr cells*

The function of Tfr cells in suppressing the T dependent humoral immune response was initially shown to affect a multitude of factors including the numbers of Tfh and GC B cells, antigen-specific antibody production, and differentiation of plasma cells [127-129, 134, 138]. Furthermore, they appear to affect the appearance of certain isotypes of antibody, notably IgE and IgA [141, 142]. Studies that looked for autoantibody production found that in a pristine-induced model of autoimmunity, they could control the development of pathogenic anti-dsDNA antibodies [131].

*Tfr cellular and molecular mechanisms of action*

T regulatory cells have a myriad of cellular targets including antigen presenting cells and effector T cells [142-144]. The ability to target both types of cells lends to their ability to effectively shut down immune responses. However, since the GC is highly interdependent on continued cross-talk between GC B cells and GC Tfh cells for its maintenance and maturation, determining specifically what and how Tfr cells exert control *in vivo* is complicated. It has been suggested that Tfr cells can control either Tfh cell numbers, the cytokines Tfh cells secrete, or directly repress GC B cells [127, 131, 143].

Tfr cells may exert control directly on GC Tfh cells. Evidence for this largely comes from *ex vivo* experiments that showed Tfr cells could suppress T cell proliferation, differentiation, and diminish T cell help to B cells [127, 134, 138, 141, 142]. *In vivo*, early work suggested that depletion of Tregs, once GCs were established (8 days post immunization), lead to an increase in Tfh cells but not GC B cells [127]. However, when Tfr were specifically depleted, both Tfh and GC B cell numbers increased significantly [127]. This may be explained because total Treg depletion might favor increased generation of Tfh cells that support non-antigen specific GC B cells and thus, even though there are increased numbers of Tfh cells, they cannot properly support the foreign antigen-specific GC population. In contrast, when Tfr cells are depleted, the brakes are taken off antigen-specific Tfh cells that can provide enhanced, cognate help to GC B cells.

Tfr cells may also directly influence cytokine secretion by Tfh cells. *In vitro* analysis with co-cultures of B cells and Tfh cells found that Tfr could suppress IFN$\gamma$, IL-10, IL-21, and TNF-$\alpha$ in Tfh cells [138]. The suppression of IFN$\gamma$, IL-10 and IL-21 was further confirmed using an *in vivo* system for the deletion of Tfr cells [131]. That IL-10 and IL-21 are increased following the removal of Tfr cells in Tfh cells is not too surprising given that both cytokines have roles that affect B cell survival, proliferation, differentiation, and affect selection and isotype switching [95, 97, 145, 146]. The increase in these cytokines may in part explain why GCs and plasma cell numbers are increased and the affinity, amount and type of antibody being produced would change.

Tfr cells may also act to deprive GC B cells of Tfh-derived signals. For instance, PD-1 signaling in Tfh cells results in IL-4 and IL-21 production [20]. However, it is also found on Tfr cells and could compete with Tfh cells for PD-L1 ligands on GC B cells. Paradoxically, PD-1-deficeint Tfr cells are *more* suppressive both *ex vivo* and *in vivo* which could be explained by the possibility of enhanced TCR activation signals in Tfr cells [134, 147]. Tfr cell CTLA-4 may also potentially interfere with Tfh - B cells communication by downregulating or competing for CD80/86 on B cells [141, 142].

Finally, Tfr may also act directly on GC B cells. *Ex vivo*, B cells cultured with Tfr cells and then subsequently activated do not proliferate or differentiate as much as unsuppressed B cells. The suppressed B cells showed significant differences in their metabolic pathways such as glycolysis suggesting that Tfr can act directly on B cells [143]. However, whether direct inhibition of GC B cells by Tfr cells occurs *in vivo* is not known. It is also unclear which factors may promote this inhibition and whether it depends on cognate recognition of self-antigens presented by GC B cells.

**Control of B and $CD8^+$ T cell response by proinflammatory chemokines**

Previous studies suggested that proinflammatory chemokines may play a role in regulating T-dependent B cell responses through regulatory T cells. They have also been shown to influence $CD8^+$ T cell response. In the section below, I will detail when B cells express proinflammatory cytokines, implicate that undifferentiated Tregs respond to these cytokines, and discuss some of the known roles that these cytokines have been shown to play in regulating T cell and APC interactions.

*Production of CCL3/4 by activated murine and human B cell subsets*

Chemokines are important factors that mediate the immune response through processes such as chemotaxis, inflammation, and development. B cells activated directly through their BCR can upregulate the production of several chemokines [148]. Notably, the proinflammatory cytokines CCL3 and CCL4 (MIP1-α and MIP1-β, respectively) are upregulated in both mouse and human B cells following antigen receptor cross-linking [148, 149]. Strong BCR crosslinking in human GC B cells also results in upregulated production of CCL3/4 *in vitro* [149]. Freshly isolated GC B cells contain gene signatures that are enriched for genes downstream of BCR signaling suggesting that GC B cells may also upregulate CCL3 and CCL4 [22]. Indeed, analysis of microarrays of either LZ or DZ GC B cells reveals that LZ GC B cells are relatively enriched for CCL3 and CCL4 transcripts [150, 151].

*Chemokine receptors that can respond to CCL3 and CCL4*

Chemokines exert their pleiotropic effects through their binding of G-protein coupled receptors. CCL3 binds to the chemokine receptors CCR1 and CCR5 while CCL4 binds to CCR5 [152]. Binding of CCL3 or CCL4 to either CCR1 or CCR5 induces a signaling cascade that induces the reorganization of actin and facilitates formation of lamellipodia [153]. In this way, CCL3 and CCL4 can promote CCR5-mediated chemotaxis and/or probing behavior. Rapid sensitization to these chemokines often occurs through the endocytosis of receptors [154].

In addition to the known chemotactic receptors CCR1 and CCR5, both CCL3 and CCL4 can bind to the chemokine scavenging receptor D6 [155]. D6 is a decoy receptor that acts as a chemokine sink since it has no known chemotaxis or signaling properties.

*Tregs can respond to CCL4 ex vivo and regulates GC responses in vivo.*

CCL4 was identified in 2001 as being able to exert control over the humoral immune response [148]. *Ex vivo*, $CD25^+$ $CD4^+$ T cells were found to migrate to activated B cell supernatant, as well as purified CCL4, but not CCL3 chemokine and could suppress B cell blasting [148]. Neutralization of CCL4 in unimmunized mice induced spontaneous formation of GCs. Moreover, it induced rapid generation of antinuclear antibodies [148]. Based on that study, it was hypothesized that CCL4 may be important for maintenance of B cell tolerance through attraction of Tregs to the activated B cells. However, this hypothesis has not been further tested or verified by intravital imaging.

*CCL3/4 and CCR5 in controlling T cell – APC interactions.*

In contrast to the mechanism of CCL3 or CCL4 action in T-B cell interactions, the role that these chemokines play in antigen priming of T cells by DCs is more understood. Similarly to activated B cells, activated DCs can secrete CCL3 and CCL4 after provision of help from antigen specific CD4 T cells. Under very specific conditions, immunization induces CCR5 expression in $CD8^+$ T cells prior to antigen recognition [156]. Intravital imaging suggested that CCL3 and CCL4 promote chemokinesis of $CD8^+$ T cells to DCs that enables more efficient scanning of the cells providing the “find me” signal.

Additionally, APC-derived CCL3 and CCL4 and T cell CCR5 may promote enhanced synapse formation, polarization in T cells, and activation [157, 158]. Thus, CCL3 and CCL4 may play various roles in promoting efficient interactions between T cells and APCs *in vivo* and enable complete activation of $CD8^+$ T cells.

*Treg control of Th cell dynamics and responses in vivo*

Given that CCL3 and CCL4 play an important role in locating cells to sites of ongoing priming and contributes to synapse formation, and therefore activation, it stands to be reasoned that specific control of these chemokines can affect the outcome of the immune response. Early imaging studies of Tregs and Th cells found that Tregs could limit the time self-reactive T cells spent in contact with antigen presenting cells [159, 160]. Importantly, based on the imaging of Tregs or Th cells and APCs it was suggested that Tregs could act directly on APCs [160]. Tregs engaged with APCs may influence many processes. One specific pathway that Tregs seem to influence in APCs is the production of CCL3 and CCL4 [161-163]. Loss of control of CCL3 and CCL4 (and CCL5) in APCs by Tregs leads to increased $CD8^+$ T cell and DC interactions and results in a marked decrease in the avidity of the immune response [163].

**Scope of dissertation**

In the past decade, significant work has been made towards understanding the regulation of T-dependent humoral responses. These works have highlighted the roles of both Tfh cells and Tfr cells in promoting and controlling GC B cells and their selection. Progress has been made in understanding the development, physiological effects, and molecular mechanisms that both Tfh and Tfr cells utilize for their control of the humoral immune response [127, 129, 131, 134, 135, 137, 138, 141-143, 164]. Considering these developments, several new and exciting questions related to the control of the humoral immune response remain to be answered.

*Can follicular T cells respond to CCL3/4 chemokines secreted by GC B cells and modify T-dependent responses?*

Since the initial implication that proinflammatory chemokines produced by B cells could control their responses through suppressive T cells, our understanding of the cells and molecules that govern the humoral responses has grown considerably. However, no study has further sought to characterize specifically the role of proinflammatory chemokines in the humoral response nor examine if CCL3/4 cytokines produced by GC B cells influence the dynamics of their interactions with either T follicular regulatory or T follicular helper cells. One of the main focuses of my thesis work has addressed whether CCL3 chemokine promotes T follicular regulatory cells response and influences the T-dependent immune response.

*Do changes in follicular T cells influence the recruitment of new B cells into ongoing GC responses?*

Follicular T cells have clearly been demonstrated to play a role in permitting entry and participation of B cells within the GC [21, 22, 77]. It has been shown that GCs can be seeded by 50-200 total B cell clones [67, 165]. Newly arriving and recently activated B cells can enter pre-existing GCs, provided they can effectively compete against other GC B cells for Tfh cell help [21, 70]. The quality of help provided by Tfh cells changes throughout the course of the GC as does the quantity of Tfh and Tfr cells [95, 96]. However, whether changes in quality and quantity of follicular T cells associated with the phase of the GC (i.e. early, peak, contraction) influences the recruitment of recently activated B cells has not been addressed. My thesis work, in part, has been to address how the temporal changes in follicular T cells can regulate B cell responses.

Understanding Tfr cells' effect on B cell participation both into and within the GC furthers our knowledge on mechanisms that shape vaccine responses and prevent autoimmune diseases. My thesis work has provided new insights into Tfr mediated control of the T-dependent humoral response.

# Chapter 2 - CCL3 production by germinal center B cells promotes their direct sampling by follicular regulatory T cells and control


## Abstract

Previous studies and our findings suggest upregulated expression of proinflammatory chemokines CCL3/4 in GC centrocytes. However, the role of CCL3/4 for centrocyte interactions with follicular T cells and regulation of humoral immunity is poorly understood. We found that B cell intrinsic production of CCL3 is required for control of GC B cell expansion and is important for restricted development of class-switched anti-nuclear antibodies. We also determined that follicular regulatory T cells (Tfr) respond to CCL3 chemokine *ex vivo* and interact more frequently with WT compared to CCL3-deficient GC B cells *in vivo* in a CCR5 receptor-dependent fashion. Our findings suggest that CCL3 secreted by B cells promotes their direct interactions and control by Tfr cells and plays a role in the elimination of potentially self-reactive B cell clones.


## Introduction

A hallmark of adaptive humoral immunity is the germinal center (GC) reaction. GCs are the primary site of antigen-dependent clonal expansion, immunoglobulin diversification, and affinity maturation. This set of coordinated processes ultimately leads to the generation of memory cells and long-lived plasma cells that secrete high-affinity antibodies and is dependent on follicular T cells [10]. Despite the wealth of studies dissecting the chemotactic cues that organize GCs [28, 166, 167], it is unclear whether additional factors enable efficient sampling of GC B cells by follicular T cells.

CCL3 and CCL4 (MIP1-$\alpha$ and MIP1-$\beta$) are proinflammatory chemokines that are secreted by various types of immune cells upon activation and play important roles in inflammatory responses and multiple other processes [168, 169]. In B cell cultures with naïve, memory or GC B cells, the cross-linking of B cell receptors (BCRs) upregulates expression and secretion of CCL3/4 [148, 149]. In addition, analysis of published GC microarray data suggests that expression of CCL3/4 may be elevated in GC centrocytes compared to centroblasts [60, 150, 151]. Despite multiple indications that CCL3/4 is secreted by activated and GC B cells, the significance of B-cell intrinsic production of proinflammatory chemokines for regulation of humoral response is unclear.

In 2001 Bystry et al. demonstrated that treatment of unimmunized mice with anti-CCL4 antibodies (Abs) leads to rapid development of GCs and generation of autoantibodies, mirroring the effects observed in mice deficient or depleted of regulatory T cells (Tregs) [170]. In addition, the study showed that a subset of splenic CD4 T cells that were $CD25^{high}$, expressed high levels of TGF-β and CTLA-4, and had a suppressive phenotype *ex vivo,* can migrate to CCL4 (but not CCL3) in transwell assays. The observed transmigration of suppressive T cells was attributed to CCR5, the primary G-protein coupled receptor for CCL3 and CCL4 [148]. The above observations raised the possibility that CCL4 may promote Tregs' interactions with activated B cells or dendritic cells (that also produce CCL3/4) to regulate B cell responses. However, whether more recently identified subsets of follicular resident Tregs can respond to CCL3 or CCL4 has been unclear [125, 127, 129, 171].

Follicular regulatory T cells (Tfr) are a subset of $FoxP3^{pos}$ Tregs that play a role in the control of GC responses. While majority of Tfr cells arise from natural Tregs, some can be induced from foreign antigen-specific Th cells [135]. Similarly to follicular helper T cells (Tfh), Tfr cells develop in the secondary lymphoid organs following foreign antigen challenge, express the transcription factor Bcl6, upregulate surface expression of CXCR5, PD1 and Icos receptors, and localize to the follicles and the GCs [127-129]. However, while Tfh cells are required for the support of GC responses, Tfr cells negatively control GCs. In some studies, deficiency in Tfr cells has been reported to

induce a 1.5 to 2-fold increase in GC size and/or lead to a modest increase in foreign antigen-specific antibody response [127-129]. Other studies suggested that Tfr deficiency affects Tfh cell class-switching [131, 134, 142] increases recruitment of non-foreign antigen-specific B cell clones into GCs [127, 131] and development of self-reactive antibodies [131]. While multiple mechanisms of Tfr cells action have been suggested based on the *in vivo* and *ex vivo* studies [125, 134, 141-143, 170]. Whether *in vivo* Tfr cells only regulate Tfh cells and thus indirectly control GC responses or can also act on the GC B cells directly remains an open-ended question.

Here we investigated the role of B cell-intrinsic production of CCL3 in the regulation of GC responses. Based on the 2-photon imaging of murine lymph nodes we found that production of CCL3 by GC B cells promotes their efficient sampling by Tfr cells in a CCR5 receptor-dependent fashion. Consistent with an important role of CCL3 in mediating GC-Tfr cells interactions, we found that immunized CCL3 deficient mice developed about 1.5-fold increase in GC responses compared to WT mice. Our data also suggests that B cell deficiency in CCL3 can lead to decreased control over anti-nuclear B cell clones. Based on these data we suggest that CCL3 secretion by B cells is required for direct Tfr cell-mediated control of both foreign antigen-specific GC B cells as well as potentially self-reactive B cell clones.

**Materials and methods**

*Mice, immunizations, and bone marrow chimeras.* C57BL/6 (B6, WT) mice were purchased from the National Cancer Institute, Charles River or Jackson Laboratories. B6-CD45.1 (002014), CCL3-KO (002676), CCR5-KO (005427), β-actin-CFP (004218), UBC-GFP (004353), Stop-tdTomato (0079009) and E2a-Cre (003724) mice were from Jackson Laboratories. HyHEL10 [61], MD4 [172], OTII [173], Foxp3$^{EGFP}$, and Foxp3$^{DTR}$ mice were from internal colonies. All mice were housed in specific-pathogen free conditions. Relevant mice were interbred to obtain HyHEL10 CFP$^{+}$, HyHEL10 GFP$^{+}$ CCL3-KO, OTII GFP$^{+}$, OTII tdTomato$^{+}$, MD4 CFP$^{+}$, tdTomato$^{+}$ Foxp3$^{EGFP}$ and tdTomato$^{+}$ Foxp3$^{EGFP}$ CCR5-KO mice. 6-12 weeks old mice were immunized either s.c.

or i.p. with the protein antigens OVA (Sigma), DEL-OVA (produced as previously described [61]), or NP-KLH (Biosearch Technologies), mixed in either Ribi (Sigma) or Complete Freund Adjuvant (CFA, Sigma). [WT/WT → WT] and [CCL3/WT → WT] mixed bone marrow chimeras were generated by reconstitution of irradiated with a single dose of 960 rads B6 mice with 50:50% bone marrow cells from B6:B6-CD45.1 or CCL3-KO:B6-CD45.1 mice. Chimeric mice were s.c. immunized with OVA in CFA at 8-10 weeks after the BM reconstitution. All experiments were performed in compliance with federal laws and institutional guidelines as approved by the University Committee on Use and Care of Animals.

*Cell isolation, flow cytometry analysis and cell sorting.* Lymphocytes were isolated by homogenizing lymph nodes (LNs) and/or spleens into a single cell suspension in DMEM medium (Corning) containing 2% fetal bovine serum (FBS, Atlanta Biologicals), antibiotics (50 IU/mL of penicillin and 50 µg/mL of streptomycin; Gibco) and 10 mM HEPES (Gibco) and straining through a 70 µm mesh filter (Falcon) in the presence of 20 µg/ml of DNase I (Sigma-Aldrich). Red blood cells were lysed using Tris-buffered $NH_4Cl$. The following antibodies and reagents were used for flow cytometry analysis: CD3 (BD, 145-2C11), CD4 (BD, RM4-5), CD8 (BD, 53-6.7), CD25 (BD, PC61.5), B220 (BD, RA3-6B2), CD19 (BD, 1D3), CXCR5 (BD, 2G8), Fas (BD, Jo2), IgM (BD, R6-60.2), $IgM^a$ (BD, DS-1), Vβ5 (Biolegend, 6D5), CD45.1 (Biolegend, A20), CD45.2 (Biolegend, 104), IgD (Biolegend, 11-26c.2a), PD-1 (Biolegend, RMP1-30), CXCR4 (eBiosciences, 2B11), CD86 (Biolegend, GL1), Foxp3 (eBiosciences, FJK-16s), GL-7 (eBiosciences, GL-7), SA-qDot607 (Life Technologies), SA-DyLight 488 (Biolegend). Single-cell suspensions were incubated with biotinylated antibodies for 20 minutes on ice, washed twice with 200 µl OBS supplemented with 2% FBS, 1 mM EDTA, and 0.1% $NaN_3$ (FACS buffer), and then incubated with fluorophore-conjugated antibodies and streptavidin for 20 minutes on ice, and washed twice more with 200 µl FACS buffer. For Foxp3 staining, the cells were permeabilized and stained using Foxp3 staining buffer (eBioscience) according to the manufactures instructions. Cells were then resuspended in FACS buffer for acquisition. Lymphocyte apoptosis analysis was measured with AnnexinV-FITC Apoptosis Detection Kit (Affymetrix) according to the manufacturers protocol. All

flow cytometry analyses and cell-sorting procedures were done using FACSCanto II and FACSAria IIIu, respectively. FlowJo Software (v 9.7, TreeStar) was used for data analyses and plot rendering.

*Cell purification and adoptive transfers.* For adoptive transfers, cells were isolated from combined spleens and LNs of donor mice and CD4 T cells or B cells were enriched using autoMACS (Miltenyi Biotec) as described before [61]. The purity of B cells was >95%, and CD4 T cells >70% for all experiments. Lymphocytes were adoptively transferred by intravenous injection into the lateral tail vein.

*Generation of mice with Tregs and Tfr cells expressing tdTomato.* In order to generate mice with fluorescent Tregs the following scheme was utilized: first, tdTomato expressing mice were crossed with $Foxp3^{EGFP}$ mice. $tdTomato^{+}$ $Foxp3^{EGFP}$ mice were also crossed to CCR5-KO mice. Second, $tdTomato^{+}Foxp3^{EGFP}$ or $tdTomato^{+}$ $Foxp3^{EGFP}$ $CCR5^{-/-}$ Tregs were sorted and adoptively transferred into $Foxp3^{DTR}$ mice where endogenous Tregs were transiently ablated by DTx treatment (Sigma). To sort tdTomato expressing Tregs, the LNs and spleens from the $tdTomato^{+}Foxp3^{EGFP}$ or $tdTomato^{+}$ $Foxp3^{EGFP}$ CCR5-KO mice were combined and lymphocyte suspension was prepared as described above. The lymphocytes were separated from RBCs using Ficoll-Paque (GE Healthcare) gradients per manufacturer's instructions using 14 mL round bottom tubes (Falcon). Single cell suspensions were enriched for CD4+ T cells as described above. Following the enrichment, $EGFP^{+}$ cells were sorted into DMEM medium supplemented with 10% FCS. The purity of sorted Tregs as determined by intracellular Foxp3 staining was > 99%. About 0.8-1.5 million of purified $tdTomato^{+}$ Tregs were then transferred into recipient $Foxp3^{DTR}$ mice via tail vein injection. Finally, one day later the endogenous nonfluorescent Tregs in the recipient $Foxp3^{DTR}$ mice were ablated by intraperitoneal injection of 5 µg/kg of DTx in PBS. The DTx treatment was repeated once more a week later.

*Cell culture and chemotaxis.* Transwells with 5 µm pore size (Corning) were used. CD4 T cells were isolated and enriched as described above from draining peripheral LNs of

mice s.c. immunized with OVA in Ribi at 10 days following immunization. T cells were resuspended with RPMI 1640 (Corning) supplemented with 2% fatty acid free BSA (Sigma-Aldrich), 10 mM HEPES, 50 IU/mL of penicillin, and 50 mg/mL of streptomycin (HyClone). For chemotaxis analysis, the lower chambers of transwells were filled with the same medium mixed with various concentrations of CCL3 or CCL4 chemokines (PeproTech). For chemokinesis analysis both upper and lower chambers of transwells were filled with either 200 ng/mL of CCL3 or with 400 ng/mL CCL4. Transwells with chemokines and resuspended CD4 T cells were incubated at 37ºC and 5% $CO_2$ for 10 minutes. After that, CD4 T cells were placed in the upper chambers of transwells at $4x10^5$ cells per well and incubated at 37ºC and 5% $CO_2$ for 3 hours. Two to three replicas per condition have been performed per experiment. The transmigrated fraction of cells was stained and analyzed via flow cytometry. Chemotactic index was calculated as the ratio of cells that transmigrated to chemokine compared to no cytokine control.

Enzyme-linked immunosorbent assay. For measuring NP-specific Abs, NUNC immunoplates were coated with 2 µg/ml of NP8-BSA or NP41-BSA (Biosearch) in borate saline buffer (100mM boric acid, pH 7.4, 0.9% NaCl). For measuring total titers of IgA, IgG1, IgG2b and IgG2c, plates were coated with 4 µg/ml of purified goat anti-mouse Ig (H+L) (Southern Biotech, cat #1010-01). Blocking was done with PBS containing 0.1% gelatin and 0.1% sodium azide. Washes were done with PBS containing 0.05% Tween-20. Serial serum dilutions were applied. For detection of IgA, IgG1, IgG2b and IgE, the plates were incubated with 1:4000 dilution of biotinylated mouse anti-mouse IgA, IgG1, rat anti-mouse IgG2b, and rat anti-mouse IgE (BD Biosciences, clones C10-1, 10.9, R12-3, and R35-72) respectively followed by streptavidin-HRP (R&D). The color was developed using a substrate solution from R&D (DY999). For detection of IgG2c the plates were incubated with AP-conjugated goat anti-mouse IgG2c Abs (Southern Biotech, cat #1079-04) and visualized by incubating with nitrophenyl phosphate (Sigma) in carbonate buffer (22mM Sodium carbonate, 34 mM sodium bicarbonate, 2.1 mM MgCl2). Plates were read with a Synergy HT microplate reader (Bio-Tek Incorporated) at 405 and 562 nm. All plates contained serial

dilutions of the serum that was used to generate the calibration curve for quantitative comparison of the samples.

*Immunofluorescence and Hep2 Staining.* Freshly isolated lymph nodes were fixed in 1% PFA for 1 hour at room temperature, washed with PBS three times, and stored at 4ºC in 30% sucrose solution overnight. Fixed samples were then transferred to OCT (Tissue-Tek) and snapfrozen. 30 µm thick sections were cut via cryostat (Leica). The sections were dried at room temperature for 3 hours. They were then blocked using normal rabbit serum (Sigma-Aldrich) and endogenous biotin was blocked via a Biotin Blocking Kit (Vector) and then stained with rat anti-CD35 (BD, 8C12) Abs overnight followed by PE-conjugated anti-rat antibodies (Santa Cruz Biotechnology) for 1 hour. Slides were then stained with anti-Foxp3-biotin (eBiosciences, FJK-16s) Abs overnight. The next day, streptavidin conjugated Alexa647 (Life Technologies), anti-CD4-PE-TexasRed (BD, RM4-5), and anti-IgD-FITC (Biolegend, 11-26c.2a) Abs were added for 1 hour. Slides were then mounted in fluoromount-G (Southern Biotech) and analyzed via confocal microscopy with Leica SP5 II (Leica Microsystems). For Hep2 staining, serum was diluted to a concentration of 1:40 before being applied to Hep2 slides (Antibodies Incorporated). After a 30-minute incubation, serum was washed off three times and FITC-conjugated anti-mouse IgM or IgG was added with 300 nM of DAPI. The slides were then mounted with fluoromount-G and imaged on a Leica SP5 II.

*Two Photon Microscopy.* Inguinal LNs (ILNs) were either explanted or surgically exposed for intravital imaging and perfused as previously described [61, 174]. ILNs were imaged with a Leica SP5 II (Leica Microsystems) fitted with a MaiTai Ti: Sapphire laser (Spectra-Physics) that was tuned to 870 nm. Each *xy* plane spanned 435µm x 435µm and with z spacing ranging from 2-3 µm detecting emission wavelengths of 430-450 nm (second harmonic emission of collagen), 465-500 nm (for $CFP^+$ cells), 520-550 nm (for $GFP^+$ cells), and >560 nm (for $tdTomato^+$ cells), every 20-25 seconds. Images were acquired by Leica Advanced Fluorescent Suite (Leica Microsystems). Analysis of the imaging data and generation of 3D rotations and time-lapse image sequences were performed using Imaris 7.6.5 x64 (Bitplane). Videos were processed with a median

noise filter. Semi-automated cell tracking in 3D was performed with Imaris 7.6.5 x64, and then verified and corrected manually. 3-dimensional GC volume was defined based on the distribution of HyHEL10 CFP B cells by combination of visual analysis and a custom-made MATLAB program that performed time integrated image rendering of CFP signal. TdTomato$^+$ Tregs and Th that transited within the follicles and GCs were tracked. Their interaction with WT and CCL3-KO B cells within defined GCs volume were visually identified and categorized either as a strict contact as defined when cell-to-cell contact was unambiguous or a non-strict contact where cells could be observed in extreme proximity (~1μm). Finally, we normalized the number of contacts to the average number of WT or CCL3-KO B cells within the GC volume accessible to Tfr or Tfh cells to arrive at a normalized contact frequency. Annotation and final compilation of videos was performed in Adobe After Effects CS5.5 (Adobe).

*RT-PCR Analysis*. RNA from sorted cells was obtained using RNeasy Kit (Qiagen) following the manufacturer's instructions. RNA was treated with DNase to remove genomic DNA (Ambion). The concentration of RNA was calculated using a NanoDrop 2000 (Thermo) and cDNA was synthesized using a SuperScript III kit (Invitrogen) following the manufacturer's instructions. Preamplification of target genes was performed using PreAmp Kit (AB Biosystems) for 10 cycles. TaqMan assays were obtained from Applied Biosystems and RT-PCR was carried out on a RealPlex 2 (Eppendorf). Expression levels of CCL3/4/5 were normalized to the level of β2m.

*Statistical analysis*. Statistical analysis of data normalized to the control samples were performed using a one-sample *t*-test. For comparisons between two groups two-sample *t*-test was utilized. Welch's correction was applied for data with unequal variances. For data in which more than two groups or more than two time points were analyzed, two-way ANOVA followed by Dunnet or Bonferonni post-hoc analysis was done. In cases where we did not assume normally distributed data and the data was from paired measurements, we used the Wilcoxon signed-rank test. Two investigators independently categorized ANA staining and significance was then tested by $\chi^2$ with trend test. All statistical tests were computed with PRISM (GraphPad) after consultation

with a University of Michigan Center for Statistical Consultation and Research representative. *P* values of less than 0.05 were considered statistically significant. Only statistically significant results were labeled. No samples were excluded from the analysis.

## Results

### GC centrocytes upregulate expression of CCL3, CCL4 and CCL5

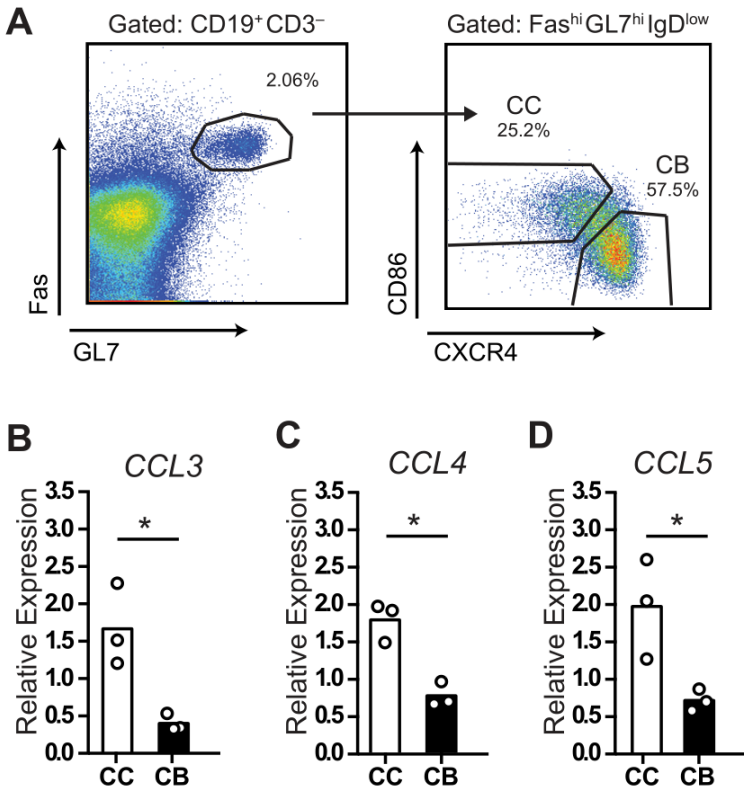


**Figure 2.1: Centrocytes express proinflammatory chemokines**
**A-D**, Relative expression of proinflammatory chemokines in GC centroblasts (CB) and centrocytes (CC) compared to non-GC B cells ($FAS^{low}$ $GL7^{low}$). Cells were sorted from peripheral LNs (pLNs) of mice at 10 days post s.c. immunization with 50 µg OVA in Ribi. **A**, Representative flow cytometry plots displaying the gating strategy for cell sorting. **B-D**, Relative expression of *Ccl3* (**B**), *Ccl4* (**C**), and *Ccl5* (**D**) mRNA from cells sorted as shown in (A) and measured by quantitative RT-PCR. Chemokine $C_T$ values were normalized to β2m $C_T$. *Ccl3-5* expression in GC B cells was then normalized to non-GC B cells. Bars represent mean ± SEM. Data represent n=3 independent experiments, 5 mice total. *, P<0.05, two-tailed Student's *t*-test with Welch's correction.

To verify expression of *Ccl3*, *-4*, and *-5* in murine GC B cells, we performed qPCR analysis of GC centroblasts, centrocytes and naive B cells sorted from the draining lymph nodes (LNs) of immunized mice at 10 days post immunization (d.p.i) (Fig 2.1A 1A). We found that expression of CCL3/4/5 is upregulated in murine GC centrocytes compared to centroblasts (Fig 2.1B-D).

**Increased GC response in CCL3-KO mice**

To determine if CCL3 plays a role in the regulation of GCs, we utilized CCL3-KO mice [175]. In unimmunized CCL3-KO and WT mice, we found no significant difference in the GC B cells numbers in peripheral lymph nodes (pLNs), spleens, mesenteric LNs (mLNs) and payer patches (PP) (Fig. 2.2A). However, upon immunization we detected a small, but significant increase in the GC response in CCL3-KO mice compared to WT that was independent of the antigen or the adjuvant used (Fig. 2.2B-E). We then tested whether in littermate-control CCL3-KO mice GCs were also elevated, and confirmed the previously observed phenotype (Fig. 2.2F, G). Additionally, we detected a trend towards increased numbers of GC B cells in immunized CCR5-KO mice (Fig. 2.2C). The observed accumulation of GC B cells was not due to a decreased clearance of apoptotic GC B cells in CCL3-KO, since the fractions of apoptotic and dead GC cells in immunized WT and CCL3-KO mice remained comparable (Fig. 2.2H-J). We also observed a small trend towards increased formation of plasmablasts in the pLNs of immunized CCL3-KO mice, but it was not statistically significant (Fig. 2.2K, L).

To determine whether the observed increase in the GC response in CCL3-KO mice was due to overexpansion of foreign-Ag specific GC B cell clones, we examined the number of NP-binding cells within the GCs of mice immunized with NP-KLH in Ribi at 10 d.p.i. While the frequency of the $NP^+$ B cells within the GC was similar between WT and CCL3-KO mice (Fig. 2.2M), their frequency relative to total lymphocytes was increased in CCL3-KO mice compared to WT counterparts (Fig. 2.2N, see inset). Despite of that small increase, no significant differences in the titers of high- or low-affinity NP-specific IgG1 antibodies (NP8, and NP41, correspondingly) was detected in the serum of CCL3-

KO vs. WT mice (Fig. 2.2O, P). Overall, these results are consistent with modest overexpansion of foreign antigen-specific GC B cells, but not plasma cells, in the immunized CCL3-KO mice at 10 d.p.i.

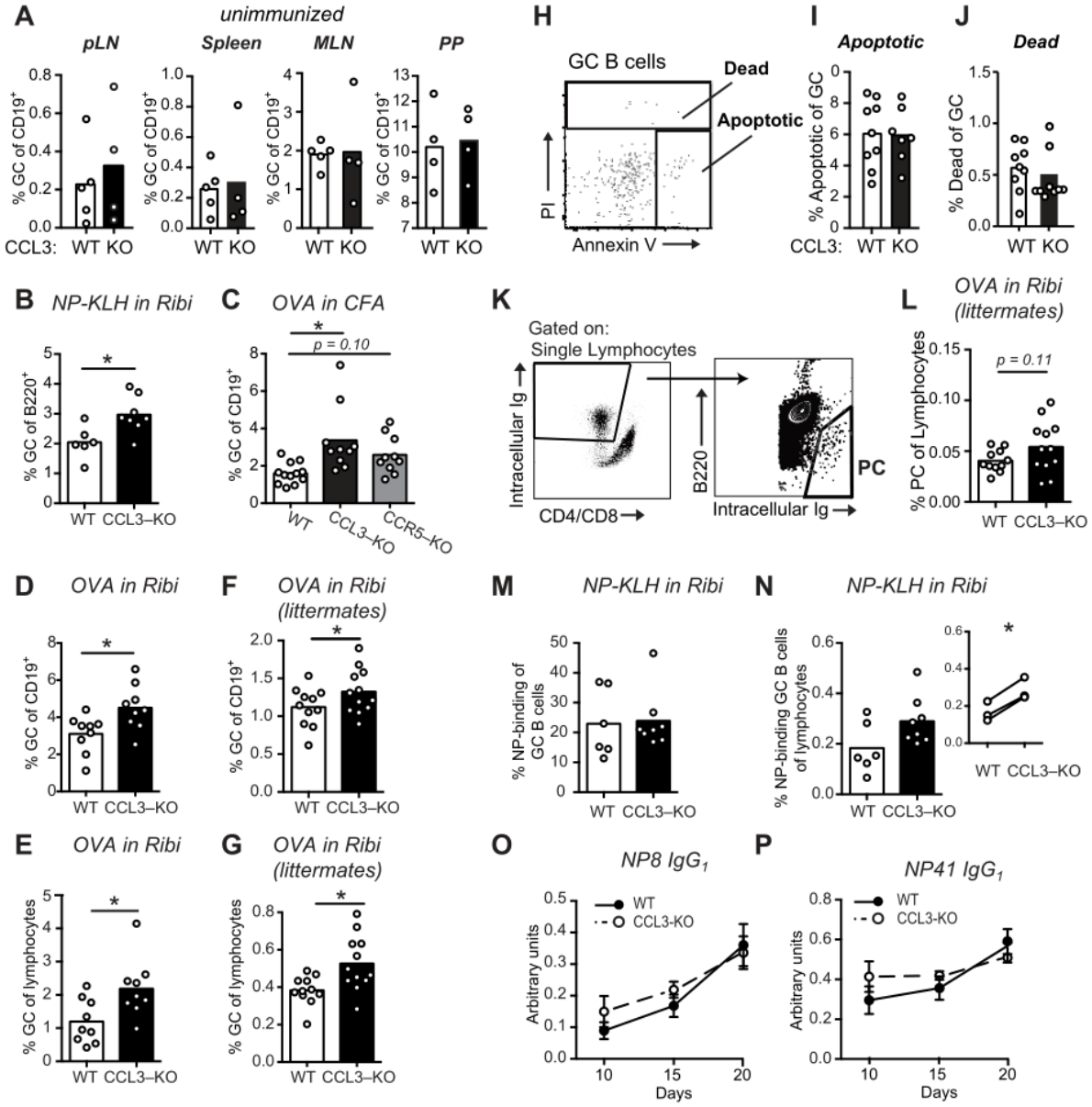


**Figure 2.2 Increased GC response in CCL3-KO mice following immunization.**
**A-G**, Flow cytometry analysis of the GC B cells ($Fas^{high}$ $GL7^{high}$ $IgD^{low}$) as a fraction of total B cells (**A-D**, **F**) or total lymphocytes (**E**, **G**) in WT, CCL3-KO, and CCR5-KO mice. **A**, Analysis of GCs in peripheral LNs (pLNs: inguinal, brachial and axillary LNs combined), spleens, mesenteric LNs (MLNs), and Peyer's Patches (PP) from unimmunized mice. **B-G**, Analysis of GCs in the antigen-draining pLNs from mice subcutaneously (s.c.) immunized with 50 µg of 4-Hydroxy-3-nitrophenyl (*NP*) acetyl-*hapten* conjugated to *Keyhole limpet hemocyanin (*KLH) in Ribi adjuvant (**B**) or 50 µg of OVA in Complete Fruend's Adjuvant (CFA) (**C**) or 50 µg OVA in Ribi (**D-G**) at 10 d.p.i.
*Legend continues next page.*

**Figure 2.2 cont.**
**F, G,** Verified in littermate-control mice. Each symbol represents one mouse. Bars represent mean. Data are derived from 2 or 3 independent experiments. *, P<0.05, Student's *t*-test (two-sided in **B-E**, one-sided in **F, G,** with Dunnet's correction in **C**). **H-J**, Flow cytometry analysis depicting apoptotic (Annexin $V^+$ $PI^-$, **H**, **I**) and dead (Annexin $V^+$ $PI^+$, **H**, **J**) GC B cells from draining pLNs of mice immunized as in **D**. **K, L**, Flow cytometry analysis of the plasma cells (PC) in pLNs of littermate-control WT and CCL3-KO mice at 10 d.p.i. with 50 ug of OVA in Ribi. PC gating strategy (**K**) and fraction of total lymphocytes (**L**). Each dot represents a single mouse and bars indicate mean from 2 independent experiments. Two-tailed Student's *t*-test. **M-P** Analysis of NP-specific GC responses (in **M**, **N**) and antibody responses (in **O**, **P**) from mice immunized with 50 µg of NP-KLH in Ribi s.c. **M, N,** Flow cytometry analysis of NP-specific GC B cells as a fraction of total GC B cells (**M**) or total lymphocytes (**N**) at 10 d.p.i. Each dot represents a single mouse and bars indicate mean from 3 independent experiments while the inlet depicts the mean of each individual experiment. *, P<0.05, two-tailed paired *t*-test. **O, P**, ELISA of NP-specific $IgG_1$ titers that have high affinity (NP8-bidning) (**O**) and overall affinity (NP41-binding) (**P**) to NP. Relative titers were determined using serial dilutions and a calibration curve from control serum. Each point represents the mean ± SEM. Data are derived from 2 independent experiments with 2-4 mice of each genotype per experiment.

## Immunization induces anti-nuclear antibody (ANA) response in CCL3-KO mice and in mice transferred with CCL3 deficient B cells

We next asked whether over-expanded GC B cells in the CCL3-KO mice may contain anti-nuclear B cell clones. The presence of ANA in the serum of NP-KLH immunized WT and CCL3-KO mice was addressed by Hep2 staining (Fig. 2.3A) [176]. While little anti-nuclear staining of Hep2 slides was observed for serum from unimmunized mice, the presence of IgG ANA was detected in most CCL3-KO but in few WT animals at 15 and 28 d.p.i. (Fig. 2.3B). We also found increased formation of ANA in the littermate control CCL3-KO compared to WT mice (Fig. 2.3C). Of note, majority of ANA from CCL3-KO mice exhibited non-homogenous nucleoplasmic patterns of Hep2 staining, while others were specific to nuclear membranes (Fig. 2.3A). Interestingly, immunized CCL3-KO mice had an increase in the titers of total IgG2c and IgA, but not other antibody isotypes in the serum of CCL3-KO mice at 28 d.p.i (Fig. 2.3D-H).

To determine whether the observed generation of ANA is dependent on B cell-intrinsic chemokine production, we transferred 35 million of purified WT or CCL3-KO B cells into $CCL3^{+/+}$ MD4 mice (with over 95% of B cells specific to Hen Egg Lysozyme) [172], which were then immunized with NP-KLH in Ribi and analyzed as described above. While only one out of thirteen MD4 mice receiving WT B cells had ANA, half of MD4

mice that received CCL3-KO B cells generated robust ANA response following immunization (Fig. 2.3I).

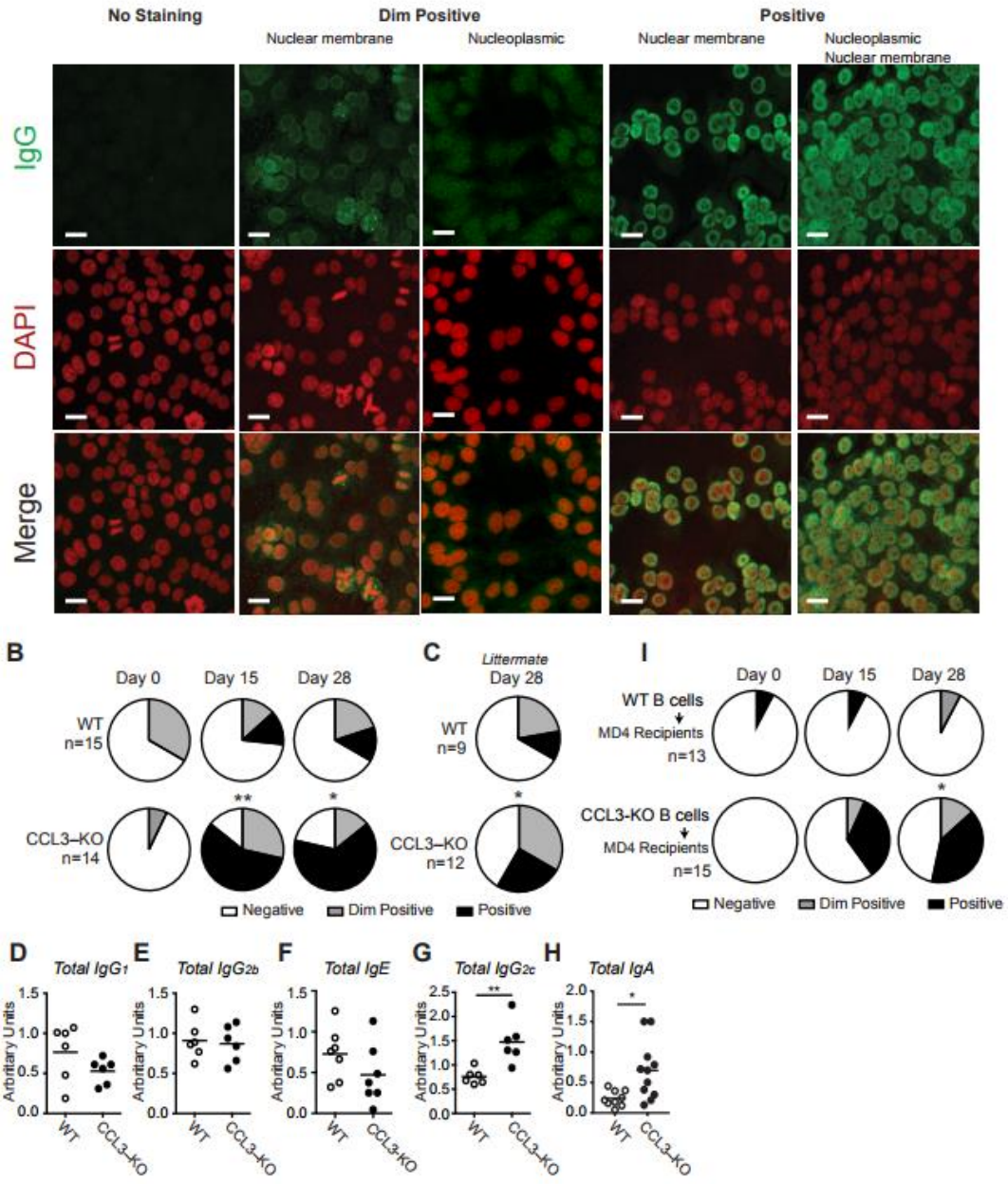


**Figure 2.3. Generation of ANA responses in CCL3-KO mice following immunization.**

**A-H**, Analysis of serum from WT and CCL3-KO mice s.c. immunized with 50 µg of NP-KLH in Ribi and boosted with the same dose of antigen in Ribi on day 24. **A-C** Analysis of anti-nuclear IgG antibodies in mouse serum by HEP2 staining. The staining was categorized into negative, dim positive, or positive nuclear staining. **A**, Representative staining examples. Scale bar – **15 µm**. **B**, Data summary for n=15 WT and 14 CCL3-KO mice.

*Legend continues next page.*

**Figure 2.3. cont.**
**C**, Analysis of anti-nuclear IgG antibodies development in the initially ANA-negative littermate-control WT and CCL3-KO mice at 28 d.p.i. Data represents 4 independent experiments. *, P<0.05. **, P<0.005. $\chi^2$ test. **D-H**, Titers of total $IgG_1$ (**D**), $IgG_{2b}$ (**E**), IgE (**F**), and $IgG_{2c}$ (**G**) on day 28 from mice in B and IgA **(H)** from mice in C. Relative titers were determined using serial dilutions and a calibration curve from control serum. Data represents 2 independent experiments with 2-4 mice of each genotype per experiment for D-G and 3 independent experiments with 3-5 mice of each genotype for H. *, P<0.05. **, P<0.005, two-tailed Student's *t*- test. **I**, MD4 recipient mice received $35x10^6$ B cells purified from WT or CCL3-KO mice and were immediately immunized s.c. and i.p. with a total of 100 µg of NP-KLH in Ribi. Mice were boosted with the same dose of Ag in Ribi on day 24. Serum was collected and tested for Hep2 reactivity as described in A. Data represents 3 independent experiments with n=13 WT and 15 $CCL3^{-/-}$ B cell recipients. *, P<0.05. $\chi^2$ test.

To summarize, the above analysis suggests that B cell-intrinsic production of CCL3 is required for control over ANA development upon immunization.

### CCL3 and CCL4 induces chemotaxis of regulatory T cells *ex vivo*

Based on the elevated expression of CCL3 and CCL4 in GC centrocytes, the observed dysregulation in GC and ANA responses in CCL3-KO mice and previously reported responsiveness of an unidentified subset of splenic Tregs to CCL4 chemokine *ex vivo* [148], we hypothesized that Tfr cells that localize to GCs may respond to CCL3 as well as CCL4 chemokines. To determine whether CCL3 and CCL4 can induce chemotaxis of Tfr cells *ex vivo* we performed transwell migration analysis of CD4 T cells isolated from pLNs of mice at 10 d.p.i. with OVA in Ribi. $CXCR5^{high}$ $PD1^{high}$ $FoxP3^{+}$ Tfr cells transmigrated in response to CCL3 chemokine (Fig. 2.4A, B). Similar trends were observed for $CXCR5^{low}$ $PD1^{low}$ $FoxP3^{+}$ and $CXCR5^{int}$ $PD1^{int}$ $FoxP3^{+}$ cells (Fig. 2.4A, B). We also observed transmigration of Tfr and other regulatory T cell subsets to CCL4 (Fig. 2.4C). The observed transmigration was predominantly due to chemotaxis rather than chemokinesis, since addition of CCL3 or CCL4 chemokines to both the upper and the lower wells of the transwell chamber did not promote Tregs' transmigration (Fig. 2.4B, C). While we also observed a slightly increased transmigration of Tfh cells ($CXCR5^{high}$ $PD1^{high}$ $FoxP3^{-}$) to CCL3 and CCL4 chemokines in the transwell assays, the trend was not significant (Fig. 2.4D, E). These data suggest that CCL3 and CCL4 can induce chemotaxis of Tfr and possibly other Treg cells *ex vivo*.

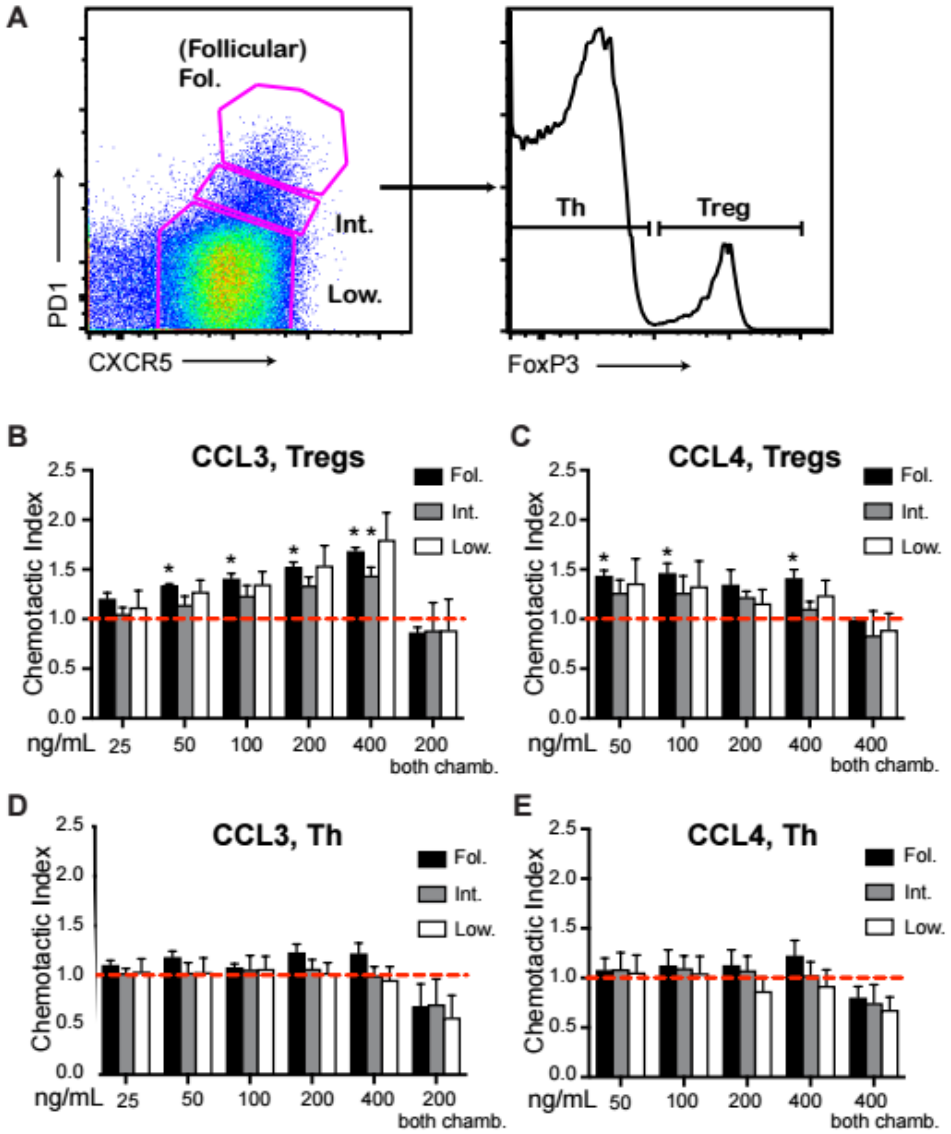


## Figure 2.4. Chemotaxis of Tfr cells to CCL3 and CCL4 *ex vivo*.

**A-E,** *Ex vivo* transwell assay of $CD4^+$ T cells purified from draining pLNs of WT mice at 10 d.p.i. with 100 µg OVA in Ribi and analyzed by flow cytometry using the gating strategy as in (**A**). Transmigration of $CXCR5^{high}PD1^{high}$ (**Fol., black bars**), $CXCR5^{int}PD^{int}$ (**Int., grey bars**), or $CXCR5^{low}PD1^{low}$ (**Low, white bars**) $CD4^{pos}$ $CD8^{neg}$ $B220^{neg}$ cell populations that also express Foxp3 (**B, C**) or were $FoxP3^{neg}$ (**D, E**) were measured against CCL3 (**B, D**) and CCL4 (**C, E**). The chemokines were added either to the lower chambers of transwells for analysis of chemotaxis or to both the upper and the lower chambers for analysis of chemokinesis. Chemotactic index was calculated as the ratio of cells that transmigrated towards the chemokine vs. no chemokine control (dashed red line). Chemotaxis and chemokinesis data are derived from 3 and 2 independent experiments correspondingly with 2 mice per experiment. Bars represent mean ± SEM, *, $P<0.05$, two-tailed, one-sample Student's *t*-test (compared to 1).

**CCL3 does not recruit Tfr cells into the GC light zone.**

Our observations that CCL3 promotes Tfr cells chemotaxis *ex vivo* and is required for control over GC response *in vivo* led us to ask whether CCL3 produced by GC centrocytes recruits Tfr cells from the follicles into the GCs. If this hypothesis is correct, the frequency of Tfr cells in the GC light zone should be reduced in CCL3-KO mice compared to WT mice. To test this, we analyzed the density of Tfr as well as Tfh cells in the GCs (both in the light and the dark zones) and in the follicles of the draining LNs from immunized CCL3–KO and WT mice. Fixed LNs were sectioned and stained with fluorescently conjugated antibodies towards IgD, CD35, CD4, and FoxP3 and analyzed by confocal microscopy (Fig. 2.5A-C). Interestingly, in WT mice, $CD4^+$ $FoxP3^+$ Tfr cells were enriched in the follicles compared to the GCs, while $CD4^+$ $FoxP3^-$ Tfh cells were more abundant in GCs light zone than in the follicle and the dark zone (Fig. 2.5C, D, F). In contrast to the expected decrease in Tfr cell frequency within the GC light zone of CCL3-KO mice, the density and recruitment index of Tfr cells in the light zones of CCL3-KO and WT mice were comparable (Fig. 2.5D, E). However, the recruitment index calculated for Tfr access into the GC dark zone relative to the follicle was higher for CCL3-KO mice (Fig. 2.5E). Similar results were found for Tfh cells (Fig. 2.5F, G). Based on this data we conclude that CCL3 is not required for Tfr or Tfh cells' recruitment into the GC light zone from the follicles, but may play a role in limiting access of follicular T cells to the GC dark zone.

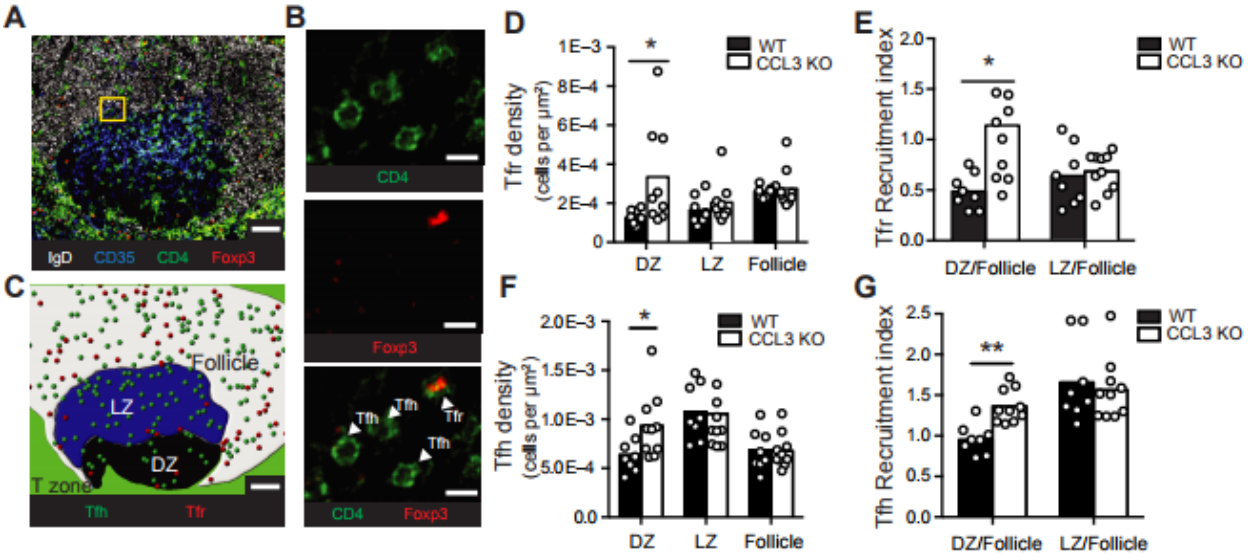


**Figure 2.5. CCL3 does not recruit Tfr or Tfh cells into the GC's light zone.**
Immunofluorescent analysis of Tfr and Tfh cells localization in the GCs and follicles of draining pLNs from WT or CCL3-KO mice at 10 d.p.i. with 50 µg OVA in Ribi. **A-C**, Representative example of a confocal image of pLN section and its analysis. **A**, Confocal image of GC-containing 10 mm thick section of pLN from WT mouse, stained with antibodies against IgD (white), CD35 (blue), CD4 (green) and anti-Foxp3 (red). **B**, Magnified image from the inset (in A) that illustrates how Tfr ($CD4^+Foxp3^+$) and Tfh ($CD4^+Foxp3^-$) cells were identified. **C**, Reconstruction of GC light zone (blue area), dark zone (black area), follicle (white area), Tfr (red circles) and Tfh cells (green circles) within the confocal image shown in (A) using manually defined surfaces in Imaris software. Scale bars 50 mm in the **A**, **C** and 10 mm in **B**. **D-G** Quantitative analysis of Tfr (**D-E**) and Tfh (**F-G**) densities in the GCs and the follicles. **D**, Density of Tfr in GC dark zone (DZ), light zone (LZ) and follicles around GCs calculated as the number of Tfr in each zone normalized to the total area of that zone. **E,** Recruitment index calculated as the density of Tfr in GC DZ or LZ normalized to their density in the GC-containing follicle. **F,** Quantitative analysis as in **D** for Tfh. **G**, Quantitative analysis as in **E** for Tfh. **D-G**, Each symbol represents a distinct GC. For each GC, three unique z-positions were analyzed and data was averaged. Data is compiled from n=3 independent experiments with 4 mice per genotype total. Bars represent mean. *, P<0.05, two-tailed Student's *t*-test.

## Adoptively transferred Tregs can become Tfr cells and be visualized by 2P microscopy

Since we found that CCL3 is not required for Tfr cells' access into the GCs, we then asked whether CCL3 could promote individual interactions of Tfr cells with GC B cells *in vivo*. To directly test this, we developed an imaging strategy that enabled visualization of adoptively transferred Tregs within the GC-containing follicles of living mice using 2-photon (2P) microscopy (Fig. 2.6A). Because intravenous injection of Tregs is insufficient to get enough of the transferred Tregs into pLNs for microscopy analysis, we utilized the fact that adoptively transferred Tregs undergo proliferation in recipient $FoxP3^{DTR}$ mice upon DTx-induced ablation of DTR-expressing resident Tregs [177]. Of

note, while treatment of FoxP3$^{DTR}$ mice with DTx leads to development of severe autoimmune disease, pre-transfer of $10^6$ polyclonal Tregs rescues FoxP3$^{DTR}$ mice from autoimmunity [177]. To generate mice with a high number of brightly fluorescent Tfr cells, we first transferred $10^6$ polyclonal Tregs that expressed both Foxp3-GFP and tdTomato into Foxp3$^{DTR}$ mice [177, 178]. We then treated the Foxp3$^{DTR}$ recipients with 5 µg of diphtheria toxin (DTx) 2 times, one weeks apart. As reported before, following transient ablation of Foxp3$^{DTR}$ Tregs, the adoptively transferred Tregs as well as the remaining endogenous Tregs underwent vigorous proliferation. At 14 days following the initial DTx treatment, tdTomato Tregs represented about 50% of all Tregs in the blood (Fig. 2.6B). We then co-transferred CCL3$^{+/+}$ HyHEL10 B cells expressing cyan fluorescent protein (CFP), ovalbumin (OVA) specific OTII CD4 T cells expressing green fluorescent protein (GFP), as well as non-fluorescent HyHEL10 B and OTII T cells into the same recipient mice and induced their recruitment into the GCs by s.c. immunization with duck egg lysozyme conjugated to OVA (DEL-OVA) as previously described [61]. By 8 d.p.i. the overall levels of Tregs in the blood had returned to normal (Fig. 2.6B). Based on confocal and flow cytometry analysis we determined that over a fifth of CD4$^+$Foxp3$^+$ cells from draining lymph nodes expressed tdTomato and that tdTomato$^+$ cells were almost exclusively Foxp3$^+$ (Fig. 2.6C, D). Additionally, tdTomato$^+$ Foxp3$^+$ cells that were also CXCR5$^{high}$ PD1$^{high}$ had increased expression of Bcl6$^+$ as expected for Tfr cells (Fig. 2.6C). In agreement with the enrichment of Tfr cells in the follicles relative to the GCs suggested by confocal analysis (Fig. 2.5C-E) we observed that at 7-8 d.p.i. a relatively minor fraction of GC-proximal Tfr cells entered into the GCs, while majority of the cells moved around GCs in proximity to the outer edge GC B cells (Fig. 2.6E, Movie S1). This data suggests that the adoptive transfer of fluorescent Tregs followed by transient ablation of non-fluorescent endogenous Tregs and immunization is sufficient to visualize Tfr cells within GC-associated follicles in living mice by 2P microscopy.

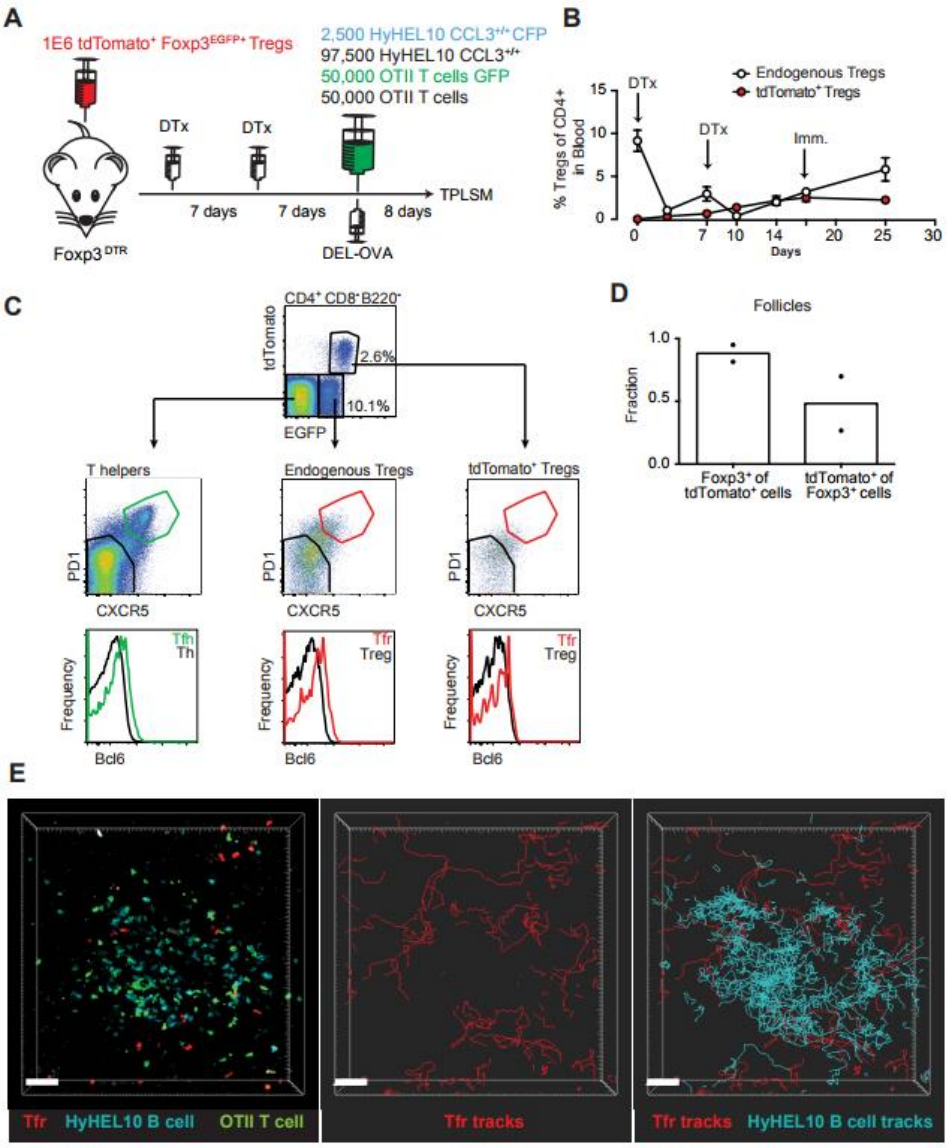


## Figure 2.6. 2P visualization of Tfr cells.

**A**, Experimental diagram for generation of recipient mice with large numbers of highly fluorescent tdTomato$^+$ Tregs and visualization of Tfr and GC B cells in the pLNs by 2P microscopy (See also **Materials and Methods**). **B**, Flow cytometry analysis of the endogenous and transferred TdTomato$^+$ Treg numbers in the blood of FoxP3$^{DTR}$ mice throughout their treatments with DTx and immunization, performed as indicated in (**A**). **C-E**, Analysis of inguinal LNs from mice generated through the procedure described in (**A**) at 8 d.p.i. **C,** Representative flow cytometry analysis of Bcl6 expression in the CXCR5$^{low}$PD1$^{low}$ and CXCR5$^{hi}$PD1$^{hi}$ subsets of TdTomato$^+$ Tregs (top panels), endogenous Tregs (middle panels) and endogenous Th cells (bottom panels). **D**, Confocal immunofluorescence analysis of inguinal LN sections for the fraction of TdTomato$^+$ cells that express Foxp3 (left bars) and fraction of Foxp3$^+$ cells that express TdTomato$^+$ (right bars) in GC-containing follicles. **E**, Representative 2P imaging analysis of Tfr cells localization with respect to GCs. A snapshot (left panel) from an intravital imaging experiment as analyzed in Imaris software (see also **Movie S1**). Tfr cells (red) and GCs containing CFP HyHEL10 B cells (cyan) and GFP OTII Tfh cells (green). Cell trajectory analysis for Tfr cells (middle panel) and both Tfr cells and GC B cells (right panel). Scale bars 40 μm.

**GC B cells' CCL3 promotes their contacts with Tfr, but not Tfh cells in a CCR5 receptor-dependent way**

To determine whether GC B cell's intrinsic production of CCL3 promotes their direct interactions with CCR5 proficient or deficient Tfr cells or with Tfh cells *in vivo* we utilized the experimental setup developed by us (Fig. 2.6) and in the previous work [61] and outlined in Figs. 2.7A and B. For analysis of T cell interactions with $CCL3^{+/+}$ and $CCL3^{-/-}$ GC B cells, recipient mice were cotransferred with $CCL3^{+/+}$ HyHEL10 B cells that expressed CFP and $CCL3^{-/-}$ HyHEL10 B cells that expressed GFP. To determine Tfr cells' interactions with GC B cells we tracked $TdTomato^{+}$ Tfr cells when they contacted or passed through the GCs, and analyzed their interactions with fluorescent $CCL3^{+/+}$ and $CCL3^{-/-}$ foreign antigen-specific HyHEL10 B cells within the same GCs (Fig. 2.7C, Movie S2). To take into account the ambiguity of correct identification of B-T cell interactions by 2P imaging, we used both "strict" and "non-strict" definitions of contacts between GC B cells and follicular T cells. By "strict" we define the interactions that based on the cell colocalization analysis in 3D have taken place with high confidence. By "non-strict" interactions we identify all likely interactions identified based on cell proximity, including the "strict" interactions. The data was analyzed in a blinded fashion to avoid possible bias in cell contact definition (Fig. 2.7D, Movie S3). We calculated the normalized contact frequency of Tfr cells with fluorescent $CCL3^{+/+}$ and $CCL3^{-/-}$ GC B cells by dividing the total number of Tfr cell contacts with $CCL3^{+/+}$ or $CCL3^{-/-}$ GC B cells by the average numbers of fluorescent B cells of each type present in the imaged GCs. Tfr cells' normalized contact frequency was lower for $CCL3^{-/-}$ compared to $CCL3^{+/+}$ GC B cells in 5 experiments, independently of the "strict" vs "non-strict" B-Tfr cell contact definition (Fig. 2.7E, F). The differences in Tfr cell contact frequencies with $CCL3^{+/+}$ and $CCL3^{-/-}$ GC B cells were not due to distinct migratory properties of $CCL3^{+/+}$ and $CCL3^{-/-}$ B cells (Fig. 2.7O-R). In contrast to WT Tregs, CCR5-KO Treg contact frequency with $CCL3^{+/+}$ and $CCL3^{-/-}$ GC B cells was not significantly different (Fig. 2.7E, F). These findings are consistent with a dominant role of CCR5 receptor on Tfr cells for sensing CCL3. Of note, duration of Tfr cell interactions with $CCL3^{+/+}$ and $CCL3^{-/-}$ GC B cells was not significantly different (Fig. 2.7G, H).

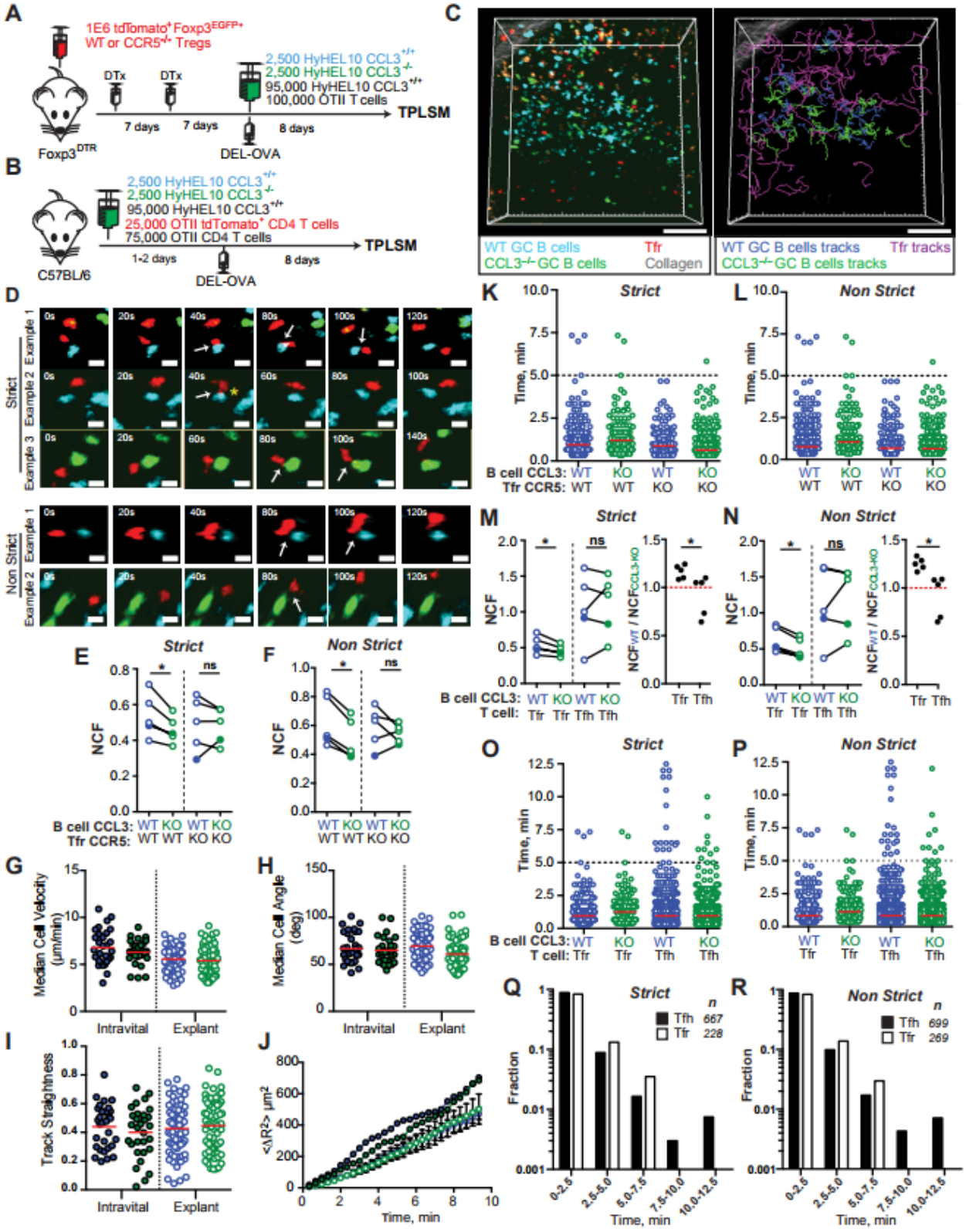


**Figure 2.7. Tfr cells make less frequent contacts with CCL3-KO B cells in GCs**
*Legend on the following page.*

**Figure 2.7. Tfr cells make less frequent contacts with CCL3-KO B cells in GCs (Previous Page)**

2P imaging analysis of Tfr and Tfh cells contacts with $CCL3^{-/-}$ and $CCL3^{-/-}$ GC B cells in the pLNs of mice at 8 d.p.i. **A, B**, Experimental diagrams for imaging GC B cell-Tfr cell interactions (A) and GC B cell-Tfh cell interactions (B). **C**, A snapshot (**left panel**) and cell trajectory analysis (**right panel**) from an intravital imaging experiment (see also **Movie S2**) performed at 8 d.p.i. as described in A**.** Scale bars - 50 mm. Left panel, Tfr cells (red), CFP HyHEL10 (cyan) and GFP $CCL3^{-/-}$ HyHEL10 (green) GC B cells, auto-fluorescent cells (orange). Right panel, Tracks of Tfr cells (purple), CFP (blue) and GFP $CCL3^{-/-}$ (green) HyHEL10 GC B cells. **D,** Time-lapse images of Tfr cells (red) interacting with $CCL3^{+/+}$ (cyan) or $CCL3^{-/-}$ (green) HyHEL10 B cells within GCs. Cell contacts were verified in 3D space and classified as Strict (definitive contacts, top three examples) and Non Strict (possible contacts, bottom two examples) (see also **Movie S3**). Defined contacts between Tfr and B cells are indicated by white arrows. Yellow star illustrates example of pseudopod extension by a Tfr cell towards CFP GC B cell. Images are displayed as 20 µm z-stacks. Scale bars - 5 mm. **E-R**, Quantitative analysis of $CCL3^{+/+}$ CFP (blue circles) and $CCL3^{-/-}$ GFP (green circles) HyHEL10 GC B cell migration (O-R) and interactions with Tfr cells (E-L) or Tfh cells (I-L). Closed symbols represent intravital and opened symbols indicate explanted pLNs imaging. Data from 5 independent experiments (5 mice) per T cell type and genotype. **E, F,** Normalized contact frequency (NCF) for Strict (E) and Non Strict (F) interactions of WT or $CCR5^{-/-}$ Tfr cells with $CCL3^{+/+}$ and $CCL3^{-/-}$ HyHEL10 B cells within defined volume of GCs normalized to the average number of HyHEL10 cells of each genotype. Linked symbols correspond to GC B cells in the same movie. (*, P<0.05, Wilcoxon matched-pairs test.) **G, H**, Contact duration between Tfr and HyHEL10 B cells of each genotype undergoing Strict (G) or Non Strict (H) interactions. Red lines represent the medians. **I, J, Left**: NCF for Strict (I) and Non Strict (J) interactions of Tfr (also shown in E, F) and Tfh cells with $CCL3^{+/+}$ or $CCL3^{-/-}$ HyHEL10 B cells calculated and analyzed as in E, F. **Right**: Ratio of the Tfr (also shown in E, F) and Tfh cell NCF with $CCL3^{+/+}$ over $CCL3^{-/-}$ HyHEL10 B cells from the same movie. (*, P<0.05, Student's t-test.) **K, L**, Contact duration between Tfr (as in G and H) or Tfh cells with HyHEL10 B cells of each genotype undergoing Strict (K) or Non Strict (L) interactions. Red lines represent the medians. **M, N,** Time histograms for duration of strict (M) and non-strict (N) contacts between Tfr and Tfh cells with WT HyHEL10 GC B cells summarized from 6 independent experiments with Tfr cells and 5 independent experiments with Tfh cells. ***n*** corresponds to the total number of contacts. **O-R**, Analysis of $CCL3^{+/+}$ and $CCL3^{-/-}$ HyHEL10 GC B cell motility from 5 movies with $CCR5^{+/+}$ Tfr cells. Median cell velocity (O), median cell angle (P), track straightness (Q), and average squared displacement (R) calculated for tracked GC B cells. The data for explanted imaging is combined from 4 mice. (No statistically significant differences according to Mann Whitney U-test.)

In contrast to Tfr cells, OTII Tfh cell contact frequency with $CCL3^{+/+}$ vs. $CCL3^{-/-}$ GC B was comparable (Fig. 2.7I, J, left panels). The ratio of T cells' contact frequency with $CCL3^{+/+}$ vs. $CCL3^{-/-}$ GC B cells was slightly but significantly lower for Tfh compared to Tfr cells (Fig. 2.7I, J, right panels). No significant difference in the duration of Tfh cell contacts with $CCL3^{+/+}$ vs. $CCL3^{-/-}$ GC B cells was observed (Fig. 2.7K, L).

The vast majority of Tfr and Tfh cell contacts with GC B cells were shorter than 5 min (Fig. 2.7K-N). However, while substantial number of both Tfh and Tfr cells also formed

more prolonged interactions with GC B cells, no Tfr cells interactions with GC B cells exceeding 7.5 min were detected (Fig. 2.7M, N).

The data presented above suggest that local production of CCL3 by GC B cells increases their sampling efficiency by Tfr but not Tfh cells *in vivo*, and that this sampling depends on the expression of CCR5 receptor on Tfr cells.

**Intrinsic production of CCL3 by B cells is required for their control in the GCs**

Since CCL3 produced by GC B cells does not promote increased entry or retention of Tfr cells in the GC light zone, but rather is important for their local contacts with GC B cells, we then asked whether intrinsic production of CCL3 by B cells is required for their control in the GCs. To address that we generated mixed bone marrow (BM) chimeras reconstituted 50:50 with either CD45.2 $CCL3^{+/+}$:CD45.1 $CCL3^{+/+}$ BMs (control chimeras, #I) or CD45.2 $CCL3^{-/-}$:CD45.1 $CCL3^{+/+}$ BMs (CCL3/WT chimeras, #II), immunized them and monitored the composition of the GCs compared to the naïve B cell compartment (Fig. 2.8A). No difference in the participation of polyclonal $CCL3^{+/+}$ and $CCL3^{-/-}$ B cells in the early GC response was observed (Fig. 2.8B, day 8). However, while $CCL3^{+/+}$ B cells were similarly engaged into the GC response in both types of chimeras, $CCL3^{-/-}$ GC B cells were overrepresented in the GCs at days 10 and 15 (Fig. 2.8B). The observed 1.5-fold increase in $CCL3^{-/-}$ GC B cells was consistent with the increase in the GC B cell numbers observed in CCL3-KO mice (Fig. 2.8B-G). Of note, the numbers of Tfh or Tfr cells were not statistically different between the CCL3/WT and control BM Chimeras at 10 d.p.i. (Fig. 2.8C and D, day 10). We also tested whether the overexpansion of $CCL3^{-/-}$ GC B cells occurred in GCs seeded exclusively by $CCL3^{-/-}$ B cells or in GCs with a mixed composition of $CCL3^{+/+}$ and $CCL3^{-/-}$ cells. Quantitative immunofluorescent analysis demonstrated that in CCL3/WT chimeras, GCs consisted of mixed $CCL3^{+/+}$ and $CCL3^{-/-}$ B cell populations with some of them containing larger fractions of GC B cells deficient for CCL3 (Fig. 2.8E and F). In summary, the BM chimera's data suggests that intrinsic production of CCL3 by B cells is required for their control in mixed GCs.

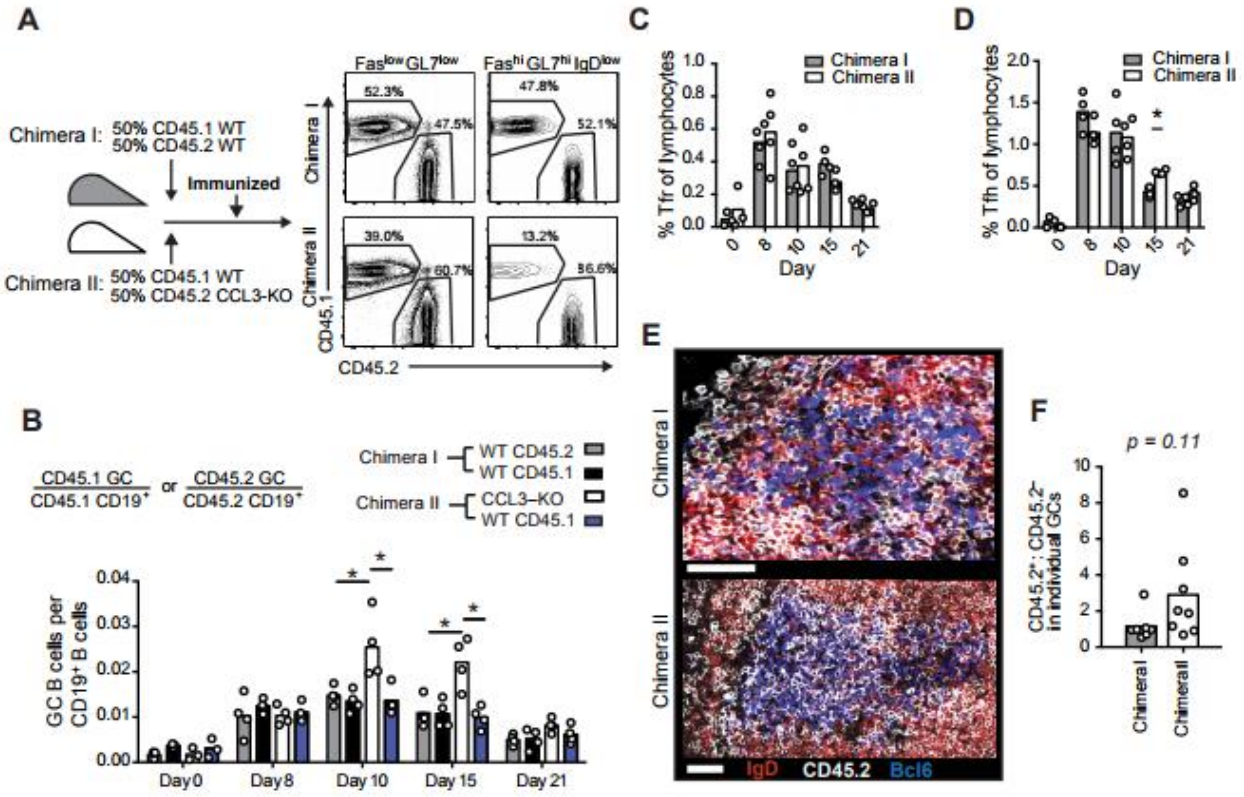


**Figure 2.8. Intrinsic production of CCL3 by B cells is required for their control in mixed GCs.**

A, Experimental outline and generation of mixed 50:50 WT/WT (Chimeras I) and WT/CCL3-KO (Chimeras II) BMChs (left) and example of flow cytometry analysis of total CD19+ cells and GC cells from draining pLNs of BMChs on day 10 p.i. with OVA in CFA (right). B-D, Flow cytometry analysis of draining pLNs from mixed BMChs at the indicated d.p.i. B, Fractions of CD45.1 or CD45.2 GC B cells relative to their respective CD19+ B cell population. C, D, Ratio of Tfr (C) or Tfh (D) cells to total lymphocytes. For B-D, data represents 4 independent experiments. Bars represent means and each symbol represents an individual mouse. (*, $P<0.05$, ANOVA with Dunnet post-analysis.) E, F, Ratio of CD45.2 to CD45.1 cells within distinct GCs of Chimera I and Chimera II as assessed by confocal microscopy analysis of pLNs at 15 d.p.i. from 2 independent experiments with 2 mice per experiment. E, Representative confocal image of draining pLN sections from WT/WT BMChs (top panel) and WT/CCL3-KO BMChs (bottom panel) stained with Bcl6 (blue), CD45.2 (white) and IgD (red)-specific antibodies. Scale bar represents 30 µm. F, Each point represents the ratio of $IgD^{low}$ $CD45.2^{+}Bcl6^{+}$ to $CD45.2^{-}Bcl6^{+}$ cells in sections calculated for individual GCs across at least 2 sections per GC. Bars represent the mean values. (Statistical analysis by two-tailed Student's *t*-test.)

**Transient depletion of Tregs leads to relative increase in CCL3$^{+/+}$ vs. CCL3$^{-/-}$ HyHEL10 GC B cells**

The simplest model that could explain the experimental observations made above is that GC B cell-secreted CCL3 promotes their direct interactions and inhibition by Tfr cells. In that case, transient depletion of Tfr cells should lead to increased expansion of CCL3-proficient compared to CCL3-KO GC B cells (Fig. 2.9A). In order to test that, we co-transferred CCL3$^{+/+}$ and CCL3$^{-/-}$ HyHEL10 B cells into recipient FoxP3$^{DTR}$ mice, immunized mice to promote HyHEL10 entry into GC response and then treated mice with DTx to promote transient depletion of FoxP3$^{+}$ cells or with PBS for control (Fig. 2.9B). First, we looked into recruitment of HyHEL10 B cells into the GCs. Surprisingly, at 6 d.p.i. twice as many CCL3$^{+/+}$ than CCL3$^{-/-}$ HyHEL10 B cells entered into GC response. However, at 9 d.p.i. we observed a trend suggesting relative expansion of CCL3$^{-/-}$ Hy10 GC B cells (Fig. 2.9C). As expected, treatment of the recipient mice with DTx led to significant drop in Tfr cells numbers in 3 days (Fig. 2.9D, E) and small increase in the GC B cell numbers (Fig. 2.9F). Upon Tfr cell depletion, we detected relative increase in CCL3$^{+/+}$ compared to CCL3$^{-/-}$ HyHEL10 GC B cells (Fig. 2.9G, H). Therefore, the data is consistent with direct CCL3-dependent inhibition of GC B cells by Tregs at the peak of GC response (Fig. 2.9A).

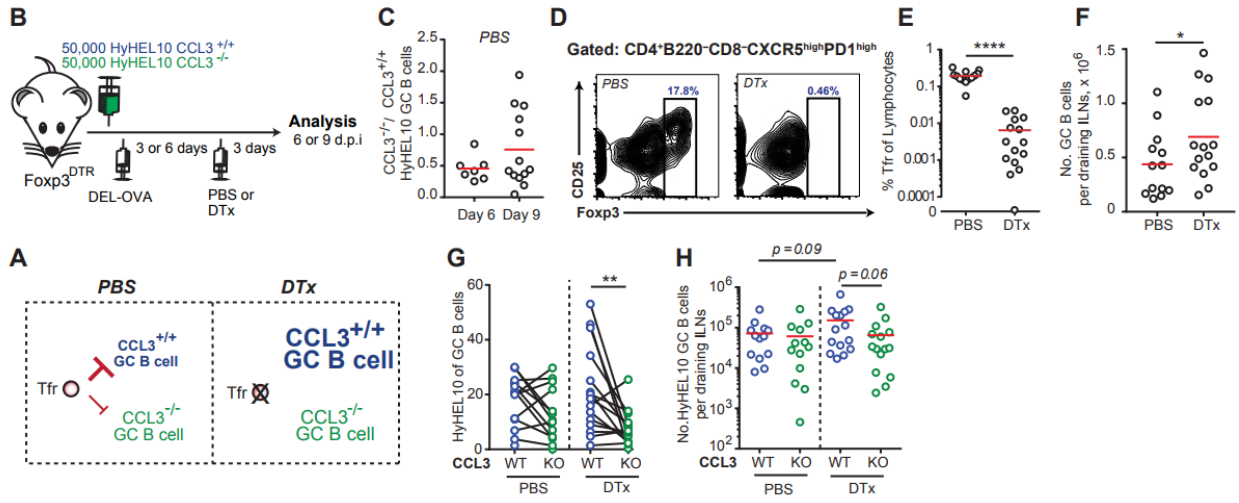


**Figure 2.9. Tregs limit B cell participation in GCs in a CCL3-dependent manner.**
**A**, Suggested model of CCL3-dependent regulation of GC B cells by Tfr cells and prediction for $CCL3^{+/+}$ and $CCL3^{-/-}$ GC B cell participation in GCs upon ablation of Tfr cells. **B**, Experimental outline. $FoxP3^{DTR}$ recipient mice were transferred with HyHEL10 B cells, immunized with 50 µg DEL-OVA in Ribi s.c. and then treated either with PBS or 5 µg DTx in PBS i.p. 3 days before analysis. **C**, The ratio of $CCL3^{-/-}$ to $CCL3^{+/+}$ HyHEL10 GC B cells ($CD19^{+}CD8^{-}CD4^{-}Fas^{high}GL7^{high}\ IgD^{low}$) at 6 and 9 d.p.i. in $FoxP3^{DTR}$ recipient mice treated with PBS. **D-H**, Flow cytometry analysis of cell participation in immune response at 9 d.p.i. in DTx-treated and control mice. **D**, **E,** DTx-mediated depletion of Tfr cells. Representative example (**D**) and Tfr fraction of total lymphocytes (**E**). (Student's t-test, ****, P<0.00001.) **F-H,** Flow cytometry analysis of total GC numbers per draining ILNs (F), the fractions of $CCL3^{+/+}$ and $CCL3^{-/-}$ HyHEL10 GC B cells in respect to the total GC cells (G), and the total numbers of HyHEL10 GC B cells of each kind per draining ILNs (H). Each dot represents a single mouse and paired analyses are indicated using a solid black line. 5 independent experiments. (One-tailed, Student's t-test was used in F; **, p<0.005. One-tailed, paired, Student's t-test used in G. ANOVA followed by Dunnet's multiple comparison test with one-tailed p values reported for H)

## Discussion

Tfr cells have been reported to control the size of GCs, decrease the magnitude of foreign antigen-specific antibody responses, restrain participation of bystander B cell clones in the GCs and prevent development of anti-dsDNA antibodies in pristane immunized-mice [125, 127-129, 131]. However, the molecular and cellular mechanisms of Tfr cell-mediated control of GCs are not fully understood. Multiple molecular players, including IL10, TGF-β, GLUT-1 and IL21 have been suggested to be involved in Tfr cell-dependent regulation [125, 131, 134, 141-143]. Tfr cells have been shown to control the numbers, specificity to foreign antigen and cytokine production by Tfh cells [131, 134, 141, 142] that could in turn affect GC responses [19, 179]. In addition, Tfr cells could inhibit B cells' expansion, class-switching and antibody production in cell culture in a GLUT-1-dependent fashion [143]. However, whether Tfr cells can directly repress GC B cells *in vivo* has not been definitively demonstrated.

Our *in vivo* data suggests that B cells' participation in GC response may depend on their direct interactions with Tfr cells. First, we determined that GC centrocytes upregulate expression of CCL3/4 compared to naïve B cells and centroblasts. We then showed that Tfr cells transmigrate to CCL3 and CCL4 in transwell assays and demonstrated that CCL3 production by GC B cells increases their encounters with Tfr cells *in vivo*. Lastly, we showed that CCL3 deficient B cells were transiently over expanded in the GCs of mixed CCL3-KO/WT BMChs and that depletion of regulatory T cells at the peak of GC response resulted in a relative increase in the numbers of CCL3-proficient compared to CCL3-KO foreign antigen-specific GC B cells. Taken together these observations suggest that production of CCL3 by GC B cells promotes their direct interactions with and control by Tfr cells (Fig 2.10A). While deletion of CCL3 is sufficient to exert an effect on GC-Tfr cell encounters and promote accumulation of GC B cells *in vivo*, future studies should address whether CCL4 chemokine secreted by GC B cells may further contribute to their interactions and regulation by Tfr cells.

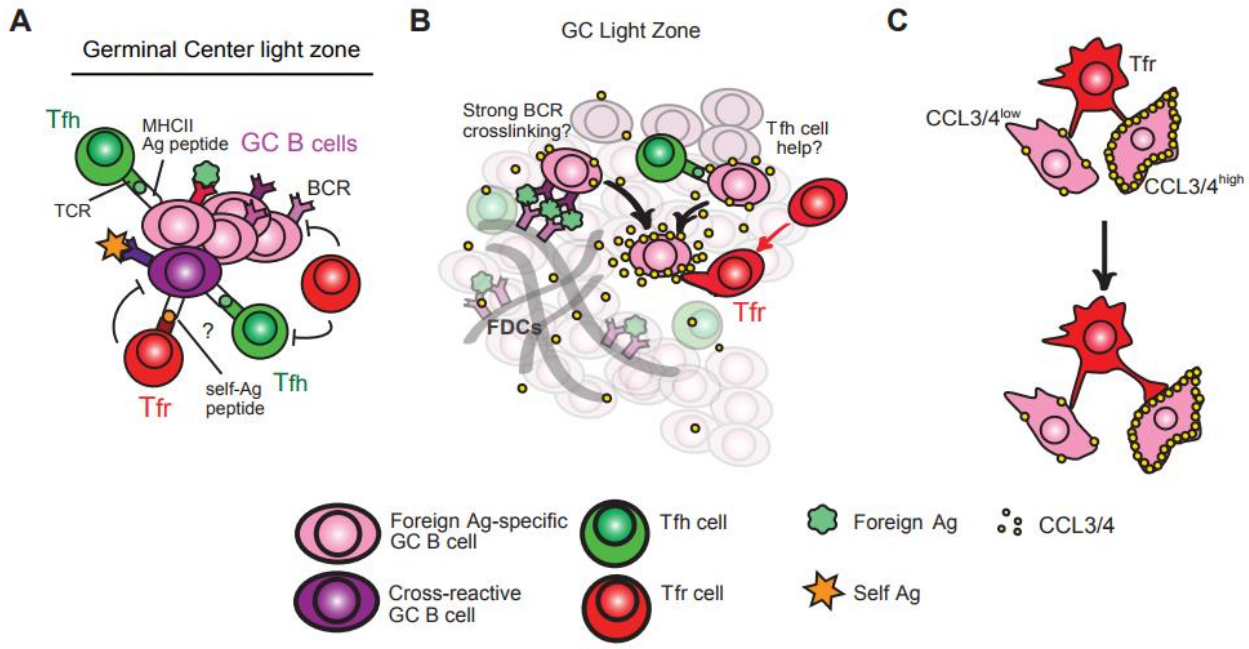


**Figure 2.10: Model of direct GC B cell regulation by Tfr cells.**
A model of direct control of foreign antigen-specific and auto-reactive GC B cell by Tfr cells suggested based on the data that CCL3 secretion by GC B cells promote their direct sampling by Tfr cells and is required for control of GC B cell expansion and elimination of anti-nuclear B cell clones. **A**, General model that illustrates a possible scenario of direct non-cognate interactions between Tfr and foreign-Ag specific GC B cells as well as cognate interactions with self-peptides presenting cross-reactive GC B cells. **B**, A model of local CCL3 gradients produced by selected GC B cells following strong BCR crosslinking (and/or T cell help). Local gradients could then enable enhanced chemotactic sampling of selected GC B cells by the rare Tfr cells traversing the GCs. **C,** A model of how secreted CCL3 immobilized on the surface of GC B cells may act to stabilize very transient interactions of Tfr cells with GC B cells and result in more extensive GC B cell control.

Similar contact frequency of CCR5 receptor-deficient Tfr cells with CCL3-proficient and CCL3-KO GC B cells observed *in vivo* suggests that CCR5 is the predominant receptor on Tfr cells for sensing CCL3 production by GC B cells in wild-type mice.

The effects observed in CCL3-KO mice are consistent, at least in part, with dysregulation of Tfr cells-mediated control. First, similar to the findings reported for mice with CXCR5-deficient Tregs that cannot access B cell follicles [129], we found a small transient increase in the total GC B cells including foreign antigen-specific GC B cells in CCL3-KO mice at 10 d.p.i. In addition, we observed increased development of IgA antibodies in the immunized CCL3-KO mice, as was previously detected in

$Bcl6^{fl/fl}Foxp3^{cre}$ mice that lack Tfr cells [131]. Finally, our data is consistent with the studies where targeted depletion or deficiency in Tfr cells leads to accumulation of non-foreign antigen-specific clones in GCs and development of autoreactive antibodies [127, 131]. Following immunization, significantly more CCL3-KO compared to WT mice, developed class-switched ANAs. Consistent with the role of B-cell intrinsic production of CCL3 for their control in GCs, we observed increased generation of ANA IgG in immunized MD4 mice that had received CCL3-KO, but not WT B cells. While increased GC size and generation of ANA could be associated with defective clearance of dying GC B cells [180, 181], this is an unlikely scenario for CCL3-KO mice, since the fractions of apoptotic GC B cells in the CCL3-KO and WT mice were comparable. Together this data suggests that CCL3 production is required for regulation of both foreign-Ag specific and anti-nuclear B cell clones.

The observed dysregulation of humoral responses in CCL3-KO mice was not due to reduced frequency of Tfr cells in the follicles or in the GCs. While we found that CCL3 is not required for Tfr cell entry into the GC light zone, in CCL3-KO mice the frequency of Tfr and Tfh cells in the GC dark zone is elevated. Future studies should address whether CCL3 secreted by follicular B cells and centrocytes reduce follicular T cells' access into the GC Dark zone and determine whether dysregulated positioning of follicular T cells or some other mechanisms may contribute to development of ANA in the immunized CCL3-KO mice.

We suggest two possible models that could explain CCL3-dependent regulation of GC B cells described in this work. First, the observed regulation could be due to local chemo-attraction of Tfr cells to a subset of CCL3-secreting B cells within GCs. Since BCR crosslinking has been reported to induce upregulation of CCL3/4 production in GC B cells [149], we hypothesize that GC centrocytes that recently acquired antigen from FDCs (and possibly T cell help) are likely to produce more CCL3 than other GC B cells, and thus could form local short-range gradients of these chemokines in the light zone (Fig. 2.10B). Since our intravital imaging system does not allow discrimination between $CCL3^{hi}$ vs. $CCL3^{low}$ GC B cells, the advantage that $CCL3^{hi}$ GC B cells may have in

attracting Tfr cells may be significantly underestimated. Alternatively, CCL3 chemokine secreted by GC B cells may serve to stabilize very transient probing interactions of GC B cells with Tfr cells that are beyond the resolution capabilities of intravital 2P microscopy (Fig. 2.10C). Both of these models can lead to decreased efficiency in sampling of CCL3 KO B cells by Tfr cells and may explain ineffective control of both foreign-Ag specific as well as bystander/self-reactive clones in the GCs.

Previous intravital imaging studies of Tfh cell interactions with cognate GC B cells revealed that majority of these encounters are transient [61].They also suggested that a small fraction of the interactions that are more prolonged (> 5-10 min) may be more efficient for productive communication between the cells and for GC B cell selection [36]. In this study we found that similarly to Tfh cells majority of interactions between foreign-antigen specific GC B cells and natural Tfr cells *in vivo* are shorter than 5 min. Interestingly, Tfr cells also formed some prolonged interactions with GC B cells. However, while a few Tfh cell contacts with GC B exceeded 7.5 min, none of these have been observed for Tfr cells. This discrepancy may be due to non-cognate interactions or very weak cognate interactions between foreign antigen specific GC B cells and natural Tfr cells. However, future studies should directly address whether Tfr cells recognize MHCII/self-peptides or MHCII/foreign peptide on GC B cells via T cell receptors (TCR), and how prevalent these cognate interactions are (Fig. 2.10A). Whether the observed transient interactions between GC B cells and Tfr cells occur in a cognate or non-cognate fashion, they appear to be sufficient for direct inhibition of GC B cells *in vivo*. Future studies should address which molecular factors, in addition to CCL3, promote the observed suppression.

In summary, our findings suggest that in addition to previously reported indirect control of GC B cells through Tfh cells, Tfr cells may also directly probe and repress GC B cells *in vivo* in a CCL3 chemokine-dependent fashion, ensuring robust control of T-dependent B cell responses.

**Description and link to movies**

Movie S1. 2-photon imaging of Tfr cells migration in respect to Tfh cells and GC B cells. Also see **Fig. 2.6E**. A time-lapse sequence of a 110 µm z-stack of a GC in an explanted inguinal lymph node imaged at 8 days after immunization. HyHEL10 GC B cell; cyan. Tfr; red. Tfh; green. Colored lines indicate the trajectories of the indicated cell types, tracked by Imaris and manually verified. Mice were generated as described in the **Fig. 2.6A**. Time is shown as hh:mm:ss and z-stacks were acquired at 20 second intervals.

Movie S2. Intravital imaging of Tfr cells in respect to the GCs containing both $CCL3^{+/+}$ and $CCL3^{-/-}$ HyHEL10 B cells**.** The data shown corresponds with the images in **Figure 7C**. A time-lapse sequence of a GC within inguinal LN of a mouse prepared as described in **Fig. 2.7A** and subjected to intravital imaging at 8 days post immunization. 180 µm z-stack. GC volume (gray surface) was defined based on the distribution of CFP HyHEL10 cells. Quantitative analysis in **Fig. 2.7** was performed for Tfr cells (red) interactions with HyHEL10 GC B cells ($CCL3^{+/+}$; cyan. $CCL3^{-/-}$; green.) within GC volumes defined in the same fashion. The tracks of individual Tfr cells outside the GC are labeled in purple while interior tracks are represented in yellow lines. Time is expressed as hh:mm:ss and z-stacks were acquired at 20 second intervals.

Movie S3. Examples of Tfr cells interactions with GC B cells identified as “strict” or “non strict” for quantitative analysis**.** A time-lapse sequence of a representative Tfr (red) entering the GC (dashed white line) and then undergoing contacts with HyHEL10 $CCL3^{+/+}$ (cyan) or $CCL3^{-/-}$ (green) HyHEL10 GC B cells within inguinal LN of a mouse prepared as described in **Fig. 2.7A** and subjected to 2P imaging at 8 days post immunization. A 40 µM slice is in view. Inlets are zoomed in and 3D rotated to visualize the contact. Time is expressed as mm:ss and z-stacks were acquired at 25 second intervals

Movie S4. 2-photon imaging of CCR5-deficient Tfr cells interacting with GC B cells. A time-lapse sequence of a GC within in an inguinal LN of a mouse prepared as described in **Fig. 7A** with $CCR5^{-/-}$ Tfr cells and subjected to explant imaging at 8 days post immunization. 120 um z-stack. Quantitative analysis was performed for CCR5-deficient Tfr cells (red) interactions with HyHEL10 GC B cells ($CCL3^{+/+}$, cyan; $CCL3^{-/-}$, green) within the GC and can be found in **Fig. 2.7E, F, K, L**. Time is shown as hh:mm:ss and z-stacks were acquired at 20 second intervals.

Movie S5. 2-photon imaging of Tfh cells interacting with GC B cells. A time-lapse sequence of a GC within an inguinal LN of a mouse prepared as described in **Figure 2.7B** and subjected to explant imaging at 8 days post immunization. 140 um z-stack**.** Quantitative analysis was performed for Tfh cells (red) interactions with HyHEL10 GC B cells ($CCL3^{+/+}$, cyan; $CCL3^{-/-}$, green) within the GC and can be found in **Fig. 2.7M-R**. Examples of long duration (>5 minutes) contacts and short duration (<5 minutes) contacts are shown in 10 um z-projections. Time is shown as hh:mm:ss for both time of the movie and for duration of the indicated contacts. Z-stacks were acquired at 20 second intervals.

# Chapter 3 -Antigen acquisition enables newly arriving B cells to enter ongoing immunization-induced germinal centers

Portions of this chapter have been published:
Turner J.S.*, Benet Z.L.*, and Grigorova I.L. Antigen Acquisition Enables Newly Arriving B cells to Enter Ongoing Immunization-Induced Germinal Centers. Journal of Immunology. 2017 Aug 15;199(4):1301-1307. PMID: 28687657. * Both authors contributed equally.

## Abstract

Modern vaccines must be designed to generate long-lasting, high-affinity, and broadly neutralizing Ab responses against pathogens. The diversity of B cell clones recruited into germinal center (GC) responses is likely to be important for the antigen-neutralization potential of the Ab-secreting cells and memory cells generated upon immunization. However, the factors that influence the diversity of B cell clones recruited into GCs are unclear. As recirculating naive antigen-specific B cells arrive in antigen-draining secondary lymphoid organs, they may join the ongoing GC response. However, the factors that limit their entry are not well understood, and it is not known how that depends on the stage of the ongoing follicular T cell and GC B cell response. In this article, we show that, in mice, naive B cells have a limited window of time during which they can undergo antigen-driven activation and join ongoing immunization-induced GC responses. However, preloading naive B cells with even a threshold-activating amount of Ag is sufficient to rescue their entry into the GC response during its initiation, peak, and contraction. Based on these results, we suggest that productive acquisition of Ag may be one of the main factors limiting entry of new B cell clones into ongoing immunization-triggered GC responses.

## Introduction

A hallmark of T-dependent B cell responses is generation of germinal centers (GCs), which are important for the development of long-term high affinity humoral immunity [66, 182]. GCs are anatomical substructures in B cell follicles that form around follicular dendritic cells (FDCs). GCs are seeded by antigen-activated B cells that have acquired cognate T cell help, proliferated, and differentiated into GC B cells. Within GCs, B cells undergo extensive proliferation, somatic hypermutation of their B cell receptors (BCRs), and class-switching and compete for Ag deposited on FDCs and for help from follicular helper T cells (Tfh) [183]. Tfh cells can drive GC B cells' affinity maturation by providing help preferentially to GC B cells that present more antigenic peptides in the context of MHCII, thus rescuing GC B cells from apoptosis and promoting their proliferation [22, 184]. In parallel, follicular regulatory T cells (Tfr) fine-tune GCs by down-regulating the magnitude of the GC response and by preventing expansion of non antigen-specific B cell clones [127, 129]. GC B cells then differentiate into long-lived plasma cells and class-switched memory B cells that harbor immunoglobulins and BCRs, respectively with higher affinity to foreign antigens [185-188].

While generation of long-lived plasma cells and memory B cells is a prerequisite for development of long-term humoral immunity, the diversity of B cell clones that participate in GC responses may contribute to the breadth of antigenic epitopes recognized by effector cells and therefore to the pathogen neutralization potential of the response.

While previous studies suggested that GCs are formed by relatively few B cells, recent works unambiguously demonstrated that GCs are seeded by 50-200 B cell clones [67, 189-191]. However, the ability of antigen-specific B cells to populate early GCs is variable. When T cell help is limiting, B cell clones with relatively low affinity to Ag are recruited into GCs less efficiently [192].

Preexisting GCs can also be populated by new B cell clones following a boosting immunization [193]. However, which factors control or limit recruitment of new B cell clones into ongoing GCs over the course of an infection or following a primary immunization is not known. Naïve antigen-specific B cells' ability to enter preexisting "late" GCs is potentially limited by multiple factors, including limited availability of antigens to naive cells, competition with pre-existing GC B cells for Tfh cell help, differences in the helper functions of Tfh cells over time [194], and increased exposure of B cells to Tfr cells. In this study, we attempted to assess how the likelihood of new B cell recruitment into GCs depends on the stage (initiation, peak, or contraction) of the Tfh/Tfr and GC response.

Our study suggests that B cells that transiently acquire a low amount of Ag can enter GCs at all stages of the response. However, the ability of naïve B cells to undergo antigen-dependent activation and recruitment into the GC response drops by 6-10 days after a standard immunization. We suggest that the main factor limiting the entry of new B cell clones into GCs after a primary immunization may be the availability of Ag for sampling by the naïve B cell repertoire.

**Materials and methods**

*Mice.* B6 (C57BL/6) mice were purchased from Charles River Laboratory. B6- CD45.1 (Ptprc$^{a}$ Pepc$^{b}$/BoyJ) were purchased from the Jackson Laboratory. BCR transgenic HyHEL10 [195] and MD4 mice [172] were generously provided by Jason Cyster. HyHEL10 mice were crossed with UBC-GFP (004353) (Jackson Laboratory) and with B6- CD45.1 mice and maintained on the B6 background. MD4 mice were crossed with B6-CD45.1 and maintained on the B6 background. Recipient mice were 6–10 weeks of age. All mice were maintained in a specific pathogen free environment and protocols were approved by the Institutional Animal Care and Use Committee of the University of Michigan.

*Antigen preparation*. Duck eggs were purchased locally. Duck egg lysozyme (DEL) was purified as previously described [195]. Ovalbumin (OVA) were purchased from Sigma. DEL was conjugated to OVA via glutaraldehyde cross-linking as previously described [195].

*Immunization and adoptive transfer and immunization*. Where indicated, recipient mice were preimmunized subcutaneously (s.c.) in the flanks and base of tail and into front foot pads (f.f.p.) with 100 µg OVA in Ribi (Sigma) or s.c. with 50 µg DEL-OVA in Ribi.

HyHEL10 B cells were enriched from donor mice by negative selection as previously described [196]. Transient exposure to antigen was performed as previously described with an Ag dose slightly above the threshold required for B cell activation [197]. In brief, purified HyHEL10 B cells were incubated with 0.5 µg/mL DEL-OVA *ex vivo* for 5 minutes at 37 °C and washed three times with room temperature DMEM supplemented with 4.5 g/L glucose, L- glutamine and sodium pyruvate, 2% FBS, 10 mM HEPES, 50 IU/mL penicillin, and 50 µg/mL streptomycin. About 5 x$10^4$ DEL-OVA-pulsed or naïve HyHEL10 B cells were then transferred into recipient mice. To study MD4 B cell activation, splenocytes from MD4 CD45.1 mice with a known frequency of transgenic B cells were transferred into recipient CD45.2 mice either unimmunized or s.c. pre-immunized with DEL-OVA in Ribi.

*Flow cytometry and cytokine staining*. The following antibodies (Abs) and reagents were used for flow cytometry analysis: biotinylated anti-mouse IgD (11-26/SBA-1, SouthernBiotech) and CXCR5 (2G8, BD Biosciences); fluorescently conjugated anti-mouse IgD-APC-Cy7 (11- 26c.2a, Biolegend), $IgM^a$-PE (DS-1, BD Pharmingen), $IgM^b$-PE (AF6-78, BD Pharmingen), PD1-PE-Cy7 (RMP1-30, Biolegend), CD25-Brilliant Violet 421 (PC61, Biolegend), CD38-PerCP-eFluor 710 (90, eBioscience), B220-V500 and B220-PerCP-Cy5.5 (RA3- 6B2, BD Pharmingen), FAS-PE-Cy7 (Jo2, BD Pharmingen), CD4-APC-Cy7 (RM4-5, Biolegend), CD8-APC-Cy7 (53-6.7, eBioscience), CD45.1-Alexa Fluor 700 (A20, Biolegend), GL7-eFluor 450 (GL7, eBioscience), FoxP3-APC (clone FJK-16s, eBioscience), CD69-PE (clone H1.2F3, Pharmingen), IL-21-PE

(clone FFA21, eBioscience), IFNγ- Alexa Fluor 700 (clone XMG1.2, Biolegends), and streptavidin-Qdot 605 (Life Technologies). Single-cell suspensions from inguinal lymph nodes (ILNs) were incubated with biotinylated antibodies for 20 minutes on ice, washed twice with 200 µl PBS supplemented with 2% FBS, 1 mM EDTA, and 0.1% $NaN_3$ (FACS buffer), and then incubated with fluorophore- conjugated antibodies and streptavidin for 20 minutes on ice, and washed twice more with 200 µl FACS buffer. For IL-21 and IFNγ cytokine staining, lymphocytes from ILNs of immunized mice were first resuspended in 10% DMEM (DMEM supplemented with 4.5 g/L glucose, L- glutamine and sodium pyruvate, 10% FBS, 10 mM HEPES, 50 IU/mL penicillin, and 50 µg/mL streptomycin) and then cultured in a $CO_2$ incubator, at 37$^oC$ and stimulated with Cell Activation Cocktail (Biolegends) that contains PMA, ionomycin and Brefeldin A for 6 hours according to the manufacturer's instructions. For FoxP3 and cytokine staining the cells were permeabilized and stained using FoxP3 staining buffer set (eBioscience) according to the manufacturer's instructions. Cells were then resuspended in FACS buffer for acquisition. Data were acquired on a FACSCanto and analyzed using FlowJo (TreeStar).

*Immunofluorescence*. The following Abs/reagents were used for confocal immunofluorescent analysis: biotinylated anti-mouse IgD (11-26/SBA-1, SouthernBiotech), CD4-CF594 (RM4-5, BD biosciences), and streptavidin-Alexa Fluor 647 (Life Technologies) or BCL6-A647(clone K112-91, BD-Pharmingen) and IgMa-PE (clone DS-1, BD-Pharmingen). Brachial lymph nodes (BLNs) were harvested from recipient mice, fixed for 1 h in 1% paraformaldehyde in PBS on ice and washed with PBS. They were then blocked overnight in 30% sucrose, 0.1% $NaN_3$ in PBS, embedded in Tissue- Tek optimum cutting temperature compound, snap-frozen in dry ice and ethanol, and stored at -70 °C. Thirty micron cryostat sections were cut from the tissue blocks, affixed to Superfrost Plus microscope slides (Fisher), and stained first with biotinylated anti-IgD Abs and then with anti-CD4 Abs and streptavidin as previously described [197]. Alternatively, they were stained with anti-Bcl6 and anti-IgMa Abs. Confocal analysis of the sections was performed using Leica SP5 with argon and helium-neon lasers, 2-channel Leica SP spectral fluorescent PMT detector, and a 20x

oil-immersion objective with a numerical aperture of 0.7. Images were processed using Imaris (Bitplane).

*Statistics*. Statistical tests were performed as indicated using Prism 6 (GraphPad). Differences between groups not annotated by an asterisk did not reach statistical significance.

## Results

### Kinetics of immunization-induced follicular T cells and GC B cell response

In order to determine whether the ability of B cells to enter immunization-triggered GCs depends on the stage of the GC response, we first analyzed the kinetics of GC B cell and follicular T cell responses in the draining lymph nodes (LNs) of mice immunized with the protein antigen ovalbumin (OVA) in Ribi adjuvant (Fig. 3.1A, B, gating strategy). In unimmunized mice there were over 3 times as many Tfr as Tfh cells (Fig. 3.2A-C). By 6 days post immunization (d.p.i.) the number of Tfh cells significantly increased, reaching a 5:1 Tfh:Tfr ratio. (Fig. 3.2A-C). This was followed by expansion of GC B cells that peaked at 10-14 d.p.i. (Fig. 3.2D, E). At 14 d.p.i Tfh cell numbers and the Tfh/Tfr cell ratio started to decrease, followed by a substantial decline in GC B cell numbers by 21 d.p.i. (Fig. 3.2A-E). Based on the observed kinetics of the GC response and previously published data, GC seeding in the draining LNs is likely to occur between 3 and 6 d.p.i. [33, 198]. This is followed by the peak of the GC response at 10 d.p.i. and its resolution after 14 d.p.i.

Previous studies indicated that Tfh cells' cytokine production and effector functions vary depending on the stage of GC response [194]. To test whether these observations would hold under our selected immunization conditions, we assessed production of IL-21 and lFNγ cytokines by Tfh cells at various times following immunization with OVA in Ribi. Consistent with previous findings [194], we observed a trend for decreased production of IL-21 by Tfh cells during the later stages of the Tfh cell response (Fig. 3.1

F-I). Interestingly, we also found that, during Tfh cells' contraction phase, production of IFN-γ by Tfh cells increased significantly (Fig. 3.1 F-H, J). To summarize, Tfh cell frequency, production of cytokines, and the Tfh/Tfr cell ratio vary during the different stages of the immunization-induced GC reaction; these might affect recruitment and participation of new B cell clones in T-dependent responses

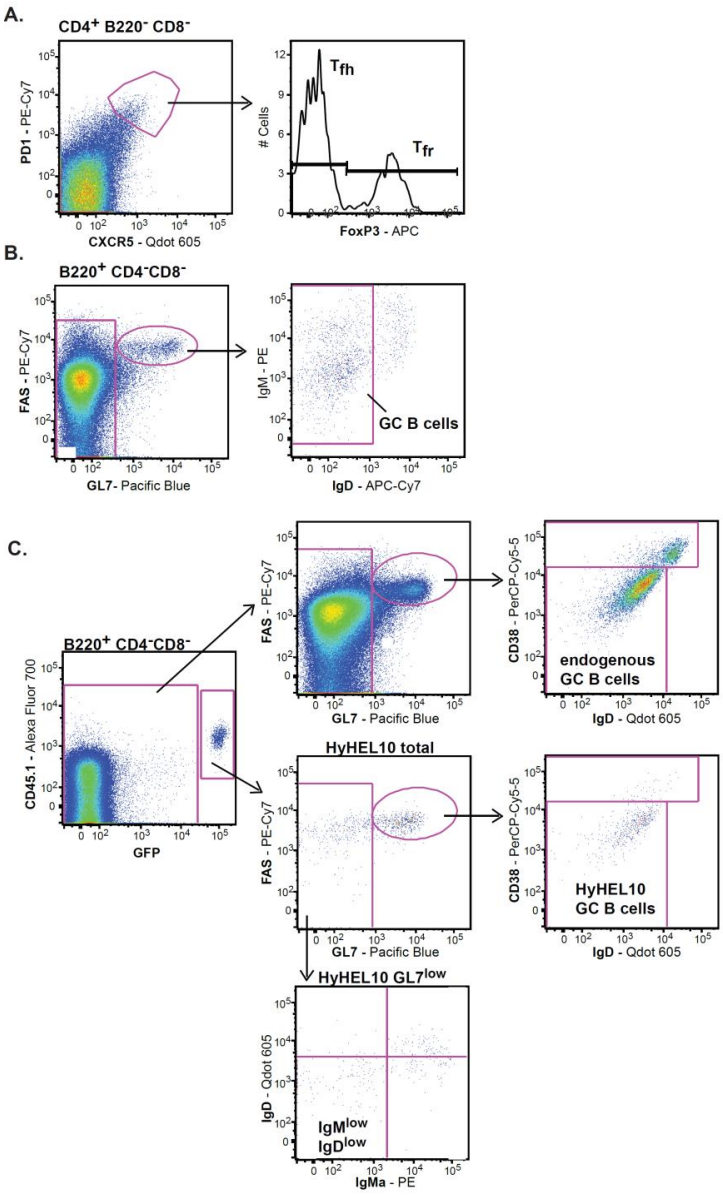


**Figure 3.1: Gating strategy for follicular T cells, GC B cells and class-switched GL7low B cells.**

(**A, B**) Flow cytometry gating strategy for endogenous Tfh and Tfr cells (**A**) and GC B cells (**B**) utilized for analysis presented in Figure 1. **C,** Flow cytometry gating strategy for total, GC, and GL7$^{low}$ class-switched HyHEL10 B cells

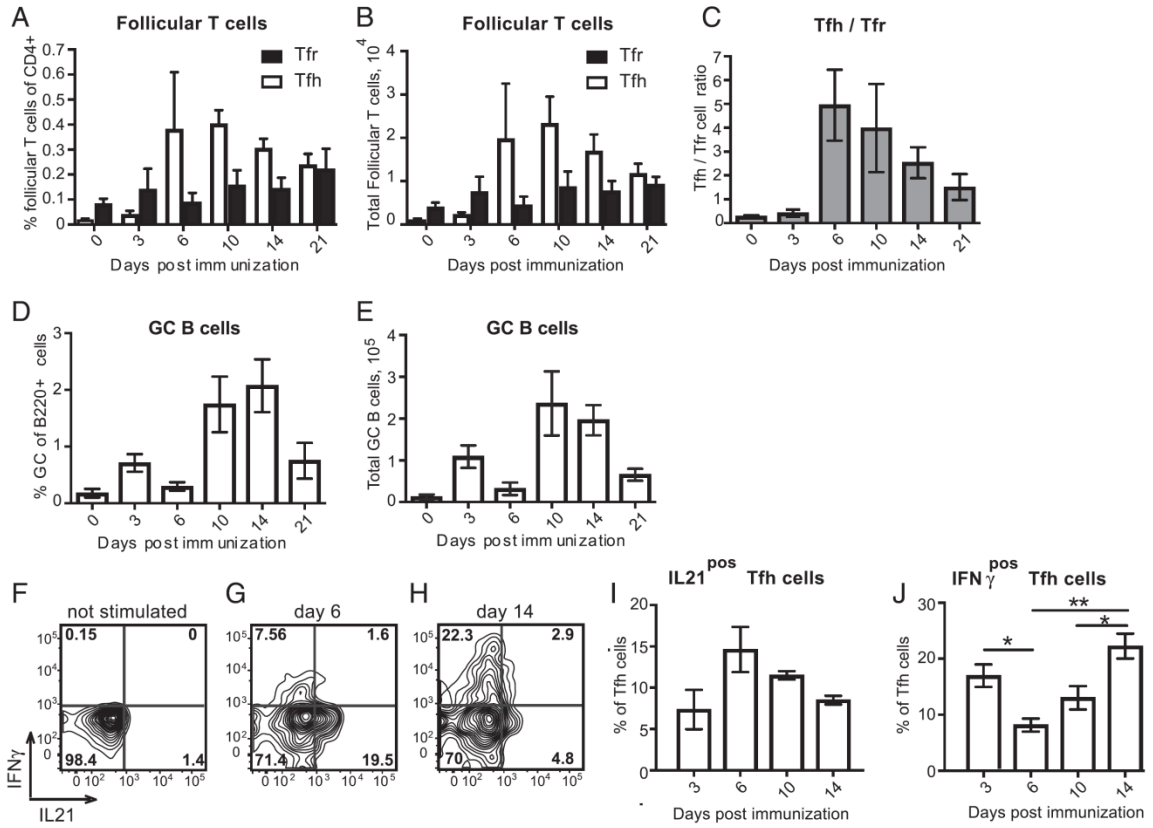


**Figure 3.2: Kinetics of immunization-induced follicular T cell and GC B cell response.**

Flow cytometry analysis of follicular T cells and GC B cells in the ILNs of mice immunized s.c. with OVA in Ribi in the flanks, base of the tail, and into the front foot pads. (**A**) Frequencies of Tfh cells and Tfr cells among $CD4^+$ $B220^-$ $CD8^-$ cells. (**B**) Total numbers of Tfh cells and Tfr cells. (**C**) Tfh/Tfr cell ratios. (**D**) Frequencies of GC B cells among $B220^+$ $CD4^-$ $CD8^-$ cells. (**E**) Total numbers of GC B cells. (**F**–**J**) Analysis of IL-21 and IFN-γ production by Tfh cells at various times following immunization. Representative examples of flow cytometry cytokine staining of $FoxP3^-$ $CXCR5^{high}$ $PD1^{high}$ Tfh cells from ILNs of mice at 6 d.p.i. (F and G) and at 14 d.p.i. (H), following ex vivo stimulation with PMA and ionomycin (G and H) or no ex vivo stimulation (F). Fraction of Tfh cells that upregulate production of IL-21 (I) or IFN-γ (J) following ex vivo stimulation. Data are from three or four independent experiments, with one to three mice per experiment. Data are mean ± SEM. *$p$ < 0.05, **$p$ < 0.01, ordinary one-way ANOVA with Tukey multiple-comparison test.

.

**Antigen-pulsed B cell recruitment into the different phases of the GC response**

To address whether B cells that acquire the same amount of antigen have a substantially different ability to enter GCs depending on the phase of the GC response we made use of a recently published experimental strategy [197](Fig. 3.3A). Transgenic HyHEL10 B cells [61] that have B cell receptors (BCR) specific to duck egg lysozyme (DEL) were incubated ex vivo for 5 minutes with DEL chemically conjugated to OVA (DEL-OVA) at a concentration only slightly above HyHEL10 B cells activation threshold [197]. The unbound antigen was then washed off and HyHEL10 B cells were transferred into mice preimmunized with OVA in Ribi. While DEL-OVA pulsed HyHEL10 B cells could not reacquire their cognate DEL Ag *in vivo*, they could present preacquired OVA Antigenic peptides in the context of MHCII molecules for recognition by OVA-specific Th cells *in vivo*. Our previous study demonstrated that antigen-pulsed B cells transferred into recipient mice preimmunized with OVA for 3 d undergo proliferation, differentiate into GC B cells, and participate in histologically defined GCs in vivo and that their ability to enter the B cell response is critically dependent on the acquisition of the antigen-linked OVA for presentation to activated Th cells [197].

To assess B cell recruitment into an immunization-driven GC response at its various stages, fifty thousand DEL-OVA pulsed HyHEL10 B cells were transferred into recipient mice at 3, 6, 10 and 14 days after immunization with OVA or, for control, into unimmunized mice (Fig. 3.3A). These times correspond to the initiation, peak and contraction phases of the Tfh cell response (Fig. 3.2A-C).

At 4 days after the transfer of antigen-pulsed HyHEL10 B cells, we observed their expansion in the draining LNs of all OVA-immunized recipient mice (Fig. 3.3B). Based on the $GL7^{high}$ $FAS^{high}$ $IgD^{low}$ $CD38^{low}$ phenotype (Fig. 3.2C), comparable numbers of HyHEL10 B cells differentiated into GC B cells in all OVA-immunized, but not in control recipient mice at 4 days after transfer (Fig. 3.3E; Fig. 3.4, black bars). At 6 days after the

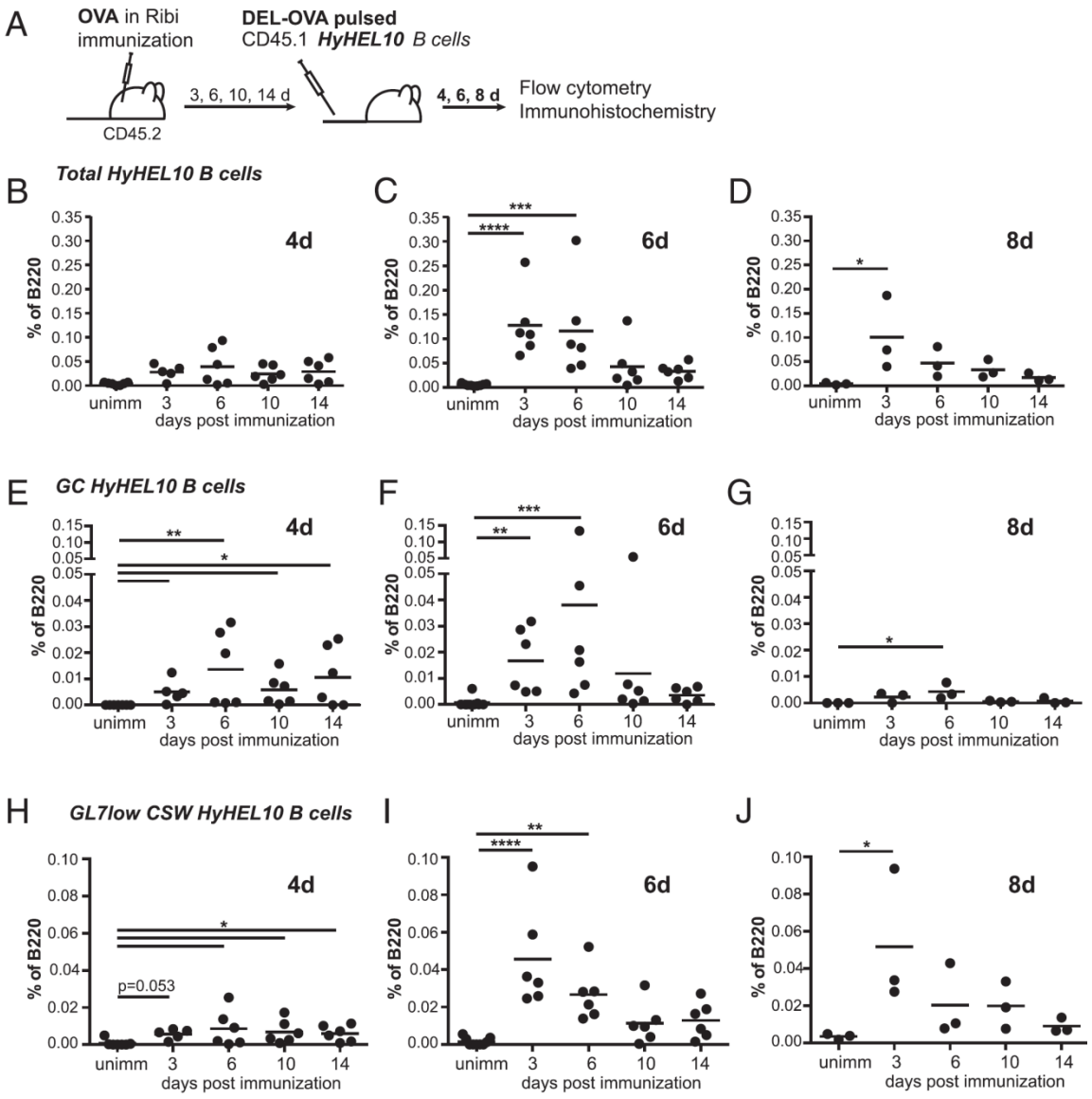


**Figure 3.3: Antigen-pulsed HyHEL10 B cell recruitment into B cell response during initiation, peak and resolution of the immunization-induced GC response.** (**A**) Experimental scheme. A total of 5 × $10^4$ HyHEL10 B cells, pulsed ex vivo with 0.5 µg/ml DEL-OVA, was transferred into unimmunized control mice or mice that were immunized with OVA in Ribi s.c. and in the front foot pads 3, 6, 10, or 14 d earlier. Flow cytometry analysis of ILNs was performed at 4, 6, and 8 d post-HyHEL10 B cell transfer. Frequencies of total HyHEL10 B cells (**B**–**D**) and $GL7^{high}$ $FAS^{high}$ $IgD^{low}$ $CD38^{low}$ HyHEL10 B cells (**E**–**G**) and $GL7^{low}$ $IgM^{low}$ $IgD^{low}$ HyHEL10 B cells (**H**–**J**) among $B220^+$ $CD4^-$ $CD8^-$ cells at 4 d (B, E, and H), 6 d (C, F, and I) and 8 d (D, G, and J) following the transfer. Data are from three to five independent experiments. Each dot represents an individual mouse. *$p \leq 0.05$, **$p \leq 0.01$, ***$p \leq 0.001$, ***$p \leq 0.0001$ versus unimmunized control, Kruskal–Wallis test, with Dunn multiple-comparison test.

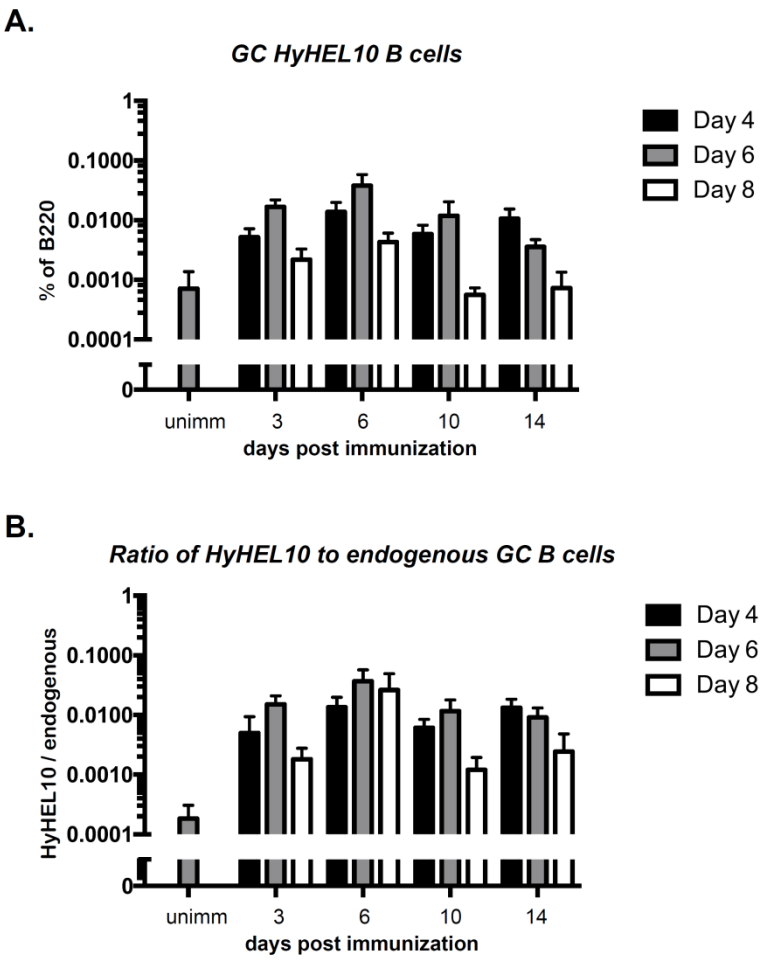


**Figure 3.4: Antigen-pulsed HyHEL10 B cell recruitment into GC responses during initiation, peak and resolution of the immunization-induced GC response.**

$GL7^{high}$ $FAS^{high}$ $IgD^{low}$ $CD38^{low}$ HyHEL10 GC B cells displayed as a fraction of $B220^{+}$ cells (A) and their ratio to endogenous GC B cells (B) at 4d (black bars), 6d (gray bars) and 8d (white bars) following the transfer of DEL-OVA-pulsed HyHEL10 B cells into unimmunized mice or mice preimmunized with OVA in Ribi for 3, 6, 10 and 14 days. Data are from 3-5 independent experiments, shown as mean ± SEM. In A, data is combined from Fig. 3.3 E-G.

transfer the numbers of HyHEL10 GC B cells either slightly increased (when transferred at 3, 6 d.p.i.) or stayed the same (at 10, 14 d.p.i.) (Fig. 3.3F; Fig. 3.4, gray bars). In all cases, HyHEL10 GC B cell numbers started to decline by 8 days after B cell transfer, as expected due to their inability to reacquire their cognate Ag DEL within GCs and compete with OVA-specific endogenous GC B cells (Fig. 3.3G; Fig. 3.4, white bars). Some of the antigen-pulsed HyHEL10 B cells also differentiated into $GL7^{low}$ class-switched B cells, which made up 20-40% of total HyHEL10 B cells by 6-8 days after

their transfer (Fig. 3.3B-D, H-J). Few, if any, HyHEL10 plasma cells were found (data not shown).

The presence of HyHEL10 B cells in the GCs of OVA-immunized, but not control mice, was confirmed by immunofluorescent analysis of draining LNs regardless of the time of transfer following immunization (Fig. 3.5, HyHEL10 B cells express GFP and are detected as green). Majority of GC resident HyHEL10 B cells also expressed Bcl6 (Fig. 3.5B; see examples 1, 4, 7, 10, 11). Of note, HyHEL10 B cells were also found in other regions of B cell follicles with some of them $IgM^a$ positive (Fig. 3.5B; examples 2, 5) and some class-switched (Fig. 3.5B; examples 3, 6, 9).

Altogether these results indicate that at various stages of the OVA-immunization induced endogenous follicular T cell/GC response, acquisition of relatively small amounts of DEL-OVA antigen by newly arriving HyHEL10 B cells is sufficient for their recruitment into the GC and class-switched $GL7^{low}$ memory B cell responses in OVA-draining lymph nodes. However, when antigen-pulsed B cells are transferred at the peak and resolution phases of the Tfh/GC response (at 10 and 14 d.p.i.), their subsequent accumulation as GC and class-switched $GL7^{low}$ B cells at 6 and 8 days after transfer is reduced.

**Naïve B cell recruitment into ongoing GC responses**

To test the ability of naïve B cells to enter the GC response during its various stages, naïve HyHEL10 B cells were transferred into mice immunized with their cognate Ag DEL-OVA in Ribi adjuvant at 0, 3, 6, 10 and 14 d.p.i (Fig. 3.6A). While HyHEL10 B cells

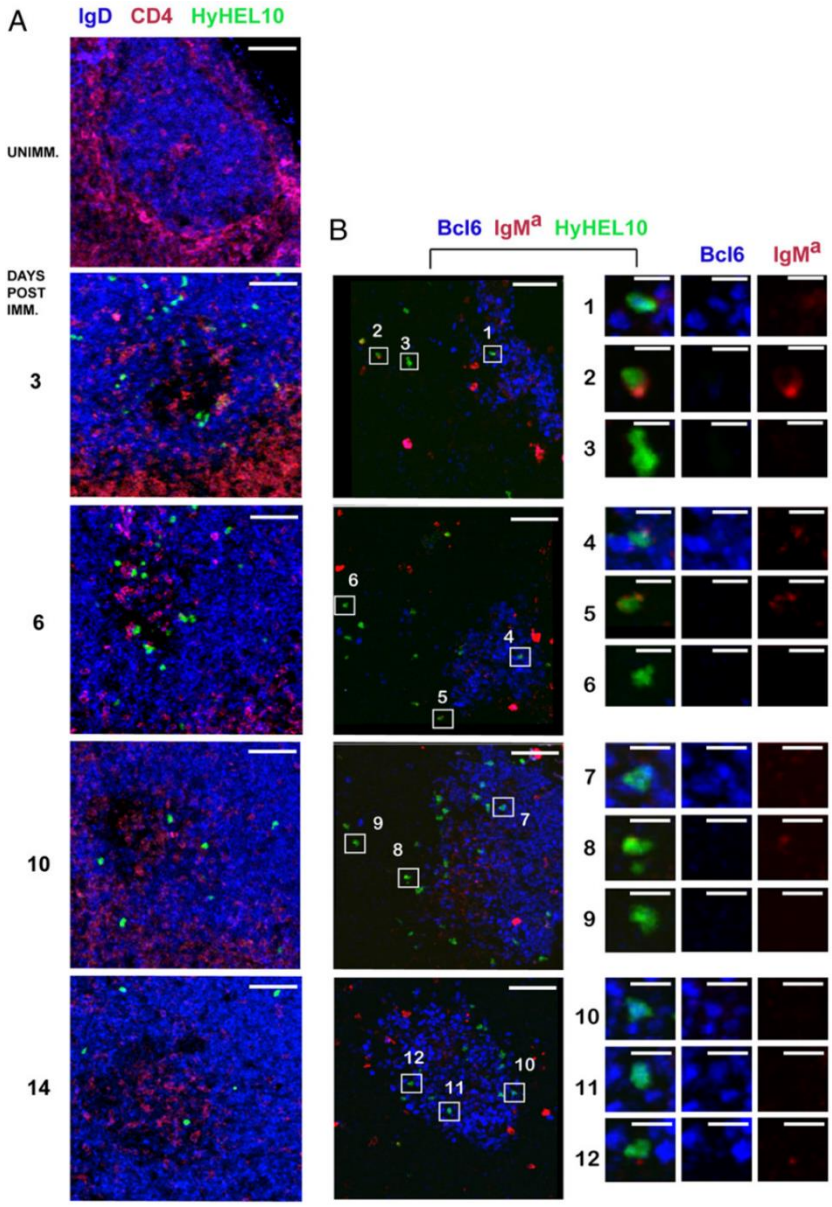


**Figure 3.5: Antigen-pulsed HyHEL10 B cells can enter GCs during the initiation, peak, and resolution of the immunization-induced GC response.**
**(A** and **B**) Examples of DEL-OVA pulsed HyHEL10 B cells' anatomical positioning with respect to GCs. Confocal immunofluorescent analysis of 14–20-μm-thick sections from the brachial LNs of mice that were immunized or not with OVA in Ribi 3, 6, 10, or 14 d before receiving DEL-OVA pulsed HyHEL10 B cells; slides were analyzed at 6 d post transfer. GFP-expressing HyHEL10 B cells are shown in green. Sections were stained with fluorescently conjugated anti-CD4 (red) and anti-IgD (blue) Abs (A) or IgMa (red) and Bcl6 (blue) (B). (B) Right panels show a zoomed-in view of the boxed HyHEL10 cells in the left panels. In (A), $IgD^{low}$ areas represent GCs. In (B), $Bcl6^{+}$ cells are GC B cells; $IgMa^{-}$ HyHEL10 B cells are CSW. Red staining not colocalized with $GFP^{+}$ HyHEL10 cells is likely due to nonspecific binding of IgMa to other cells, presumably to macrophages and FDCs. The data are representative of three independent experiments, with one mouse per experiment. Scale bars: 50 μm (A and B, left panels), 10 μm (B, right panels).

transferred into recipient mice prior to or 3 days after the immunization mounted a vigorous GC B cell response, their ability to form GC B cells began to decline when they were transferred 6 days following the immunization and completely disappeared at later times (Fig. 3.6B, white bars). Naïve HyHEL10 B cells also formed substantially smaller class-switched B cell responses when transferred into DEL-OVA immunized mice with a 10-14 day delay (Fig. 3.6C, white bars). However, HyHEL10 B cells pulsed with a low dose of Ag (0.5 μg/ml of DEL-OVA) formed GC B cells and class-switched GL7$^{low}$ cells when transferred into DEL-OVA immunized mice even at the peak and prior to contraction phases of the GC response, similarly to antigen-pulsed cells transferred into OVA-immunized mice (Fig. 3.6B, C, gray bars, Fig. 3.3E-J).

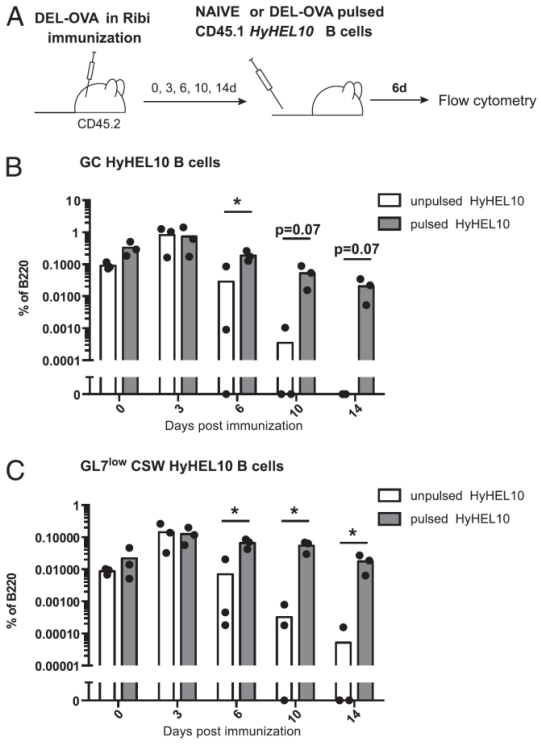


**Figure 3.6: Recruitment of naïve and DEL-OVA-pulsed HyHEL10 B cells into B cell response during initiation, peak and resolution of GC response in DEL-OVA immunized mice.**

(A) Experimental scheme A total of 5 × 104 HyHEL10 B cells (naive or pulsed ex vivo with 0.5 μg/ml DEL-OVA) was transferred into mice immunized s.c. with DEL-OVA in Ribi 0, 3, 6, 10, or 14 d earlier. Flow cytometry analysis of ILNs was performed at 6 d post-HyHEL10 B cell transfer. Frequencies of unpulsed or DEL-OVA–pulsed HyHEL10 GL7high FAShigh IgDlow CD38low (B) and HyHEL10 GL7low IgMlow IgDlow (C) B cells among B220+ CD4− CD8− cells. Data are from three independent experiments. Each point represents one mouse. *p < 0.05, multiple t tests with the Holm–Sidak correction for multiple comparisons.

To test whether B cells have a limited window of time to undergo Antigen-driven activation following a standard protein immunization, we utilized BCR transgenic B cells from MD4 mice that have the same specificity to DEL as HyHEL10 B cells. While MD4 B cells cannot undergo class-switching as HyHEL10 B cells, they are better for enumeration of Antigen-specific B cells by flow cytometry because they constitute the majority (>95%) of B cells in MD4 mice. Splenocytes from CD45.1 MD4 mice were transferred into recipient CD45.2 mice preimmunized with DEL-OVA in Ribi for 3, 6 and 10 days or into unimmunized control mice. One day later Antigen-driven activation of the recently arriving MD4 B cells was assessed in the ILNs of preimmunized mice based on their upregulation of surface CD69 (Fig. 3.7A). We found that many MD4 B

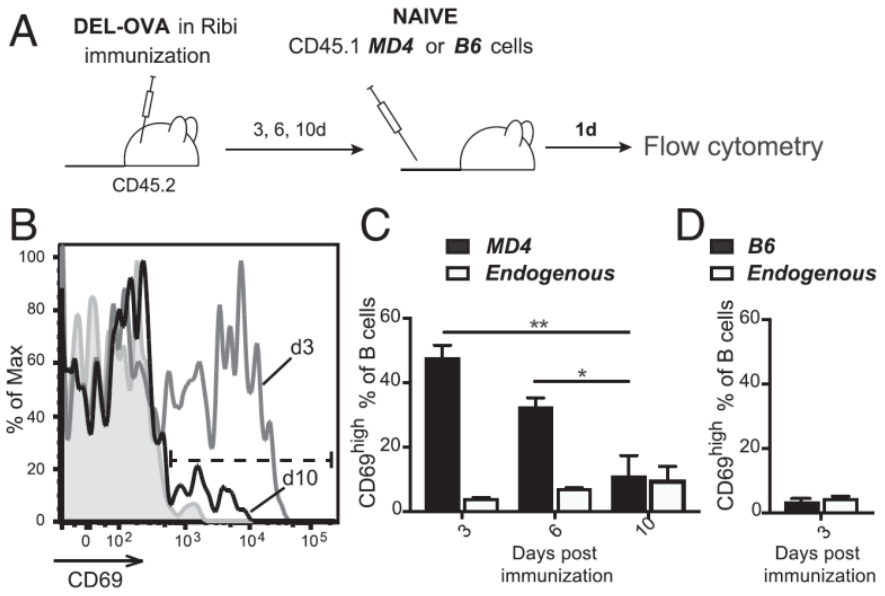


**Figure 3.7: Antigen-dependent activation of B cells at various times post immunization.**

(**A**–**D**) Upregulation of CD69 by naive MD4 or B6 B cells transferred into DEL-OVA–preimmunized mice. (A) Experimental scheme. A total of 2–10 × $10^5$ naive CD45.1 MD4 B cells was transferred into mice immunized with DEL-OVA in Ribi s.c. 3, 6, or 10 d earlier or into unimmunized control mice. Similar numbers of CD45.1 B6 B cells were transferred into mice immunized with DEL-OVA in Ribi s.c. 3 d earlier. Flow cytometry analysis of ILNs was performed 1 d post–B cell transfer. (B) Representative flow cytometry analysis of MD4 B cell CD69 surface staining after their transfer into unimmunized mice (shaded graph) or mice immunized 3 d earlier (gray line) or 10 d earlier (black line). (C) Frequencies of $CD69^{high}$ MD4 B cells ($B220^+$ $CD4^-$ $CD8^-$ $CD45.1^+$ $CD45.2^-$; black bars) and endogenous B cells ($B220^+$ $CD4^-$ $CD8^-$ $CD45.1^-$ $CD45.2^+$; white bars). Data are from three independent experiments, with one mouse per experiment. (D) Frequencies of $CD69^{high}$ $B220^+$ $CD4^-$ $CD8^-$ $CD45.1^+$ $CD45.2^-$ B6 B cells that were transferred at 3 d post–DEL-OVA immunization (black bars) and $CD45.1^-$ $CD45.2^+$ endogenous B cells (white bars). Data are from two independent experiments, with four recipient mice. Data are mean ± SEM. *$p < 0.05$, **$p < 0.01$, ordinary one-way ANOVA, Tukey multiple-comparison test.

cells transferred at 3 days post immunization underwent activation (Fig. 3.7B, C). In contrast, transferred non-transgenic CD45.1 B cells did not upregulate CD69 in ILNs of DEL-OVA mice preimmunized for 3 days (Fig. 3.7D). The fraction of MD4 B cells that underwent antigen-dependent activation and upregulated CD69 significantly decreased between 3 and 10 days following DEL-OVA immunization (Fig. 3.7B, C). Based on these observations and the findings described above, we conclude that following immunization with standard protein antigen in Ribi adjuvant, antigen-driven activation becomes the predominant factor limiting the entry of new antigen-specific B cells into the ongoing GC B cell response.

## Discussion

While the cellular and molecular mechanisms of GC B cell affinity maturation and their differentiation into memory B cells and plasma cells have been analyzed in a great level of detail, the factors that control clonal diversity of B cell responses are much less understood. In this work, we addressed which factors may limit the access of new antigen-specific B cell clones into GC and memory B cell responses following a standard protein/adjuvant immunization. First, we asked whether the ability of B cells uniformly exposed to the same small dose of cognate antigen to enter GC responses would be different during the initiation, peak, and resolution of the follicular T cell / GC B cell response. Our studies suggest that the initial expansion of antigen-experienced B cells *in vivo* and the generation of GC B cells do not strongly depend on the phase of the follicular T cell/GC response. We also confirmed histologically that B cells can enter GCs during various phases of follicular T cell/GC response (Fig 3.8A). However, when antigen-exposed B cells enter the GC response during the peak or contraction phase their subsequent expansion as GC B cells and their differentiation into memory-like $GL7^{low}$ class-switched B cells is reduced (Fig 3.8A). We speculate that the observed trend may be explained by the decreased ability of Tfh cells to support proliferation and survival of both older and newer GC B cell clones possibly due to the decrease in Tfh cell numbers and altered cytokine-mediated activity and/or the relative increase in the contribution of Tfr cells that negatively impact GC sustainability [95, 127, 129].

We then assessed the ability of naïve antigen-specific B cells to enter the GC response at various times following immunization with their cognate Ag. We found that in contrast to B cells that pre-acquired a small amount of Ag, naïve B cells' ability to enter both the GC and $GL7^{low}$ CSW B cell responses drops by 6-10 days following immunization. That correlated with significantly decreased ability of antigen-specific B cells to undergo "early" activation (Fig. 3.8B). This outcome is consistent with naïve B cell access to Ag becoming relatively limited *in vivo* after a few days following the immunization, suggesting it is a critical factor for new antigen-specific B cell clones' recruitment into the GC response. The fact that boosting immunizations promote recruitment of new antigen-specific B cell clones into preexisting GCs is consistent with this hypothesis [193].

One possibility is that over time naïve B cells' access to antigen becomes more restricted. Formation of immune complexes leads to antigen redistribution onto FDCs [199]. While antigens persist on FDCs for prolonged periods of time supporting the GC response, a previous study indicated progressive loss in naïve B cells' ability to acquire antigens from FDCs over time [200]. Gradual degradation of antigen and formation of GCs around FDCs may partially limit access of naïve B cells to FDC-presented antigens. Steric hindrance by the antibodies generated during the early B cell response in some cases may additionally limit antigen acquisition by newly arriving B cell clones [201]. Further studies are necessary to discriminate between these possibilities and thus decipher factors controlling recruitment of new B cell clones into ongoing immunization-induced GCs. Future studies should also address whether various adjuvants or antigen administration protocols affect the window of time in which new B cells may enter ongoing GCs following immunization. Dissecting these factors may be important for improving the diversity of B cell clones entering GCs following vaccinations and thus increasing the chances of generating broadly neutralizing antibody responses.

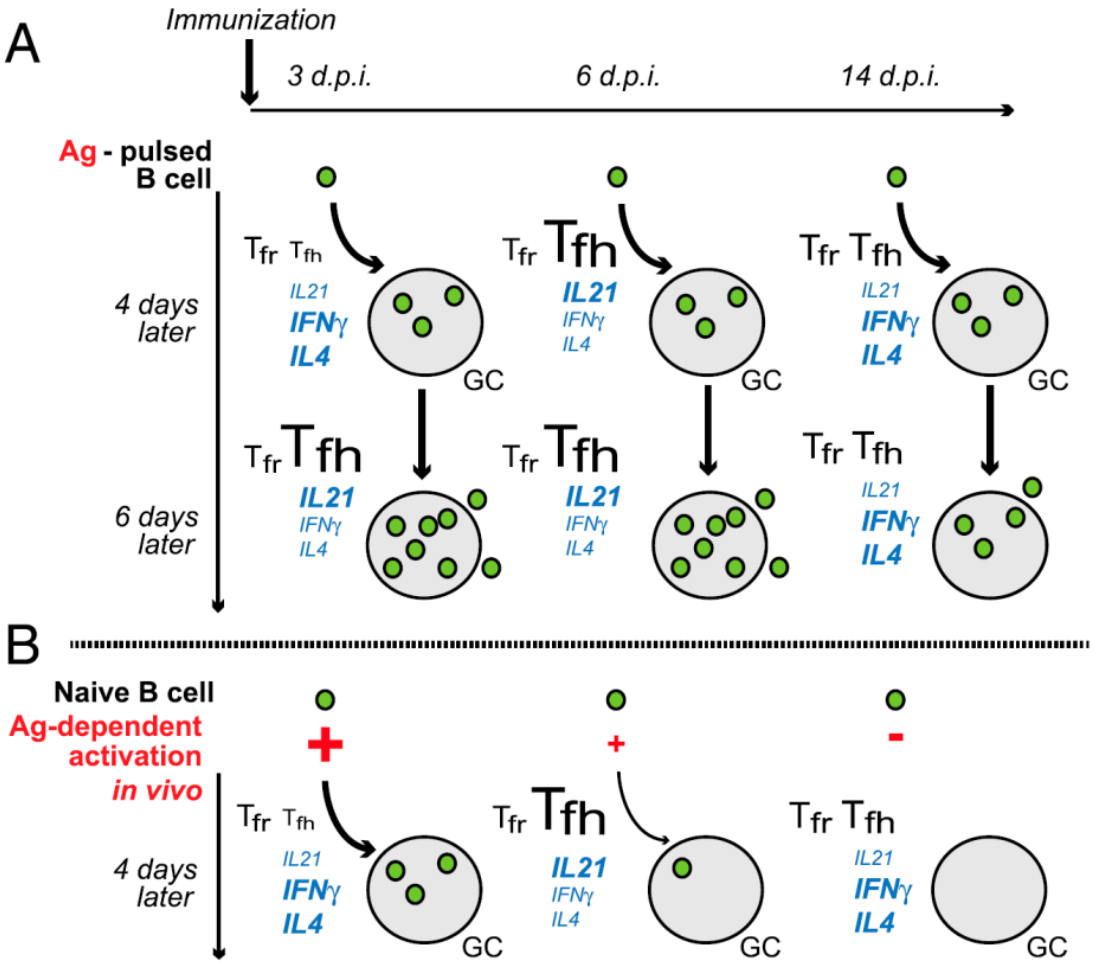


**Figure 3.8: Model of new B cell entry into the GC response at various times after immunization.**

(**A**) B cells exposed to a threshold-activating dose of Ag and cognate T cell help can enter the GC response with comparable efficiency at various times after immunization, including the initiation, peak, and resolution phases of the follicular T cell response. However, their subsequent expansion in GCs and formation of memory cells are reduced during the Tfh/GC resolution phase, possibly due to their decreased exposure to Tfh cell–produced IL-21 and/or increased repression from Tfr cells. (**B**) Following immunization, naive antigen-specific B cells have a limited window of time during which they can enter the GC response. This is determined by antigen-dependent activation of the naive B cells entering into antigen-draining LNs. In mice immunized s.c. with DEL-OVA in Ribi, antigen-dependent activation and entry into GCs starts to decrease at 6 d.p.i.

# Chapter 4 - Conclusions and future directions

In this dissertation, we have investigated several factors which influence B cell participation in the immune response by Tfr cells. In chapter 2, we suggest a role for the proinflammatory chemokine CCL3 in promoting Tfr mediated surveillance and suppression of GC B cells. In chapter 3, we find that antigen-dependent activation of B cells is the dominant factor rather than the phase of the Tfr and Tfh cell responses in controlling B cell entry and participation within the GC.

## Discussion of results from Chapter 2

The study summarized in Chapter 2 suggests that CCL3 plays an important role in the regulation of T-dependent humoral immune response. Unimmunized WT and CCL3-KO have comparable GC B cells. In contrast, immunization leads to an accumulation of GC B cells in CCL3-KO mice. We did not observe alterations in the frequencies of preapoptotic or apoptotic GC B cells between WT and CCL3-KO mice.

The increase in GC can be partly attributed to the accumulation of foreign-antigen specific GC B cells. Despite increased numbers of foreign-antigen specific cells, foreign-antigen specific IgG1 antibodies were not increased in the primary immune response. This result is consistent with the similar numbers of PCs in WT and CCL3-KO mice. Unexpectedly, secondary immunization led to significantly increased antigen-specific IgG1 antibodies in WT mice but not in CCL3-KO mice (see Appendix A1, Fig. A1.A-C).

In addition to the accumulation of foreign-antigen specific cells in the GCs, CCL3-KO mice were more likely to develop ANA responses following immunization. Hep2 staining patterns did not suggest that loss of CCL3 contributed significantly to the development of anti-dsDNA antibodies. Histological analysis of the kidneys and livers did not show

deposition of immune complexes or any gross anatomical changes related to autoimmunity in CCL3-KO mice at 40 d.p.i.

This study suggests that B-cell intrinsic production of CCL3 is partly responsible for the dysregulation of humoral responses in CCL3-KO mice. CCL3-KO B cells were overrepresented, although transiently, in the GCs of mixed bone marrow chimeras at 10 and 15 d.p.i. Additionally, transfer of CCL3-KO but not WT B cells into MD4 mice resulted in the development of ANAs following immunization.

According to a previous study, CCL4, but not CCL3, may promote interactions between Tregs and B cells or DCs and that these interactions could influence the T-dependent humoral immune response and the development of autoimmunity [148]. However, this hypothesis was never directly tested *in vivo*. Additionally, this study did not address how CCL3 or CCL4 contribute to follicular T cell interactions. To address this, we first isolated CD4 T cells from immunized mice and analyzed their responsiveness to CCL3 and CCL4 chemokines *ex vivo*. We confirmed that CCL4 could promote chemotaxis of Tregs but, in contrast to the previous study, found that CCL3 also promoted their chemotaxis. More importantly, CCL3 and CCL4 could both promote chemotaxis *ex vivo*. Many aspects of the dysregulation of the humoral immune response observed in CCL3-KO mice are consistent with previous findings where Tfr cells were ablated or do not form. Based on this, we suggest that CCL3 produced by GC B cells could be important for their interactions with Tfr cells and for the control of GC responses.

Previous microarray data suggested that CCL3 and CCL4 may be slightly upregulated by GC B cells in the LZ compared to the DZ. QPCR analysis of sorted GC B cells was able to confirm this observation. We then asked whether CCL3 promoted Tfr localization and recruitment into the LZ from the follicle. Unexpectedly, we found that the frequency of Tfr cells in the LZ of WT and CCL3-KO mice was comparable and that increased numbers of both Tfr and Tfh cells were found in the DZ of CCL3-KO mice.

Since there was no defect in Tfr localization to the GC light zone, we sought to test whether CCL3 may promote local interactions between GC B cells and Tfr cells. To address this, we developed a novel system that enabled intravital 2P imaging of Tfr cell migration in respect to GCs and their interactions with GC B cells in the peripheral LNs of mice. Analysis of Tfr cell migration in GCs 8 d.p.i. suggests that the majority of Tfr cells migrated along the perimeter of GCs. These Tfr cells made contacts with GC B cells along the outer border with only a few Tfr cells moving inside the GC. Quantitative analysis of interactions between foreign antigen-specific transgenic GC B cells and Tfr cells (derived from polyclonal, natural Tregs) suggested that Tfr cells formed more frequent interactions with CCL3 proficient vs. CCL3 deficient GC B cells. The observed effect was small but was consistent across multiple experiments. In contrast, we found no difference in the duration of Tfr interactions with CCL3 proficient vs. deficient GC B cells.

For comparison, we also imaged and analyzed interactions with Tfh cells with GC B cells. We found that in contrast to Tfr cells, the frequency in which Tfh cells interaction with CCL3 proficient and deficient GC B cells is the same.

We then asked whether expression of CCR5 on Tfr cells was important for Tfr cell contacts with CCL3-proficient GC B cells by 2P imaging. We found that CCR5 deficient Tfr cells did not preferentially interact with either CCL3-proficient or deficient GC B cells. This data is consistent with CCR5 being the predominant receptor on Tfr cells for sensing CCL3 produced by GC B cells.

Based on the observed dysregulation of GC responses and the 2P imaging data, we suggest a model wherein CCL3 promotes direct sampling and regulation of GC B cells by Tfr cells *in vivo*. In accord with this model, transient ablation of Tregs (including Tfr cells) during the peak of the GC response resulted in increased accumulation of CCL3 proficient but not deficient GC B cells.

Altogether, my data provides *in vivo* evidence suggesting that CCL3 produced by GC B cells and CCR5 on Tfr cells promote Tfr – GC B cell interactions and is important for control of GC responses. Moreover, this data is consistent with direct Tfr-mediated suppression of GC B cells *in vivo*. Thus, we show that, in addition to acting on Tfh cells, Tfr cells can directly suppress GC B cells in a contact-dependent fashion, ensuring robust control of GC responses.

**Future directions for chapter 2:**

We suggest a role for CCL3 in mediating control over the GC in a Tfr-dependent manner. However, the chemokine and chemokine receptor system is noted for its redundancy [152]. CCL4 expression is also elevated in activated B cells, as well as in LZ GC B cells. Previous studies suggested that CCL4 promotes Treg migration and is important for control of GC responses [148], We found that Tfr cells undergo chemotaxis to both CCL3 and CCL4 *ex vivo*. It is therefore likely that both CCL3 and CCL4 chemokines secreted by GC B cells may promote their interactions with Tfr cells. While in our initial studies we found no increase in GC responses in WT or CCL3-KO mice treated with anti-CCL4 antibodies (data not shown), future studies should examine various clones of CCL4-neutralizing Abs to determine whether they may induce or contribute to dysregulation of GC responses *in vivo*. The antibodies efficiently neutralizing CCL4 *in vivo* should then be tested in conjunction with Tfr intravital imaging system to determine whether CCL4 contributes to GC B cell scanning by Tfr cells and together with CCL3 promote negative control of GC B cells by Tfr cells.

The intravital imaging experiments enabled us to suggest that GC B cell-secreted CCL3 promotes their direct contacts with Tfr cells. However, we could detect only small differences in Tfr contact frequencies with CCL3 proficient vs. deficient GC B cells (10-25%). Interestingly, single cell qPCR analysis of B cell subsets that I performed suggests that only a minor fraction of LZ GC B cells have significant upregulation in CCL3/4 expression (Appendix II, Figure A1). Our 2P imaging system does not allow discrimination between CCL3/4$^{hi}$ and CCL3/4$^{low}$ GC B cells. Therefore, our interaction

data may significantly underestimate Tfr interaction frequency with CCL3/4$^{hi}$ GC B cells. In the future, this may be addressed using a fluorescent CCL3 reporter or a CCL3 overexpression system to determine how the amount of CCL3 being expressed by GC B cells relates to their interaction frequency with Tfr cells.

Another direction that has not been addressed in my thesis work is the nature of molecular signals that trigger proinflammatory chemokine expression in LZ GC B cells. It is tempting to suggest that the few LZ GC B cells that upregulate CCL3/4 expression are GC B cells that have undergone positive selection in the LZ and therefore specifically require attention of Tfr cells. Both Ag and T cell help may be available for GC B cells in the LZ, and expression of CCL3/4 chemokines has been shown to be upregulated due to BCR cross-linking or through CD40 stimulation of B cells [148, 149, 202]. It is possible that either signal alone is sufficient to trigger proinflammatory chemokines or that both are required for high levels of CCL3/4 expression [203]. It is also possible that other signals can promote CCL3/4 upregulation in GC B cells, such as Toll-like receptor ligands. TLRs play an important role in humoral immune response dysregulation [204, 205]. Therefore, it would be interesting to assess whether acquisition of TLR7 or TLR9 ligand-linked antigens promotes increased production of CCL3/4 by GC B cells and thus increased attention of Tfr cells. Of note, Tfr-mediated suppression of GC B cells that acquire TLR ligands may contribute to better control of B cell clones specific to anti-nuclear antigens.

While this work provides evidence for the role of CCL3 in Tfr-mediated repression of foreign antigen-specific GC B cells, how it controls ANA responses remains an opened question. Based on the development of ANA responses in MD4 mice transferred with CCL3-KO B cells, we suggest that this effect is B cell intrinsic. However, whether CCL3 expression is required during B cell development in the bone marrow, shortly after B cell activation, or within the GC remains unclear. In the future, conditional CCL3-KO mouse model may be instrumental in addressing the stage of B cell development or response when CCL3 expression is required for better control of ANA responses.

Tfr cells are largely thought to be derived from natural Tregs and thus specific to self-antigens although under certain experimental conditions foreign antigen Tfr cells can arise [127, 129, 135, 137]. Cognate B cells and Tfh cells can engage in interactions with durations much longer than noncognate cells [31, 36]. Within the GC, it is believed that productive interactions require durations lasting longer than 5-10 minutes [36]. Interestingly, we observed GC B cell interactions with “natural” Tfr cells or that lasted over five minutes. However, we did not detect any Tfr-GC B cell interactions that lasted longer than 7.5 minutes. While no definitive conclusions can be made, it is possible that 5-7.5 minute long interactions represent Tfr cells that are weakly reactive to foreign antigen or B cells which inadvertently acquired self-antigen. Future studies will need to address how Tfr and GC B cells interact with one another when GC B cells are known to present cognate antigen, and determine how prevalent or important cognate GC-Tfr cell interactions are *in vivo*.

**Conclusions from chapter 3**

GCs can be seeded by 50-200 unique B cell clones by 6 days post immunization [67]. Entry into the GC may continue past this point as newly activated B cells can be seen entering the GC [68]. However, these analyses were done coinciding with either the initiation or just prior to the peak of GC B cell responses when Tfr cell numbers are only beginning to ramp up. Therefore, it is unclear whether activated B cells could continuously seed the GC as the immune response progressed and follicular T cell numbers changed.

In chapter 3, we investigated factors that mediate continuous B cell recruitment into an immunization-induced immune response. The purpose of the study was to determine whether different phases of the GC would affect recently activated B cell recruitment into ongoing GCs. While highly dominant prior to and during the peak, Tfh cell numbers decrease over time. In contrast, Tfr cell numbers slowly increase. In Chapter 2, we have suggested that Tfr cells can act directly on GC B cells to limit their participation within the GC. However, whether Tfr cells directly interact with newly arriving B cells in the

same manner as they do with GC B cells and limit their recruitment into GCs has been unclear. In addition, whether Tfr cell interactions with activated B cells may change over time as Tfr cells become more prevalent was not known.

Published work also suggested that Tfr cells alter cytokine production in Tfh cells which our results and others have suggested change over time [131]. Therefore, the role of Tfr cells in modulating newly arriving B cell fate and different phases of the GC response either through direct interactions or through Tfh cells has not been previously assessed. Analysis of these factors is important for increasing the efficiency of existing vaccines and increasing diversity of B cell clones recruited into humoral immune response.

We found that naïve antigen specific B cells have impaired recruitment into GC responses as early as 6 days post immunization. However, exposure to a threshold activation dose of antigen was sufficient to rescue B cell participation. The initial proliferation of antigen-exposed B cells and recruitment into the GCs was unaffected by the phase of GC or follicular T cell response. However, once in the GCs, recently activated B cells that joined the response during its peak or contraction phase proliferated less and formed reduced numbers of class-switched memory cells. Overall, these data suggest that antigen-dependent activation is the critical factor for initial recruitment of B cells into the ongoing immunization-induced GC response, but other factors within the GC contribute to their further proliferation and differentiation. Based on this study we suggest that the frequency of Tfr cells is not likely to be critical for the recruitment of new B cell clones into the ongoing GC response. However, it may still be important for proliferation and differentiation of the newly formed GC B cells.

**Future directions for chapter 3**

Our study made use of a single antigen stimulation condition with a large number of B cells being specific to an identical epitope. In reality, B cell responses to foreign antigen are highly diverse, consisting of 50-200 unique clones in each GC [67]. Increased diversity is likely to lead to enhanced protection through increased breadth of antibody

epitope specificities. However, the potential to recruit B cells into the response with cross-reactive specificities to self-antigen may increase with each additional unique clone being recruited. It has been shown previously that cross-reactive B cells can participate within GCs [206]. Interestingly, their cross reactivity can be selected against via affinity maturation thereby increasing clonal diversity and keeping self-tolerance intact [206]. However, it is not known how early these types of B cells are recruited into the response. Cross-reactive B cell recruited earlier would face less Tfr-mediated suppression within the GC and potentially have more rounds of SHM to increase their affinity towards foreign antigen. Our data suggested that antigen alone is sufficient for the recruitment of B cells into the GC yet that antigen is not normally thought of as being able to be recognized by Tfr cells. This can be addressed by pulsing our foreign antigen-specific B cells with foreign antigen conjugated with a self-peptide. We can then assess recruitment of either B cells pulsed with foreign antigen alone or the self-peptide conjugated antigen. If Tfr cells block the entry of recently activated clones through a self antigen-specific mechanism, then recruitment of B cells that received the self-peptide conjugated to foreign antigen would be diminished compared to those only pulsed with foreign antigen.

We and others have found that Tfh cells alter their cytokine production from IL-21$^{+}$ cells to IFNγ (or IL-4) cells [95]. It is possible that the reason we see differences in participation of the recruited B cells within the GC between the initiation and peak vs. the contraction phase is a result of altered cytokine production by Tfh cells. Interestingly, Tfr have been implicated in changing the levels of cytokine production in Tfh cells directly *ex vivo* and evidence exists for this function *in vivo*. However, those studies did not look at the kinetics of cytokine production by Tfh cells. Therefore, it is possible that Tfr cells indirectly regulate GC B cell participation through alterations in Tfh cell cytokine production profile. This question can be addressed using Tfr-deficient mouse models and kinetically analyzing Tfh cytokine production. If indeed Tfr cells can mediate the switch in cytokine production it would suggest that Tfr control the fate of GC B cells through Tfh cells.

Our finding that naïve B cells, but not antigen-pulsed B cells, have reduced chances of participating in ongoing responses past 6 days post immunization suggests that antigen acquisition may be the limiting factor in B cell recruitment. One factor that may contribute to the loss of available antigen is its sequestration by immune complexes [199]. Immune complexes are deposited on FDCs within the GC either through FcγRIIB or complement receptors (such as CD35)[199, 207]. Immune complexes may also bind to FcγRIIB on B cells and prevent activation of other antigen specific clones [208]. Both factors may be responsible for the loss in GC participation of naïve B cells. This may be addressed by transferring FcγRIIB deficient naïve B cells into immunized mice at various time points. If inhibitory Fc receptors on B cells are playing a role, then the participation windows of FcγRIIB -KO B cells should be increased relative to WT B cells. Mixed bone marrow chimeras wherein FcγRIIB-KO mice are reconstituted with WT bone marrow would allow one to address the role of FcγRIIB on FDCs in limiting recruitment of newly activated B cells.

**Final thoughts**

The findings from this thesis answer important and fundamental questions about how Tfr cells regulate B cell responses. We found that while Tfr cells do not appear to prevent the recruitment of foreign antigen-specific B cells into the T-dependent humoral response, but are critical in directly controlling B cells within the GCs. Efficient regulation of GC B cells was dependent on their intrinsic expression of CCL3 which potentiated Tfr contacts through CCR5.

These results leave open the most fundamental and unresolved question of Tfr cell biology: do Tfr cells regulate humoral responses in an antigen-specific manner? Our studies were not designed to address this question but nonetheless provide insight into the antigen-dependency of Tfr cells. Given the data presented in Chapter 2, one could hypothesize that Tfr have an ability to suppress B cells within the GC in both an antigen-dependent and -independent manner. We also observed that despite developing from polyclonal Tregs, Tfr cells could engage in contact durations of 5-7.5 minutes with

antigen-specific B cells. This finding is interesting given that it is believed that contact durations over 5 minutes between Tfh cells and GC B cells are considered productive [36, 108, 116]. Our imaging studies could not address whether active signaling occurred between Tfr and GC B cell pairs that underwent durable interactions. Additionally, we cannot preclude the ability of foreign-antigen specific B cells to either a) acquire self-antigen or b) develop cross-reactive affinities. These factors may promote durable interactions between foreign antigen-specific cells and self-antigen-specific Tfr cells.

In Chapter 3, we pulsed antigen-specific B cells *ex vivo* with foreign antigen and found that Tfr cell numbers or their ratio to Tfh cells did not make a difference towards their recruitment. However, since foreign antigen-specific B cells were pulsed exclusively with foreign antigen and were unable to acquire additional antigen within the GC through their BCR, Tfr cells may simply not be able to suppress these B cells well. Alternatively, Tfr cells may simply be ignorant of ongoing recruitment of B cells into the GC and only respond to GC B cells that express certain unknown GC-acquired molecules. While we know BCR signaling can trigger the expression of CCL3, recently recruited B cells may not currently be secreting the chemokine by the time they arrive into the GC. However, once in the GC, some unknown stimuli can promote CCL3 expression by GC B cells and then promote their interactions with Tfr cells.

Overall, my thesis findings, along with a number of reported observations, allow us to develop a model of Tfr mediated regulation of the GC. Irrespective of their cross reactivity to self, B cells that are activated via foreign antigen are capable of seeding or being recruited into GCs. Cross-reactive GC B cells that were recruited early can mutate away from self-reactivity and increase their foreign antigen affinity. An unknown mechanism, possibly BCR cross-linking, triggers the expression of CCL3 within GC B cells. Tfr cells sample CCL3-secreting B cells and potentially suppress them directly. However, these interactions may promote further differentiation or proliferation of Tfr cells and this may be enhanced during interactions with cross-reactive GC B cells. The increase in Tfr numbers may also affect cytokine production by Tfh cells either directly or indirectly. This in turn affects further participation within the GC by GC B cells –

regardless of when they were recruited or their specificity. This model assumes a constant supply of foreign antigen while, in most physiological circumstances, foreign antigen is often limiting. However, self-antigen is not limiting. This model posits an interesting feedback loop wherein Tfr could short-circuit GC reactions provided enough self-reactive or cross-reactive B cells were recruited into the GC.

In conclusion, my thesis work has identified that CCL3 can promote the control of T dependent humoral responses by Tfr cells. Tfr cells can directly interaction with GC B cells and we believe that these interactions are responsible for some of their suppressive effects *in vivo*. While not tested directly, it is likely Tfr cells undergo cognate interactions similar to Tfh cells when presented with cognate antigen. The understanding of Tfr cell biology may prove critical in understanding the causes of autoimmune diseases in humans. We hope that these studies will promote further interest into understanding the molecular and cellular mechanisms of GC regulation.

# Appendix A – Supplementary Information for Chapter 2

## Appendix A.1 – Secondary Humoral Responses in CCL3-KO Mice

A hallmark of the adaptive immune system is the generation of memory cells. Memory cells enable the rapid clearance of pathogens and is a goal of vaccine development. As an extension to the work performed in Fig. 2 and Fig. 3, we addressed if CCL3 could affect the memory recall response. WT and CCL3-KO littermate mice were immunized with NP-KLH in Ribi and serum draws were taken at 0, 10, 15, and 20 days. On day 24, mice were boosted and a final serum draw occurred on day 28. Despite greater numbers of GC B cells in CCL3-KO mice, there was no increase in either low affinity or high affinity NP-specific IgG1 antibodies during the primary response (Fig. A.1A-B). In contrast to the primary response, antigen boosting significantly increased the titers of NP-specific IgG1 in WT but not CCL3-KO mice (Fig. A.1A-B). The overall affinity of the responding B cells was not affected by CCL3 (Fig. A.1C). This piece of data suggests that CCL3 may play a role in memory B cell responses.

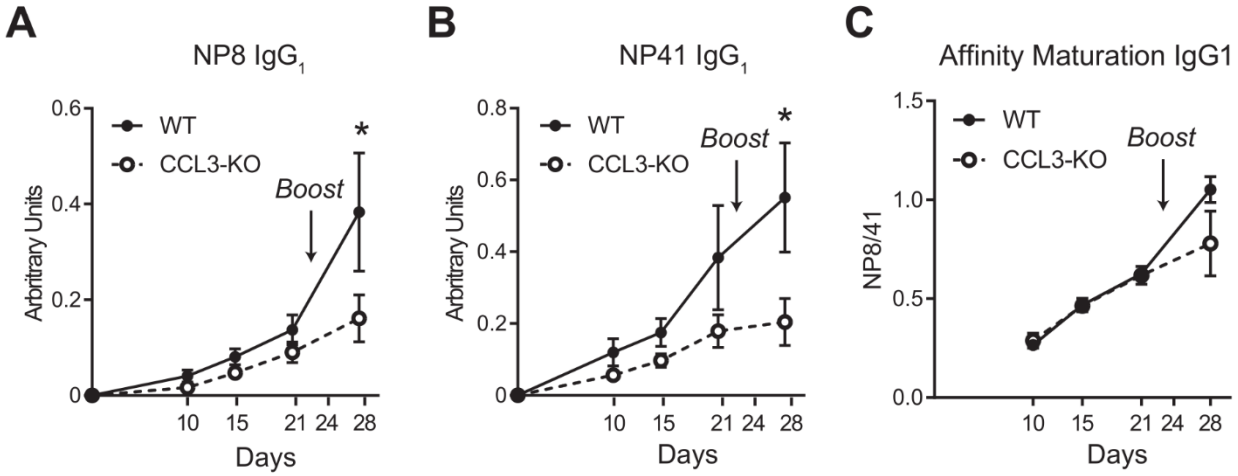


**Figure A.1: NP-specific IgG1 recall response.**

**A,B**, ELISA of NP-specific $IgG_1$ titers that have high affinity (NP8-binding) (**A**) and overall affinity (NP41-binding) (**B**) to NP from mice immunized with 50 µg NP-KLH in Ribi and boosted with the same dose at day 24. **C**, affinity maturation as measured by the NP8- to NP41-binding ratio. Black line with filled in circles, WT mice. Dashed line with open circles, CCL3-KO mice. *, $P < 0.05$, Student's *t*-test.

## Appendix A.2 – Heterogenous expression of CCL3 and CCL4 in LZ GC B cells

We hypothesize that certain events such as antigen recognition, provision of T cell help, or stimulation via pattern recognition receptors within the LZ may trigger the expression of CCL3 and CCL4 in GC B cells and promote efficient Tfr mediated surveillance of B cells. If this were true, then only a fraction of B cells within the LZ might express relatively high levels of CCL3 and CCL4. To test this hypothesis, we performed qPCR analysis of CCL3, CCL4, and B2m on single cell sorted centrocytes, centroblasts, and naïve B cells. We performed two independent experiments and in both we observed that a few centrocytes, but not centroblasts or naïve B cells, expressed noticeably higher levels of CCL3 and CCL4 compared to the rest of the population (Fig. A.2A). We used an alternative normalization gene, HPRT1, to confirm our results with B2m. All cells which showed higher expression of CCL3 or CCL4 relative to B2m showed similar increases relative to HPRT1 (Fig. A.2B). Maximum likelihood analysis was then done to determine if the observed data was likely to derive from two or more separate distributions. We found that for the two experiments, the data is more likely to derive from at least two separate populations (Fig A.2C, one experiment shown). This finding suggests that signals that induce CCL3 and CCL4 expression in centrocytes is relatively rare. Interestingly, the fraction of centrocytes expressing higher levels of CCL3 and CCL4 is around 5-10%, a proportion similar to the fraction of centrocytes which can be observed to migrate from the light zone to the dark zone.

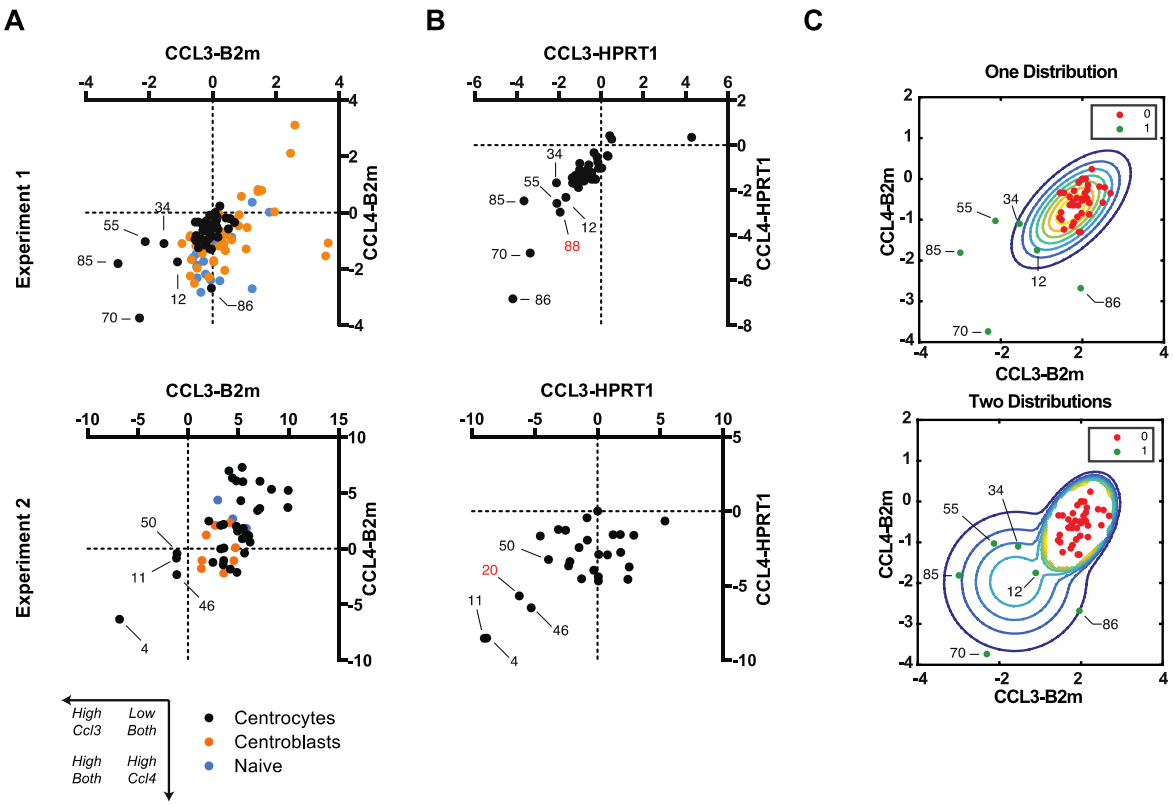


**Figure A.2: Single qPCR analysis of centrocytes, centroblasts, and naïve B cells.** **A-C**, Single cell qPCR of centrocytes, centroblasts, and naïve B cells sorted from mice immunized with OVA in Ribi on day 10. **A,** QPCR of CCL3 (*x* axis) and CCL4 (y axis) relative to B2m for centrocytes, centroblasts, and naïve B cells. Centrocytes with visually higher expression of either CCL3 or CCL4 are labeled with their ID number. **B,** QPCR of CCL3 and CCL4 relative to HPRT1 for centrocytes. Red numbering indicates cells which had higher expression of CCL3 or CCL4 relative to HPRT1 but not B2m. **C,** Maximum likelihood distributions of centrocytes in (**A, top**) from either one distribution (top) or two distributions (bottom). Red dots indicate low expressing cells. Green dots indicate high expressing cells. Numbers indicate cell ID number.

## Appendix A.3 – Treg-mediated CCL3-dependent effects on B cell participation at different stages of the GC response

We addressed how Treg-mediated, CCL3-dependent control over B cell participation within the GC changed as the response contracts. To test this, we transferred HyHEL10 B cells as described in Fig 2.9 into Foxp3$^{DTR}$. Mice were immunized with DEL-OVA and at 12 d.p.i. were treated with PBS or DTx. Three days later, the participation of WT and CCL3-KO HyHEL10 B cells within the GC was analyzed. In contrast to the mixed bone marrow chimeras (Fig. 2.8), WT HyHEL10 B cells were found to dominate the GC relative to CCL3-KO HyHEL10 B cells during contraction phase of the GC (Fig. A.3A-C). Furthermore, treatment of DTx did not appear to benefit the participation of WT HyHEL10 B cells since the ratio of CCL3$^{-/-}$ to CCL3+/+ HyHEL10 B cells within the GC increased due a slight expansion of the numbers of CCL3$^{-/-}$ HyHEL10 B cells. Combined with Fig. 2.8, these data suggest that CCL3 may play different roles in the participation of GC B cells depending on the phase of the GC.

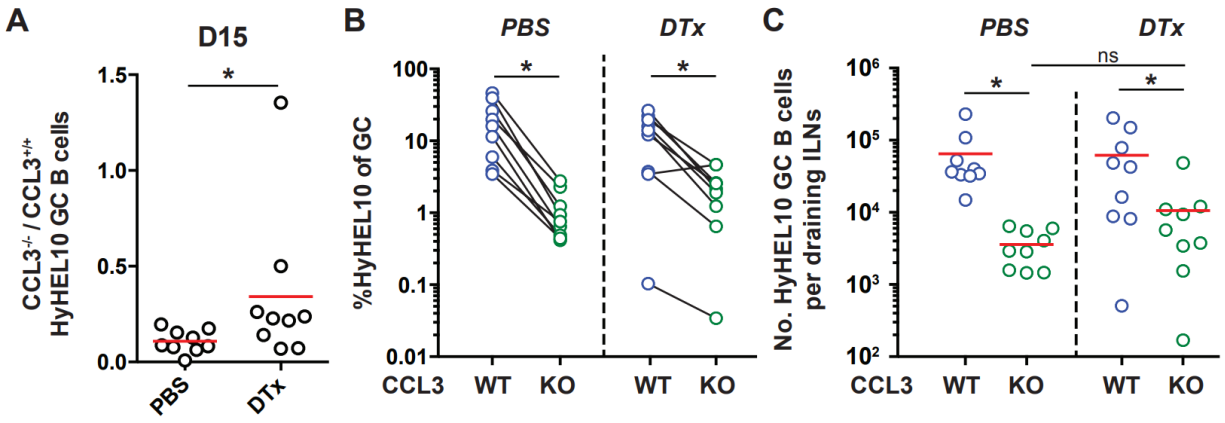


**Figure A.3: CCL3 promotes Ag specific B cell participation during the contraction of GC responses**

**A-C,** Flow cytometry analysis of HyHEL10 cell participation in the GC at 15 d.p.i. in Foxp3DTR recipient mice treated with PBS or DTx 12 d.p.i. **A**, ratio of CCL3$^{-/-}$ to CCL3$^{+/+}$ HyHEL10 GC B cells (CD19$^{+}$CD8$^{-}$CD4$^{-}$Fas$^{high}$GL7$^{high}$ IgD$^{low}$) in PBS or DTx treated mice. **B**, **C,** Flow cytometry analysis of total GC numbers per draining ILNs. The fractions of CCL3$^{+/+}$ and CCL3$^{-/-}$ HyHEL10 GC B cells of total GCs (**B**), and the total numbers of HyHEL10 GC B cells of each kind per draining ILNs (**C**). Each dot represents a single mouse and paired analyses are indicated using a solid black line. 3 independent experiments. (*, P<0.05. Two-tailed, Student's t-test was used in A. Paired t-test used in B. ANOVA followed by Dunnet's multiple comparison test with one-tailed p values reported for C.)

## References


1. von Behring, E. and S. Kitasato, *[The mechanism of diphtheria immunity and tetanus immunity in animals. 1890]*. Mol Immunol, 1991. **28**(12): p. 1317, 1319-20.

2. Fagraeus, A., *Plasma cellular reaction and its relation to the formation of antibodies in vitro.* Nature, 1947. **159**(4041): p. 499.

3. Ordman, C.W., C.G. Jennings, and C.A. Janeway, *Chemical, Clinical, and Immunological Studies on the Products of Human Plasma Fractionation. Xii. The Use of Concentrated Normal Human Serum Gamma Globulin (Human Immune Serum Globulin) in the Prevention and Attenuation of Measles.* J Clin Invest, 1944. **23**(4): p. 541-9.

4. Eibl, M.M., L. Cairns, and F.S. Rosen, *Safety and efficacy of a monomeric, functionally intact intravenous IgG preparation in patients with primary immunodeficiency syndromes.* Clin Immunol Immunopathol, 1984. **31**(1): p. 151-60.

5. Reth, M., *Antigen receptors on B lymphocytes.* Annu Rev Immunol, 1992. **10**: p. 97-121.

6. Harwood, N.E. and F.D. Batista, *Early events in B cell activation.* Annu Rev Immunol, 2010. **28**: p. 185-210.

7. MacLennan, I.C., *Germinal centers.* Annu Rev Immunol, 1994. **12**: p. 117-39.

8. Alugupalli, K.R., et al., *B1b lymphocytes confer T cell-independent long-lasting immunity.* Immunity, 2004. **21**(3): p. 379-90.

9. Obukhanych, T.V. and M.C. Nussenzweig, *T-independent type II immune responses generate memory B cells.* J Exp Med, 2006. **203**(2): p. 305-10.

10. Victora, G.D. and M.C. Nussenzweig, *Germinal centers.* Annu Rev Immunol, 2012. **30**: p. 429-57.

11. Nutt, S.L., et al., *The generation of antibody-secreting plasma cells.* Nat Rev Immunol, 2015. **15**(3): p. 160-71.

12. Bossaller, L., et al., *ICOS deficiency is associated with a severe reduction of CXCR5+CD4 germinal center Th cells.* J Immunol, 2006. **177**(7): p. 4927-32.

13. Grimbacher, B., et al., *Homozygous loss of ICOS is associated with adult-onset common variable immunodeficiency.* Nat Immunol, 2003. **4**(3): p. 261-8.

14. Warnatz, K., et al., *Human ICOS deficiency abrogates the germinal center reaction and provides a monogenic model for common variable immunodeficiency.* Blood, 2006. **107**(8): p. 3045-52.

15. Linterman, M.A., et al., *Follicular helper T cells are required for systemic autoimmunity.* J Exp Med, 2009. **206**(3): p. 561-76.

16. Vinuesa, C.G., et al., *A RING-type ubiquitin ligase family member required to repress follicular helper T cells and autoimmunity.* Nature, 2005. **435**(7041): p. 452-8.

17. Alegre, M.L., K.A. Frauwirth, and C.B. Thompson, *T-cell regulation by CD28 and CTLA-4.* Nat Rev Immunol, 2001. **1**(3): p. 220-8.

18. Nurieva, R.I., et al., *Generation of T follicular helper cells is mediated by interleukin-21 but independent of T helper 1, 2, or 17 cell lineages.* Immunity, 2008. **29**(1): p. 138-49.

19. Crotty, S., *T follicular helper cell differentiation, function, and roles in disease.* Immunity, 2014. **41**(4): p. 529-42.

20. Good-Jacobson, K.L., et al., *PD-1 regulates germinal center B cell survival and the formation and affinity of long-lived plasma cells.* Nat Immunol, 2010. **11**(6): p. 535-42.

21. Schwickert, T.A., et al., *A dynamic T cell-limited checkpoint regulates affinity-dependent B cell entry into the germinal center.* J Exp Med, 2011. **208**(6): p. 1243-52.

22. Victora, G.D., et al., *Germinal center dynamics revealed by multiphoton microscopy with a photoactivatable fluorescent reporter.* Cell, 2010. **143**(4): p. 592-605.

23. Batista, F.D. and N.E. Harwood, *The who, how and where of antigen presentation to B cells.* Nat Rev Immunol, 2009. **9**(1): p. 15-27.

24. Pereira, J.P., L.M. Kelly, and J.G. Cyster, *Finding the right niche: B-cell migration in the early phases of T-dependent antibody responses.* Int Immunol, 2010. **22**(6): p. 413-9.

25. Cyster, J.G., *B cell follicles and antigen encounters of the third kind.* Nat Immunol, 2010. **11**(11): p. 989-96.

26. Ansel, K.M., et al., *A chemokine-driven positive feedback loop organizes lymphoid follicles.* Nature, 2000. **406**(6793): p. 309-14.

27. Liu, C., et al., *Oxysterols direct B-cell migration through EBI2.* Nature, 2011. **475**(7357): p. 519-23.

28. Pereira, J.P., et al., *EBI2 mediates B cell segregation between the outer and centre follicle.* Nature, 2009. **460**(7259): p. 1122-6.

29. Yi, T., et al., *Oxysterol gradient generation by lymphoid stromal cells guides activated B cell movement during humoral responses.* Immunity, 2012. **37**(3): p. 535-48.

30. Kelly, L.M., et al., *EBI2 guides serial movements of activated B cells and ligand activity is detectable in lymphoid and nonlymphoid tissues.* J Immunol, 2011. **187**(6): p. 3026-32.

31. Okada, T., et al., *Antigen-engaged B cells undergo chemotaxis toward the T zone and form motile conjugates with helper T cells.* PLoS Biol, 2005. **3**(6): p. e150.

32. Luther, S.A., et al., *Coexpression of the chemokines ELC and SLC by T zone stromal cells and deletion of the ELC gene in the plt/plt mouse.* Proc Natl Acad Sci U S A, 2000. **97**(23): p. 12694-9.

33. Kerfoot, S.M., et al., *Germinal center B cell and T follicular helper cell development initiates in the interfollicular zone.* Immunity, 2011. **34**(6): p. 947-60.

34. Gatto, D., et al., *Guidance of B cells by the orphan G protein-coupled receptor EBI2 shapes humoral immune responses.* Immunity, 2009. **31**(2): p. 259-69.

35. Cannons, J.L., et al., *Optimal germinal center responses require a multistage T cell:B cell adhesion process involving integrins, SLAM-associated protein, and CD84.* Immunity, 2010. **32**(2): p. 253-65.

36. Qi, H., et al., *SAP-controlled T-B cell interactions underlie germinal centre formation.* Nature, 2008. **455**(7214): p. 764-9.

37. Veillette, A., et al., *SAP expression in T cells, not in B cells, is required for humoral immunity.* Proc Natl Acad Sci U S A, 2008. **105**(4): p. 1273-8.

38. Taylor, J.J., M.K. Jenkins, and K.A. Pape, *Heterogeneity in the differentiation and function of memory B cells.* Trends Immunol, 2012. **33**(12): p. 590-7.

39. Johnston, R.J., et al., *Bcl6 and Blimp-1 are reciprocal and antagonistic regulators of T follicular helper cell differentiation.* Science, 2009. **325**(5943): p. 1006-10.

40. Chan, T.D., et al., *Antigen affinity controls rapid T-dependent antibody production by driving the expansion rather than the differentiation or extrafollicular migration of early plasmablasts.* J Immunol, 2009. **183**(5): p. 3139-49.

41. Paus, D., et al., *Antigen recognition strength regulates the choice between extrafollicular plasma cell and germinal center B cell differentiation.* J Exp Med, 2006. **203**(4): p. 1081-91.

42. Kwon, H., et al., *Analysis of interleukin-21-induced Prdm1 gene regulation reveals functional cooperation of STAT3 and IRF4 transcription factors.* Immunity, 2009. **31**(6): p. 941-52.

43. Sciammas, R., et al., *Graded expression of interferon regulatory factor-4 coordinates isotype switching with plasma cell differentiation.* Immunity, 2006. **25**(2): p. 225-36.

44. Taylor, J.J., K.A. Pape, and M.K. Jenkins, *A germinal center-independent pathway generates unswitched memory B cells early in the primary response.* J Exp Med, 2012. **209**(3): p. 597-606.

45. Ochiai, K., et al., *Transcriptional regulation of germinal center B and plasma cell fates by dynamical control of IRF4.* Immunity, 2013. **38**(5): p. 918-29.

46. Sciammas, R., et al., *An incoherent regulatory network architecture that orchestrates B cell diversification in response to antigen signaling.* Mol Syst Biol, 2011. **7**: p. 495.

47. Allen, C.D. and J.G. Cyster, *Follicular dendritic cell networks of primary follicles and germinal centers: phenotype and function.* Semin Immunol, 2008. **20**(1): p. 14-25.

48. Cyster, J.G., et al., *Follicular stromal cells and lymphocyte homing to follicles.* Immunol Rev, 2000. **176**: p. 181-93.

49. Rodda, L.B., et al., *Phenotypic and Morphological Properties of Germinal Center Dark Zone Cxcl12-Expressing Reticular Cells.* J Immunol, 2015. **195**(10): p. 4781-91.

50. Allen, C.D., et al., *Germinal center dark and light zone organization is mediated by CXCR4 and CXCR5.* Nat Immunol, 2004. **5**(9): p. 943-52.

51. Dominguez-Sola, D., et al., *The FOXO1 Transcription Factor Instructs the Germinal Center Dark Zone Program.* Immunity, 2015. **43**(6): p. 1064-74.

52. Sander, S., et al., *PI3 Kinase and FOXO1 Transcription Factor Activity Differentially Control B Cells in the Germinal Center Light and Dark Zones.* Immunity, 2015. **43**(6): p. 1075-86.

53. Mandel, T.E., et al., *The follicular dendritic cell: long term antigen retention during immunity.* Immunol Rev, 1980. **53**: p. 29-59.

54. Mandel, T.E., et al., *Long-term antigen retention by dendritic cells in the popliteal lymph node of immunized mice.* Immunology, 1981. **43**(2): p. 353-62.

55. Szakal, A.K., et al., *Isolated follicular dendritic cells: cytochemical antigen localization, Nomarski, SEM, and TEM morphology.* J Immunol, 1985. **134**(3): p. 1349-59.

56. Kopf, M., et al., *Interleukin 6 influences germinal center development and antibody production via a contribution of C3 complement component.* J Exp Med, 1998. **188**(10): p. 1895-906.

57. Kosco-Vilbois, M.H. and D. Scheidegger, *Follicular dendritic cells: antigen retention, B cell activation, and cytokine production.* Curr Top Microbiol Immunol, 1995. **201**: p. 69-82.

58. Nishikawa, Y., et al., *Establishment of lymphotoxin beta receptor signaling-dependent cell lines with follicular dendritic cell phenotypes from mouse lymph nodes.* J Immunol, 2006. **177**(8): p. 5204-14.

59. Shinnakasu, R., et al., *Regulated selection of germinal-center cells into the memory B cell compartment.* Nat Immunol, 2016. **17**(7): p. 861-9.

60. Victora, G.D., et al., *Identification of human germinal center light and dark zone cells and their relationship to human B-cell lymphomas.* Blood, 2012. **120**(11): p. 2240-8.

61. Allen, C.D., et al., *Imaging of germinal center selection events during affinity maturation.* Science, 2007. **315**(5811): p. 528-31.

62. Hauser, A.E., et al., *Definition of germinal-center B cell migration in vivo reveals predominant intrazonal circulation patterns.* Immunity, 2007. **26**(5): p. 655-67.

63. Pavri, R. and M.C. Nussenzweig, *AID targeting in antibody diversity.* Adv Immunol, 2011. **110**: p. 1-26.

64. Hanna, M.G., Jr., *An Autoradiographic Study of the Germinal Center in Spleen White Pulp during Early Intervals of the Immune Response.* Lab Invest, 1964. **13**: p. 95-104.

65. Jacob, J., R. Kassir, and G. Kelsoe, *In situ studies of the primary immune response to (4-hydroxy-3-nitrophenyl)acetyl. I. The architecture and dynamics of responding cell populations.* J Exp Med, 1991. **173**(5): p. 1165-75.

66. Jacob, J., et al., *Intraclonal generation of antibody mutants in germinal centres.* Nature, 1991. **354**(6352): p. 389-92.

67. Tas, J.M., et al., *Visualizing antibody affinity maturation in germinal centers.* Science, 2016. **351**(6277): p. 1048-54.

68. Schwickert, T.A., et al., *In vivo imaging of germinal centres reveals a dynamic open structure.* Nature, 2007. **446**(7131): p. 83-7.

69. Bannard, O., et al., *Germinal center centroblasts transition to a centrocyte phenotype according to a timed program and depend on the dark zone for effective selection.* Immunity, 2013. **39**(5): p. 912-24.

70. Dal Porto, J.M., et al., *Very low affinity B cells form germinal centers, become memory B cells, and participate in secondary immune responses when higher affinity competition is reduced.* J Exp Med, 2002. **195**(9): p. 1215-21.

71. Shih, T.A., et al., *Role of BCR affinity in T cell dependent antibody responses in vivo.* Nat Immunol, 2002. **3**(6): p. 570-5.

72. Khalil, A.M., J.C. Cambier, and M.J. Shlomchik, *B cell receptor signal transduction in the GC is short-circuited by high phosphatase activity.* Science, 2012. **336**(6085): p. 1178-81.

73. Pratama, A. and C.G. Vinuesa, *Control of TFH cell numbers: why and how?* Immunol Cell Biol, 2014. **92**(1): p. 40-8.

74. Bentebibel, S.E., et al., *Induction of ICOS+CXCR3+CXCR5+ TH cells correlates with antibody responses to influenza vaccination.* Sci Transl Med, 2013. **5**(176): p. 176ra32.

75. Duan, Z., et al., *Genetic polymorphisms of CXCR5 and CXCL13 are associated with non-responsiveness to the hepatitis B vaccine.* Vaccine, 2014. **32**(41): p. 5316-22.

76. Gitlin, A.D., et al., *HUMORAL IMMUNITY. T cell help controls the speed of the cell cycle in germinal center B cells.* Science, 2015. **349**(6248): p. 643-6.

77. Gitlin, A.D., Z. Shulman, and M.C. Nussenzweig, *Clonal selection in the germinal centre by regulated proliferation and hypermutation.* Nature, 2014. **509**(7502): p. 637-40.

78. Smith, K.G., et al., *The extent of affinity maturation differs between the memory and antibody-forming cell compartments in the primary immune response.* EMBO J, 1997. **16**(11): p. 2996-3006.

79. Smith, K.G., et al., *Bcl-2 increases memory B cell recruitment but does not perturb selection in germinal centers.* Immunity, 1994. **1**(9): p. 803-13.

80. Weisel, F.J., et al., *A Temporal Switch in the Germinal Center Determines Differential Output of Memory B and Plasma Cells.* Immunity, 2016. **44**(1): p. 116-30.

81. Nurieva, R.I., et al., *Bcl6 mediates the development of T follicular helper cells.* Science, 2009. **325**(5943): p. 1001-5.

82. Yu, D., et al., *The transcriptional repressor Bcl-6 directs T follicular helper cell lineage commitment.* Immunity, 2009. **31**(3): p. 457-68.

83. Fazilleau, N., et al., *The function of follicular helper T cells is regulated by the strength of T cell antigen receptor binding.* Nat Immunol, 2009. **10**(4): p. 375-84.

84. Fukuda, T., et al., *The murine BCL6 gene is induced in activated lymphocytes as an immediate early gene.* Oncogene, 1995. **11**(8): p. 1657-63.

85. Choi, Y.S., et al., *Cutting edge: STAT1 is required for IL-6-mediated Bcl6 induction for early follicular helper cell differentiation.* J Immunol, 2013. **190**(7): p. 3049-53.

86. Ballesteros-Tato, A., et al., *Interleukin-2 inhibits germinal center formation by limiting T follicular helper cell differentiation.* Immunity, 2012. **36**(5): p. 847-56.

87. Stone, E.L., et al., *ICOS coreceptor signaling inactivates the transcription factor FOXO1 to promote Tfh cell differentiation.* Immunity, 2015. **42**(2): p. 239-51.

88. Chen, X., et al., *Phenotypic Tfh development promoted by CXCR5-controlled re-localization and IL-6 from radiation-resistant cells.* Protein Cell, 2015. **6**(11): p. 825-32.

89. Haynes, N.M., et al., *Role of CXCR5 and CCR7 in follicular Th cell positioning and appearance of a programmed cell death gene-1high germinal center-associated subpopulation.* J Immunol, 2007. **179**(8): p. 5099-108.

90. Li, J., et al., *EBI2 augments Tfh cell fate by promoting interaction with IL-2-quenching dendritic cells.* Nature, 2016. **533**(7601): p. 110-4.

91. Suan, D., et al., *T follicular helper cells have distinct modes of migration and molecular signatures in naive and memory immune responses.* Immunity, 2015. **42**(4): p. 704-18.

92. Moriyama, S., et al., *Sphingosine-1-phosphate receptor 2 is critical for follicular helper T cell retention in germinal centers.* J Exp Med, 2014. **211**(7): p. 1297-305.

93. Shulman, Z., et al., *T follicular helper cell dynamics in germinal centers.* Science, 2013. **341**(6146): p. 673-7.

94. Turner, J.S., Z.L. Benet, and I.L. Grigorova, *Antigen Acquisition Enables Newly Arriving B Cells To Enter Ongoing Immunization-Induced Germinal Centers.* J Immunol, 2017. **199**(4): p. 1301-1307.

95. Weinstein, J.S., et al., *TFH cells progressively differentiate to regulate the germinal center response.* Nat Immunol, 2016. **17**(10): p. 1197-1205.

96. Turner, J.S., Z.L. Benet, and I.L. Grigorova, *Antigen Acquisition Enables Newly Arriving B Cells To Enter Ongoing Immunization-Induced Germinal Centers.* J Immunol, 2017.

97. Zotos, D., et al., *IL-21 regulates germinal center B cell differentiation and proliferation through a B cell-intrinsic mechanism.* J Exp Med, 2010. **207**(2): p. 365-78.

98. King, I.L. and M. Mohrs, *IL-4-producing CD4+ T cells in reactive lymph nodes during helminth infection are T follicular helper cells.* J Exp Med, 2009. **206**(5): p. 1001-7.

99. Wurster, A.L., et al., *Interleukin-4-mediated protection of primary B cells from apoptosis through Stat6-dependent up-regulation of Bcl-xL.* J Biol Chem, 2002. **277**(30): p. 27169-75.

100. Reinhardt, R.L., H.E. Liang, and R.M. Locksley, *Cytokine-secreting follicular T cells shape the antibody repertoire.* Nat Immunol, 2009. **10**(4): p. 385-93.

101. Snapper, C.M. and W.E. Paul, *Interferon-gamma and B cell stimulatory factor-1 reciprocally regulate Ig isotype production.* Science, 1987. **236**(4804): p. 944-7.

102. Han, S., et al., *Cellular interaction in germinal centers. Roles of CD40 ligand and B7-2 in established germinal centers.* J Immunol, 1995. **155**(2): p. 556-67.

103. Bolduc, A., et al., *Constitutive CD40L expression on B cells prematurely terminates germinal center response and leads to augmented plasma cell production in T cell areas.* J Immunol, 2010. **185**(1): p. 220-30.

104. Kishi, Y., et al., *Augmented antibody response with premature germinal center regression in CD40L transgenic mice.* J Immunol, 2010. **185**(1): p. 211-9.

105. Angelin-Duclos, C., et al., *Commitment of B lymphocytes to a plasma cell fate is associated with Blimp-1 expression in vivo.* J Immunol, 2000. **165**(10): p. 5462-71.

106. Shapiro-Shelef, M., et al., *Blimp-1 is required for the formation of immunoglobulin secreting plasma cells and pre-plasma memory B cells.* Immunity, 2003. **19**(4): p. 607-20.

107. Saito, M., et al., *A signaling pathway mediating downregulation of BCL6 in germinal center B cells is blocked by BCL6 gene alterations in B cell lymphoma.* Cancer Cell, 2007. **12**(3): p. 280-92.

108. Liu, D., et al., *T-B-cell entanglement and ICOSL-driven feed-forward regulation of germinal centre reaction.* Nature, 2015. **517**(7533): p. 214-8.

109. Grakoui, A., et al., *The immunological synapse: a molecular machine controlling T cell activation.* Science, 1999. **285**(5425): p. 221-7.

110. Huppa, J.B. and M.M. Davis, *T-cell-antigen recognition and the immunological synapse.* Nat Rev Immunol, 2003. **3**(12): p. 973-83.

111. Negulescu, P.A., et al., *Polarity of T cell shape, motility, and sensitivity to antigen.* Immunity, 1996. **4**(5): p. 421-30.

112. Wulfing, C., et al., *Costimulation and endogenous MHC ligands contribute to T cell recognition.* Nat Immunol, 2002. **3**(1): p. 42-7.

113. Kageyama, R., et al., *The receptor Ly108 functions as a SAP adaptor-dependent on-off switch for T cell help to B cells and NKT cell development.* Immunity, 2012. **36**(6): p. 986-1002.

114. Shulman, Z., et al., *Dynamic signaling by T follicular helper cells during germinal center B cell selection.* Science, 2014. **345**(6200): p. 1058-62.

115. Faroudi, M., et al., *Cutting edge: T lymphocyte activation by repeated immunological synapse formation and intermittent signaling.* J Immunol, 2003. **171**(3): p. 1128-32.

116. Qi, H., *T follicular helper cells in space-time.* Nat Rev Immunol, 2016. **16**(10): p. 612-25.

117. Papa, I., et al., *TFH-derived dopamine accelerates productive synapses in germinal centres.* Nature, 2017. **547**(7663): p. 318-323.

118. Bubier, J.A., et al., *A critical role for IL-21 receptor signaling in the pathogenesis of systemic lupus erythematosus in BXSB-Yaa mice.* Proc Natl Acad Sci U S A, 2009. **106**(5): p. 1518-23.

119. Lee, S.K., et al., *Interferon-gamma excess leads to pathogenic accumulation of follicular helper T cells and germinal centers.* Immunity, 2012. **37**(5): p. 880-92.

120. Odegard, J.M., et al., *ICOS-dependent extrafollicular helper T cells elicit IgG production via IL-21 in systemic autoimmunity.* J Exp Med, 2008. **205**(12): p. 2873-86.

121. Ma, J., et al., *Increased frequency of circulating follicular helper T cells in patients with rheumatoid arthritis.* Clin Dev Immunol, 2012. **2012**: p. 827480.

122. Simpson, N., et al., *Expansion of circulating T cells resembling follicular helper T cells is a fixed phenotype that identifies a subset of severe systemic lupus erythematosus.* Arthritis Rheum, 2010. **62**(1): p. 234-44.

123. Zhu, C., et al., *Increased frequency of follicular helper T cells in patients with autoimmune thyroid disease.* J Clin Endocrinol Metab, 2012. **97**(3): p. 943-50.

124. Lim, H.W., P. Hillsamer, and C.H. Kim, *Regulatory T cells can migrate to follicles upon T cell activation and suppress GC-Th cells and GC-Th cell-driven B cell responses.* J Clin Invest, 2004. **114**(11): p. 1640-9.

125. Alexander, C.M., et al., *T regulatory cells participate in the control of germinal centre reactions.* Immunology, 2011. **133**(4): p. 452-68.

126. Li, X. and Y. Zheng, *Regulatory T cell identity: formation and maintenance.* Trends Immunol, 2015. **36**(6): p. 344-53.

127. Linterman, M.A., et al., *Foxp3+ follicular regulatory T cells control the germinal center response.* Nat Med, 2011. **17**(8): p. 975-82.

128. Wollenberg, I., et al., *Regulation of the germinal center reaction by Foxp3+ follicular regulatory T cells.* J Immunol, 2011. **187**(9): p. 4553-60.

129. Chung, Y., et al., *Follicular regulatory T cells expressing Foxp3 and Bcl-6 suppress germinal center reactions.* Nat Med, 2011. **17**(8): p. 983-8.

130. Vaeth, M., et al., *Follicular regulatory T cells control humoral autoimmunity via NFAT2-regulated CXCR5 expression.* J Exp Med, 2014. **211**(3): p. 545-61.

131. Wu, H., et al., *Follicular regulatory T cells repress cytokine production by follicular helper T cells and optimize IgG responses in mice.* Eur J Immunol, 2016. **46**(5): p. 1152-61.

132. Cretney, E., et al., *The transcription factors Blimp-1 and IRF4 jointly control the differentiation and function of effector regulatory T cells.* Nat Immunol, 2011. **12**(4): p. 304-11.

133. Fontenot, J.D., M.A. Gavin, and A.Y. Rudensky, *Foxp3 programs the development and function of CD4+CD25+ regulatory T cells.* Nat Immunol, 2003. **4**(4): p. 330-6.

134. Sage, P.T., et al., *The receptor PD-1 controls follicular regulatory T cells in the lymph nodes and blood.* Nat Immunol, 2013. **14**(2): p. 152-61.

135. Aloulou, M., et al., *Follicular regulatory T cells can be specific for the immunizing antigen and derive from naive T cells.* Nat Commun, 2016. **7**: p. 10579.

136. Shrestha, S., et al., *Treg cells require the phosphatase PTEN to restrain TH1 and TFH cell responses.* Nat Immunol, 2015. **16**(2): p. 178-87.

137. Maceiras, A.R., et al., *T follicular helper and T follicular regulatory cells have different TCR specificity.* Nat Commun, 2017. **8**: p. 15067.

138. Sage, P.T., et al., *Circulating T follicular regulatory and helper cells have memory-like properties.* J Clin Invest, 2014. **124**(12): p. 5191-204.

139. Linterman, M.A., et al., *CD28 expression is required after T cell priming for helper T cell responses and protective immunity to infection.* Elife, 2014. **3**.

140. Josefowicz, S.Z., L.F. Lu, and A.Y. Rudensky, *Regulatory T cells: mechanisms of differentiation and function.* Annu Rev Immunol, 2012. **30**: p. 531-64.

141. Wing, J.B., et al., *Regulatory T cells control antigen-specific expansion of Tfh cell number and humoral immune responses via the coreceptor CTLA-4.* Immunity, 2014. **41**(6): p. 1013-25.

142. Sage, P.T., et al., *The coinhibitory receptor CTLA-4 controls B cell responses by modulating T follicular helper, T follicular regulatory, and T regulatory cells.* Immunity, 2014. **41**(6): p. 1026-39.

143. Sage, P.T., et al., *Suppression by TFR cells leads to durable and selective inhibition of B cell effector function.* Nat Immunol, 2016. **17**(12): p. 1436-1446.

144. Sojka, D.K., Y.H. Huang, and D.J. Fowell, *Mechanisms of regulatory T-cell suppression - a diverse arsenal for a moving target.* Immunology, 2008. **124**(1): p. 13-22.

145. Linterman, M.A., et al., *IL-21 acts directly on B cells to regulate Bcl-6 expression and germinal center responses.* J Exp Med, 2010. **207**(2): p. 353-63.

146. Moore, K.W., et al., *Interleukin-10 and the interleukin-10 receptor.* Annu Rev Immunol, 2001. **19**: p. 683-765.

147. Fife, B.T., et al., *Interactions between PD-1 and PD-L1 promote tolerance by blocking the TCR-induced stop signal.* Nat Immunol, 2009. **10**(11): p. 1185-92.

148. Bystry, R.S., et al., *B cells and professional APCs recruit regulatory T cells via CCL4.* Nat Immunol, 2001. **2**(12): p. 1126-32.

149. Krzysiek, R., et al., *Antigen receptor engagement selectively induces macrophage inflammatory protein-1 alpha (MIP-1 alpha) and MIP-1 beta chemokine production in human B cells.* J Immunol, 1999. **162**(8): p. 4455-63.

150. Caron, G., et al., *CXCR4 expression functionally discriminates centroblasts versus centrocytes within human germinal center B cells.* J Immunol, 2009. **182**(12): p. 7595-602.

151. Compagno, M., et al., *Mutations of multiple genes cause deregulation of NF-kappaB in diffuse large B-cell lymphoma.* Nature, 2009. **459**(7247): p. 717-21.

152. Griffith, J.W., C.L. Sokol, and A.D. Luster, *Chemokines and chemokine receptors: positioning cells for host defense and immunity.* Annu Rev Immunol, 2014. **32**: p. 659-702.

153. Di Marzio, P., et al., *Role of Rho family GTPases in CCR1- and CCR5-induced actin reorganization in macrophages.* Biochem Biophys Res Commun, 2005. **331**(4): p. 909-16.

154. Oppermann, M., *Chemokine receptor CCR5: insights into structure, function, and regulation.* Cell Signal, 2004. **16**(11): p. 1201-10.

155. Bordon, Y., et al., *The atypical chemokine receptor D6 contributes to the development of experimental colitis.* J Immunol, 2009. **182**(8): p. 5032-40.

156. Castellino, F., et al., *Chemokines enhance immunity by guiding naive CD8+ T cells to sites of CD4+ T cell-dendritic cell interaction.* Nature, 2006. **440**(7086): p. 890-5.

157. Contento, R.L., et al., *CXCR4-CCR5: a couple modulating T cell functions.* Proc Natl Acad Sci U S A, 2008. **105**(29): p. 10101-6.

158. Molon, B., et al., *T cell costimulation by chemokine receptors.* Nat Immunol, 2005. **6**(5): p. 465-71.

159. Tadokoro, C.E., et al., *Regulatory T cells inhibit stable contacts between CD4+ T cells and dendritic cells in vivo.* J Exp Med, 2006. **203**(3): p. 505-11.

160. Tang, Q., et al., *Visualizing regulatory T cell control of autoimmune responses in nonobese diabetic mice.* Nat Immunol, 2006. **7**(1): p. 83-92.

161. Dal Secco, V., et al., *Tunable chemokine production by antigen presenting dendritic cells in response to changes in regulatory T cell frequency in mouse reactive lymph nodes.* PLoS One, 2009. **4**(11): p. e7696.

162. Morlacchi, S., et al., *Regulatory T cells target chemokine secretion by dendritic cells independently of their capacity to regulate T cell proliferation.* J Immunol, 2011. **186**(12): p. 6807-14.

163. Pace, L., et al., *Regulatory T cells increase the avidity of primary CD8+ T cell responses and promote memory.* Science, 2012. **338**(6106): p. 532-6.

164. Vinuesa, C.G., et al., *Follicular Helper T Cells.* Annu Rev Immunol, 2016. **34**: p. 335-68.

165. Jacob, J. and G. Kelsoe, *In situ studies of the primary immune response to (4-hydroxy-3-nitrophenyl)acetyl. II. A common clonal origin for periarteriolar lymphoid sheath-associated foci and germinal centers.* J Exp Med, 1992. **176**(3): p. 679-87.

166. Allen, C.D., T. Okada, and J.G. Cyster, *Germinal-center organization and cellular dynamics.* Immunity, 2007. **27**(2): p. 190-202.

167. Green, J.A., et al., *The sphingosine 1-phosphate receptor S1P(2) maintains the homeostasis of germinal center B cells and promotes niche confinement.* Nat Immunol, 2011. **12**(7): p. 672-80.

168. Menten, P., A. Wuyts, and J. Van Damme, *Macrophage inflammatory protein-1.* Cytokine Growth Factor Rev, 2002. **13**(6): p. 455-81.

169. Maurer, M. and E. von Stebut, *Macrophage inflammatory protein-1.* Int J Biochem Cell Biol, 2004. **36**(10): p. 1882-6.

170. Wing, J.B. and S. Sakaguchi, *Foxp3(+) T(reg) cells in humoral immunity.* Int Immunol, 2014. **26**(2): p. 61-9.

171. Lim, H.W., et al., *Cutting edge: direct suppression of B cells by CD4+ CD25+ regulatory T cells.* J Immunol, 2005. **175**(7): p. 4180-3.

172. Goodnow, C.C., et al., *Altered immunoglobulin expression and functional silencing of self-reactive B lymphocytes in transgenic mice.* Nature, 1988. **334**(6184): p. 676-82.

173. Barnden, M.J., et al., *Defective TCR expression in transgenic mice constructed using cDNA-based alpha- and beta-chain genes under the control of heterologous regulatory elements.* Immunol Cell Biol, 1998. **76**(1): p. 34-40.

174. Grigorova, I.L., et al., *Cortical sinus probing, S1P1-dependent entry and flow-based capture of egressing T cells.* Nat Immunol, 2009. **10**(1): p. 58-65.

175. Cook, D.N., et al., *Requirement of MIP-1 alpha for an inflammatory response to viral infection.* Science, 1995. **269**(5230): p. 1583-5.

176. Wiik, A.S., et al., *Antinuclear antibodies: a contemporary nomenclature using HEp-2 cells.* J Autoimmun, 2010. **35**(3): p. 276-90.

177. Kim, J.M., J.P. Rasmussen, and A.Y. Rudensky, *Regulatory T cells prevent catastrophic autoimmunity throughout the lifespan of mice.* Nat Immunol, 2007. **8**(2): p. 191-7.

178. Bettelli, E., et al., *Reciprocal developmental pathways for the generation of pathogenic effector TH17 and regulatory T cells.* Nature, 2006. **441**(7090): p. 235-8.

179. Baumjohann, D., et al., *Persistent antigen and germinal center B cells sustain T follicular helper cell responses and phenotype.* Immunity, 2013. **38**(3): p. 596-605.

180. Rahman, Z.S., et al., *Impaired apoptotic cell clearance in the germinal center by Mer-deficient tingible body macrophages leads to enhanced antibody-forming cell and germinal center responses.* J Immunol, 2010. **185**(10): p. 5859-68.

181. Khan, T.N., et al., *Prolonged apoptotic cell accumulation in germinal centers of Mer-deficient mice causes elevated B cell and CD4+ Th cell responses leading to autoantibody production.* J Immunol, 2013. **190**(4): p. 1433-46.

182. Berek, C., A. Berger, and M. Apel, *Maturation of the immune response in germinal centers.* Cell, 1991. **67**(6): p. 1121-9.

183. Mesin, L., J. Ersching, and G.D. Victora, *Germinal Center B Cell Dynamics.* Immunity, 2016. **45**(3): p. 471-82.

184. Gitlin, A.D., Z. Shulman, and M.C. Nussenzweig, *Clonal selection in the germinal centre by regulated proliferation and hypermutation.* Nature, 2014. **509**(7502): p. 637-640.

185. McHeyzer-Williams, M., et al., *Molecular programming of B cell memory.* Nature Reviews Immunology, 2012. **12**(1): p. 24-34.

186. Brink, R., et al., *Visualizing the effects of antigen affinity on T-dependent B-cell differentiation.* Immunol Cell Biol, 2008. **86**(1): p. 31-9.

187. Oracki, S.A., et al., *Plasma cell development and survival.* Immunol Rev, 2010. **237**(1): p. 140-59.

188. McHeyzer-Williams, L.J. and M.G. McHeyzer-Williams, *Antigen-specific memory B cell development.* Annual Review of Immunology, 2005. **23**(9): p. 487-513.

189. Kroese, F.G., et al., *Germinal centers develop oligoclonally.* Eur J Immunol, 1987. **17**(7): p. 1069-72.

190. Liu, Y.J., et al., *Sites of specific B cell activation in primary and secondary responses to T cell-dependent and T cell-independent antigens.* Eur J Immunol, 1991. **21**(12): p. 2951-62.

191. Jacob, J., et al., *In situ studies of the primary immune response to (4-hydroxy-3-nitrophenyl)acetyl. III. The kinetics of V region mutation and selection in germinal center B cells.* J Exp Med, 1993. **178**(4): p. 1293-307.

192. Schwickert, T.A., et al., *A dynamic T cell-limited checkpoint regulates affinity-dependent B cell entry into the germinal center.* Journal of Experimental Medicine, 2011. **208**(6): p. 1243-52.

193. Schwickert, T.A., et al., *Germinal center reutilization by newly activated B cells.* Journal of Experimental Medicine, 2009. **206**(13): p. 2907-14.

194. Weinstein, J.S., et al., *TFH cells progressively differentiate to regulate the germinal center response.* Nature Immunology, 2016. **17**(10): p. 1197-1205.

195. Allen, C.D.C., et al., *Imaging of germinal center selection events during affinity maturation.* Science, 2007. **315**(5811): p. 528-531.

196. Allen, C.D.C., et al., *Germinal center dark and light zone organization is mediated by CXCR4 and CXCR5.* Nature Immunology, 2004. **5**(9): p. 943-952.

197. Turner, J.S., et al., *Transiently antigen-primed B cells return to naive-like state in absence of T-cell help.* Nature Communications, 2017. **8**: p. 15072-15072.

198. Kitano, M., et al., *Bcl6 protein expression shapes pre-germinal center B cell dynamics and follicular helper T cell heterogeneity.* Immunity, 2011. **34**(6): p. 961-72.

199. Heesters, B.A., R.C. Myers, and M.C. Carroll, *Follicular dendritic cells: dynamic antigen libraries.* Nat Rev Immunol, 2014. **14**(7): p. 495-504.

200. Suzuki, K., et al., *Visualizing B cell capture of cognate antigen from follicular dendritic cells.* J Exp Med, 2009. **206**(7): p. 1485-93.

201. Nicasio, M., et al., *Neutralization interfering antibodies: a "novel" example of humoral immune dysfunction facilitating viral escape?* Viruses, 2012. **4**(9): p. 1731-52.

202. Basso, K., et al., *Tracking CD40 signaling during germinal center development.* Blood, 2004. **104**(13): p. 4088-96.

203. Polo, J.M., et al., *Reversible disruption of BCL6 repression complexes by CD40 signaling in normal and malignant B cells.* Blood, 2008. **112**(3): p. 644-51.

204. Mohammad Hosseini, A., et al., *Toll-Like Receptors in the Pathogenesis of Autoimmune Diseases.* Adv Pharm Bull, 2015. **5**(Suppl 1): p. 605-14.

205. Hanten, J.A., et al., *Comparison of human B cell activation by TLR7 and TLR9 agonists.* BMC Immunol, 2008. **9**: p. 39.

206. Sabouri, Z., et al., *Redemption of autoantibodies on anergic B cells by variable-region glycosylation and mutation away from self-reactivity.* Proc Natl Acad Sci U S A, 2014. **111**(25): p. E2567-75.

207. El Shikh, M.E., et al., *Activation of B cells by antigens on follicular dendritic cells.* Trends Immunol, 2010. **31**(6): p. 205-11.

208. Pritchard, N.R. and K.G. Smith, *B cell inhibitory receptors and autoimmunity.* Immunology, 2003. **108**(3): p. 263-73.